

**“Analysis of mice
deficient in late endosomal SNARE
proteins VAMP8/endobrevin and Vti1b”**

PhD Thesis

in partial fulfilment of the requirements
for the degree of “Doctor of Philosophy (PhD)”
in the molecular biology program
at the Georg August University Göttingen
Faculty of Biology

submitted by

Namita Kanwar

born in

Faridabad, India

Göttingen, December 2006

I hereby declare that the Ph.D. thesis entitled “Analysis of mice deficient in late endosomal SNARE proteins VAMP8/endobrevin and Vti1b” has been written independently and with no other sources and aids than quoted.

Namita Kanwar

Table of contents

Acknowledgements	IV
Abstract	V
List of figures	VI
Abbreviations	VIII
List of chemicals	X
1. Introduction	1
1.1. Protein trafficking and the endosomal system	1
1.1.1. Compartments of the endosomal system	2
1.1.2. Endosomal pathways and their role in protein sorting	4
1.2. SNAREs the central component of membrane fusion machinery	6
1.2.1. SNARE proteins: history, discovery and structure	6
1.2.2. SNARE proteins: Classification	9
1.2.3. Components of fusion machinery and their function	10
1.2.3.1. <i>Rab</i> proteins: The <i>rab</i> cycle	10
1.2.3.2. <i>Tethering and docking factors</i>	11
1.2.3.3. <i>The SNARE cycle</i> :	11
1.2.3.5. <i>Sec1/Munc18 family of proteins</i>	12
1.2.3.6. <i>Synaptotagmins</i>	12
1.2.4. Mammalian SNAREs and their complexes	13
1.2.4.1. <i>VAMP Family with special emphasis on VAMP8/Endobrevin</i>	13
1.2.4.2. <i>Mammalian Syntaxins</i>	16
1.2.4.3. <i>Mammalian Vti1 homologs: Vti1a and Vti1b</i>	18
1.2.4.4. <i>Mammalian SNAP25 family members</i>	19
1.2.5. Mammalian SNARE complexes: emphasis on VAMP8 complexes	20
1.3. Thymus and its role in development of T-lymphocytes	21
1.3.1. Thymus: structure and function	21
1.3.2. T-cell development	23
1.3.2.1. <i>Developmental stages of T-lymphocytes</i>	23
1.3.2.2. <i>Thymic selection of the T cells</i>	24
1.4. Background information and objective of the project	26
1.4.1. Creation and analysis of Vti1b knock out mice	26
1.4.2. VAMP8 knock out mice	27
1.4.3. Initial findings	27
1.4.4. Initial findings	29
1.4.5. Objective of the study	30
2. Materials and Methods	32
2.1 DNA Techniques	32
2.1.1. DNA extraction from mouse tail biopsy	32
2.1.2. PCR amplification of genomic DNA to determine genotype	32
2.1.3. Agarose gel electrophoresis for DNA separation	34

2.1.4. Determination of DNA concentration	34
2.2. Protein Techniques	35
2.2.1. Tissue homogenate preparation	35
2.2.2. Determination of protein concentration	35
2.2.3. Measurement of lysosomal enzyme activities in tissue homogenates	35
2.2.4. Triton X-114 extraction of proteins	36
2.2.5. Preparation of protein samples for SDS page separation	37
2.2.6. SDS polyacrylamide gel separation of proteins	37
2.2.7. Semi dry protein transfer	38
2.2.8. Western blotting	39
2.3 Tissue culture techniques	39
2.3.1. Isolation of Primary fibroblasts from mouse embryos	39
2.3.2. Maintenance of cells	40
2.3.3. Immortalization of primary fibroblasts by passaging	40
2.3.4. Isolation of murine peritoneal macrophages	41
2.3.5. Cryoconservation of cells	41
2.3.6. Histological analysis	42
2.4. FACS techniques	42
2.4.1. Preparation of T- lymphocytes from thymus	42
2.4.2. Preparation of T- lymphocytes from spleen	42
2.4.3. Phenotyping of primary T- lymphocytes from Thymus or Spleen	43
2.4.4. Induction of apoptosis by dexamethasone treatment	46
2.4.5. Annexin V and propidium Iodide co-staining to visualize dead cells	46
2.4.6. Sub G1 peak assay to determine dead cells	46
2.4.7. Induction of apoptosis by plate bound anti CD3 ϵ and CD28 antibodies.	47
2.4.7.1. Preparation of ELISA plates:	47
2.4.7.2. Induction of apoptosis:	47
2.4.8. Induction of apoptosis using Anti-FAS (CD95) antibody	48
2.4.9. Preparation of cells for bone marrow and transplantation	48
2.4.10. Analysis of transplanted RAG2 ^{-/-} γ c ^{-/-} mice	48
2.5. Immunofluorescence techniques	49
2.5.1. Growing cells for immunofluorescence	49
2.5.2. Uptake of fluorescently labeled LDL	49
2.5.3. Uptake of fluorescently labelled beads by peritoneal macrophages	50
2.5.4. Methanol fixation	50
2.5.5. PFA fixation	50
2.5.6. Immunofluorescence for lamp1/2 and DAPI staining	51
3. Results	56
3.1 Ablation of VAMP8/endobrevin causes partial early mortality	56
3.1.1. Progressively degenerating health and early death in VAMP8 ^{-/-} mice	56
3.1.2. Heterogeneity in the VAMP8 ^{-/-} phenotype	58
3.2. Ablation of VAMP8 causes defects in Thymus	59
3.2.1. Morphological defect	59
3.2.2. Reduction in thymus size and total cell count	61
3.2.3. SNARE proteins in the thymus	63
3.3. Deficiency of VAMP8 leads to defective T-cell maturation	64
3.3.1. Development of CD4 ⁺ CD8 ⁻ DN1-4 subsets is disturbed in sick VAMP8 ^{-/-} mice	65
3.3.2. Development of CD4/CD8 subsets is disturbed in sick VAMP8 ^{-/-} mice	67

3.3.3. Development of CD4/CD8 subsets is disturbed in sick VAMP8 ^{-/-} Vti1b ^{-/-} mice	70
3.3.4. Vti1b ^{-/-} mice do not show defect in T lymphocyte maturation	71
3.3.5. T cell receptor expression unaltered in VAMP8 ^{-/-} small and sick mice	71
3.3.6. VAMP8 deficiency does not cause defect in adult peripheral T-cell reservoir	73
3.4. Thymocytes show high cell death	74
3.4.1. Thymus from small and sick mice have high cell death <i>in vivo</i>	74
3.4.2. Dexamethasone induced apoptosis	76
3.4.2.1. Thymocytes from VAMP8 ^{-/-} small not sick are sensitive to apoptosis	76
3.4.2.2. Few live thymocytes in VAMP8 ^{-/-} sick mice: not sensitive to induction	80
3.4.2.3. Thymocytes from adult mice: no increased sensitivity to apoptosis	82
3.4.2.4. Thymocytes from Vti1b ^{-/-} mice: no increased sensitivity to apoptosis	84
3.4.3. FAS induced apoptosis	86
3.4.2. Apoptosis by crosslinking with anti CD3 and anti CD28 antibodies	87
3.5. Thymic stroma is affected due to the lack of VAMP8	88
3.6. Studies on mouse cells derived from VAMP8^{-/-} mice	92
3.6.1. Lamp staining VAMP8 ^{-/-} MEFs	93
3.6.2. Uptake and degradation of fluorescently labeled LDL	94
3.6.3. Bead uptake in VAMP8 ^{-/-} Vti1b ^{-/-} peritoneal macrophages	96
3.7. Level of lysosomal enzymes	98
4. Discussion	100
4.1. Heterogeneity in phenotype manifestation	100
4.2 Thymus specific effect of VAMP8 ablation	101
4.2.1. Effect of VAMP8 ablation on T cell development and thymic stroma	101
4.2.1.1. Defect in thymic stroma	103
4.2.1.2. Defect in DN subsets	104
4.2.1.3. Defect in CD4/CD8 subsets	105
4.2.1.4. Loss of cortico-medullary morphology	106
4.2.2. Cell death in VAMP8 ^{-/-} thymus and thymus cellularity	106
4.2.3. Thymic morphology and T cell defect: Similarities to other knock out models	108
4.2.4 Is thymus defect the cause of death of the mice?	114
4.3 Endosomal trafficking in VAMP8 ^{-/-} mice	115
4.4 What could functionally replace VAMP8?	116
5. Summary	119
6. Conclusion and Outlook	122
7. Bibliography	124
Publications	140
Curriculum Vitae	141

Acknowledgements

I take this occasion to express my gratitude towards Prof. Dr. Fischer von Mollard for giving me this PhD project to work on. I would like to thank her for her patience, encouragement and ideas during scientific discussions. Her mentorship and encouragement developed a sense of confidence and independent thinking in me during the course of the present work.

I would like to thank Dr. Ralf Dressel from the bottom of my heart for his excellent support during the entire period of my work. I owe all my knowledge about immunology and immunology based experiments to Dr. Dressel. His patience, encouragement, discussions and guidance have been the key to the success of this work.

I wish to extend my warm thanks to Subbulakshmi Chidambaram, my colleague in Göttingen as well as in Bielefeld, for her friendly advises and her support during the difficult times. I also thank her for introducing me to the laboratory in my initial days at work.

I am thankful to Beate Veith and Christiane Weigand for their excellent technical help in Göttingen and Bielefeld respectively. I also wish to thank Leslie Elsner for her technical support and friendly discussions during the time I spent at the Department for Immunogenetics.

I express my gratitude to all my colleagues in Bielefeld- Bianca, Jana, Marius, Sascha, Ivar for creating a healthy work environment. I would also like to thank my colleagues in Göttingen- Fotini, Christiane, Santosh, Karthik, Malayalam, Constanze, Jenny and Tanya for their help and support.

I would like to thank all the people involved in the International Graduate School for Molecular Biology especially Dr. Steffen Burkhardt who is an excellent and the efficient most program co-ordinator I have ever come across. I also wish to thank him and Ivana for all their help in the troubled times and instantly providing all the solutions they could.

Above everything else I take this opportunity to express my love and gratitude to my family - my mother Smt. Sharda Kanwar, my father Shri. L.S. Kanwar, my brother Anshuman Kanwar and my fiancée Ravi Dwivedi for all their constant guidance, love, good wishes, moral support and constant encouragement. I wouldn't be here without them.

Abstract

Membrane fusion requires a synchronized interplay between several proteins that form the membrane fusion machinery. SNAREs are the central component of this fusion machinery. Cognate SNARE proteins localized to transport vesicles and their target membranes interact with each other via coiled-coil interaction to form core complexes. Vesicle associated membrane protein-8 (VAMP8) or endobrevin is a mammalian R-SNARE that participates in the formation of two complexes. First, VAMP8 in a complex with syntaxin8, syntaxin7 and Vti1b, mediates the homotypic late endosomal fusion. Second, VAMP8 forms a complex with SNAP23 and syntaxin 4 and mediates exocytosis of zymogen granules in the pancreatic acinar cells. VAMP8 is also required for exocytosis of granules from mast cells and platelets.

This study was aimed at understanding the physiological role of VAMP8 using VAMP8 knock out mice. VAMP8^{-/-} mice were normal at birth, however, by 10-12 days of age nearly one thirds of the mice were dead. These one third mice started to loose weight at postnatal day 8-9 (small not sick stage) and after 2-3 consecutive days of weight loss (small and sick stage), the mice died. The survivors became healthy adults but were lighter than littermates. The small and sick VAMP8^{-/-} mice were half the weight of the littermates and had an extremely small thymus. The thymic medulla was reduced to mere remnants and there was no clear cortico-medullary boundary. The developing thymocytes including the CD4⁻CD8⁻ DN1-4 subsets and CD4/CD8 populations showed a major maturational disturbance. The thymus of small and sick VAMP8^{-/-} mice showed high number of dead cells and the thymocytes from small not sick VAMP8^{-/-} mice were highly sensitive to apoptotic stimuli *in vitro*. Bone marrow derived hemopoietic progenitors from small and sick VAMP8^{-/-} mice could develop into functional T and B lymphocytes in the RAG2^{-/-} γ c^{-/-} mice, indicating that the thymic stromal cells could be defective in the VAMP8^{-/-} mice but the thymocyte precursors are normal. Hence, VAMP8 is important in proper development and function of thymus in mice and the loss of VAMP8 has severe implications on the thymocytes and the thymic stroma. However processes such as endocytosis, endosomal traffic, phagocytosis and lysosomal degradation are not affected in the cells derived from VAMP8^{-/-} mice, indicating that VAMP8 is probably not essential for the late endosomal fusion events.

List of figures

Figure 1.1. A scheme of membrane and protein trafficking through mammalian cells	1
Figure 1.2. A scheme showing assembly of neuronal SNARE proteins to form a core complex	7
Figure 1.3. The structure of neuronal SNARE proteins	8
Figure 1.4. Structure of SNARE core complex	9
Figure 1.5. The SNARE cycle	12
Figure 1.6. Mammalian endosomal SNARE complexes	21
Figure 1.7. Structural organization of thymus.	22
Figure 1.8. A scheme showing vector design for 3' trapping of the VAMP8 gene	27
Figure 1.9. Morphological Defect in thymus from VAMP8 ^{-/-} Vti1b ^{-/-} mice	28
Figure 1.10. High number of dead cells in VAMP8 ^{-/-} Vti1b ^{-/-} thymus:	29
Figure 3.1. High early mortality in VAMP8/endobrevin ^{-/-} genotypes:	56
Figure 3.2. Weight gain pattern in VAMP8 ^{-/-} mice:	57
Figure 3.3. Massive weight loss in small VAMP8 ^{-/-} mice	57
Figure 3.4. VAMP8 ^{-/-} Vti1b ^{-/-} mice show high early mortality:	58
Figure 3.5. Morphology of thymus is disrupted in VAMP8 ^{-/-} small and sick mice	60
Figure 3.6. Thymus cellularity is progressively reduced in VAMP8 ^{-/-} small and sick mice	62
Figure 3.7. The cellularity of thymus is reduced in small and sick VAMP8 ^{-/-} Vti1b ^{-/-} but not in Vti1b ^{-/-} mice:	62
Figure 3.8A. SNARE profile of the thymus from healthy VAMP8 ^{-/-} mouse	64
Figure 3.8B. SNARE profile of thymus from VAMP8 ^{-/-} Vti1b ^{-/-} mouse	64
Figure 3.9. Analysis of DN1-4 thymocyte precursor subsets in small and sick VAMP8 ^{-/-} mice:	66
Figure 3.10. Analysis of DN1-4 thymocyte precursor subsets in small not sick VAMP8 ^{-/-} mice	67
Figure 3.11. CD4/CD8 phenotyping of developing T lymphocytes from small and sick VAMP8 ^{-/-} mice	68
Figure 3.12. CD4/CD8 phenotyping from small not sick VAMP8 ^{-/-} mice	69
Figure 3.13. CD4/CD8 phenotyping from adult VAMP8 ^{-/-} mice	69
Figure 3.14. CD4/CD8 phenotyping of thymocytes from small not sick VAMP8 ^{-/-} Vti1b ^{-/-} mice.	70
Figure 3.15. CD4/CD8 phenotyping of thymocytes from Vti1b ^{-/-} mice:	71
Figure 3.16. Analysis of TCR expression on the thymocytes from small and sick VAMP8 ^{-/-} mice	72
Figure 3.17. Analysis of peripheral repertoire of lymphocytes and natural killer cells from adult VAMP8 ^{-/-} mice	73
Figure 3.18. Thymus from small and sick VAMP8 ^{-/-} Vti1b ^{-/-} mice show high number of dead cells	74
Figure 3.19. Analysis of dead cells in the thymus of small and sick VAMP8 ^{-/-} mice	75
Figure 3.20. Thymocytes from small not sick VAMP8 ^{-/-} mice show high sensitivity to cell death (dexamethasone treatment)	77
Figure 3.21. Thymocytes from small not sick VAMP8 ^{-/-} mice show high sensitivity to cell death (dexamethasone treatment)	78
Figure 3.22. Thymocytes from small not sick VAMP8 ^{-/-} mice show high sensitivity to cell death (dexamethasone treatment)	79

Figure 3.23. Few live thymocytes in small and sick <i>VAMP8</i> ^{-/-} mice: not exceptionally sensitive to (dexamethasone treatment)	81
Figure 3.24. Few live Thymocytes in small and sick <i>VAMP8</i> ^{-/-} mice: not increasingly sensitive to (dexamethasone treatment):	82
Figure 3.25. Thymocytes from adult <i>VAMP8</i> ^{-/-} mice do not show high sensitivity to cell death (dexamethasone treatment):	83
Figure 3.26. Thymocytes from adult <i>VAMP8</i> ^{-/-} mice do not show high sensitivity to cell death (dexamethasone treatment)	84
Figure 3.27. Thymocytes from <i>Vti1b</i> ^{-/-} mice do not show high sensitivity to cell death (dexamethasone treatment)	85
Figure 3.28. Thymocytes from <i>Vti1b</i> ^{-/-} mice do not show high sensitivity to cell death (dexamethasone treatment)	85
Figure 3.29. Thymocytes from small not sick <i>VAMP8</i> ^{-/-} mice show high sensitivity to cell death (anti-FAS antibody treatment):	86
Figure 3.30. Thymocytes from small not sick <i>VAMP8</i> ^{-/-} mice show high sensitivity to cell death (anti-CD3+CD28 antibody treatment):	88
Figure 3.31. Bone marrow cells from <i>VAMP8</i> ^{-/-} sick mice develop into normal B-lymphocytes in <i>RAG2</i> ^{-/-} <i>γc</i> ^{-/-} mice:	90
Figure 3.32. Bone marrow cells from <i>VAMP8</i> ^{-/-} sick mice develop into normal T-lymphocytes in <i>RAG2</i> ^{-/-} <i>γc</i> ^{-/-} mice:	91
Figure 3.33. Bone marrow cells from <i>VAMP8</i> ^{-/-} sick mice develop into normal T-lymphocytes in <i>RAG2</i> ^{-/-} <i>γc</i> ^{-/-} mice:	92
Figure 3.34. The morphology of endosomal system is normal in <i>VAMP8</i> ^{-/-} fibroblasts	93
Figure 3.35. Endocytosis, endosomal transport and lysosomal degradation of LDL not affected in <i>VAMP8</i> ^{-/-} fibroblasts	95
Figure 3.36. Phagocytic uptake and lysosomal delivery is not affected in <i>VAMP8</i> ^{-/-} <i>Vti1b</i> ^{-/-} macrophages	97
Figure 3.37. Lysosomal enzymes function normally in small <i>VAMP8</i> ^{-/-} mice	98

Abbreviations

DMEM	Dulbecco's Modified Eagle Medium
DMP	Dimethyl pimelimidate
DMSO	Dimethylsulfoxime
FITC	Fluorescein isothiocyanate
PE	Phycoerythrin
TC	Tricolor
FACS	Fluorescence assisted cell sorting
EDTA	Ethylene diamine tetra-acetic acid
ELISA	Enzyme linked immuno sorbent assay
FCS	Fetal calf serum
CD4	Cluster of differentiation 4
CD8	Cluster of differentiation 8
CD 25	Cluster of differentiation 25
CD 44	Cluster of differentiation 44
MHC	Major histocompatibility complex
PFA	Para formaldehyde
TCR	T cell receptor
SDS	Sodium dodecyl sulphate
TEMED	N'N'N'N'Tetramethylethylenediamine
APS	Ammonium Peroxodisulfate
PI	Propidium iodide
DNA	Deoxyribonucleic acid
PCR	Polymerase chain reaction
BSA	Bovine serum albumin
PMSF	Phenylmethylsulfonylchloride
DTT	Dithiotreitol
LDL	Low density lipoprotein
RPMI 1640	Roswell Park Memorial Institute medium
Fas L	Fas ligand

Units

°C	Degree Celsius
Mg	Microgram
µl	Microlitre
Mm	Micrometer
µM	Micromolar
aa	Amino acid
G	Gram (weight)
h	Hour
M	Molar (= mol/l)
mA	Milliampere

Mg	Milligram
Min.	Minute
ml	Milliliter
mM	Millimolar
mol	Mole
Rpm	Revolutions per minute
v/v	Volume per volume
w/v	Weight per volume

List of chemicals

Acetic acid	Merck
Acetone	Merck
30% Acrylamide / 0,8% Bisacrylamide	Roth
Agarose	Roth
Ammonium acetate	Fluka
Bromphenol blue	BioRad
Calcium chloride	MerckDM
Chloroform	Merck
DAKO® mounting media	Carpinteria
Dimethylsulfoxide (DMSO)	Merck
Dithiotreitol (DTT)	Serva
Ethanol	Merck
Ethidiumbromide	Serva
EDTA	Merck
Isopropanol	Merck
Leupeptin	Sigma
Magnesiumsulfate	Merck
β-Mercaptoethanol	Sigma
Methanol	Merck
Para formaldehyde	Sigma
Phenol	Fluka
Potassium chloride	Merck
Phenyl methyl sulfonylchloride	Serva
Saccharose	Roth
Sodium acetate	Merck
Sodium azide (NaN ₃)	Sigma
Sodium carbonate (Na ₂ CO ₃)	Merck
Sodium chloride (NaCl)	Roth
Sodium citrate	Merck
Sodium dodecylsulfate (SDS)	Sigma
Sodium hydrogen carbonate (NaHCO ₃)	Merck
Sodium hydroxide (NaOH)	Merck
Sucrose	Roth
TEMED	Sigma
Bovine serum albumin BSA	Carl Roth GmbH
Proteinase K	Carl Roth GmbH
Xylenecyanol FF	Sigma Aldrich
Fetal calf serum	Gibco
Penicillin	Gibco
Sterptomycin	Gibco
Trypsin EDTA	Gibco

Bradford reagent	Bio-Rad Laboratories, GmbH
Glycine	Carl Roth GmbH
Triton X 100	Carl Roth GmbH
Triton X 114	Carl Roth GmbH
Tris	Carl Roth GmbH
APS	Merck
Tween	Fluka Chemie AG
Goat serum	PAA, Germany
Protein A Sepharose beads	Amersham Biosciences
Potassium phosphate	Merck
Dimethyl pimelimidate (DMP)	Fluka Biochemika
DMEM	PAN Biotech GmbH
RPMI-1640	Gibco
Ammonium chloride (NH ₄ Cl)	Merck
Potassium hydrogen carbonate (KHCO ₃)	Fluka Chemie AG
Annexin binding buffer	Becton Dickinson, BD Pharmingen
Dexamethasone	Sigma Aldrich
Propidium Iodide	Sigma
BODIPY-FL-Low Density	Invitrogen™ Molecular probes, Eugene USA
Lipopolysaccharide	
10x PCR buffer	Roche
DNATaq polymerase	Roche, Acu prime
Deoxyribonucleotides	Roche
Primers	Iba, Göttingen
Fluoresbrite® BB Carboxylated	Polysciences, Inc. USA
Microspheres 1.00µm	

List of devices

Analytical balances	
CP320	Sartorius, Göttingen
Lab style 3002	Mettler Toledo, Switzerland
Centrifuges	
Table top centrifuge	Schütt, Göttingen
Biofuge Fresco	Heraeus
Multifuge 1L	Heraeus
Ultracentrifuge TL-100	Beckmann Coulter, München
Cooling centrifuge J21C and J2 MC	Beckmann Coulter, München
Rotors	
JA-10, JA-20	Heraeus, Osterode
TLA-100.3	Beckmann Coulter, München
Fluorescence spectrophotometer	
F1200 HITACHI	Hitachi, Tokyo, Japan
LS 50B	Perkin Elmer

pH meter	Schött, Göttingen
CG 820	Mettler Toledo, Switzerland
Sevenmulti	CTI GmbH, Idstein
Semi Dry blot Assembly	Eppendorf, Kottberg, Göttingen
Thermomixer compact	In house production institute workshop
SDS PAGE chamber	In house production institute workshop
Agarose gel electrophoresis chamber	Bender and Hobein, Zurich
Vortex	Janke & Kunkel, Stufen
Homogenizer Ultra turrax T25	Pharmacia Biotech
Spectrophotometer:	Varian
GeneQuant II	
Cary 50 Bio	
PCR thermocycler	
Gene Amp PCR system 9600	Perkin elmer Cetus, USA
Mastercycler Gradient	Eppendorf, Hamburg
Mastercycler Personal	Eppendorf, Hamburg
Eppendorf tubes	Sarsted, Germany
FACS tubes	Becton Dickinson, BD falcon
ELISA plate	F96 Maxisorp, Nunc, Roskilde, Denmark
Falcon tube	Sarsted, Germany
Corex ^(R) II	Corex, USA
Parafilm	Pechiney Plastic Packaging, USA
Fluorescence assisted cell sorter	Becton Dickinson, BD FACScan
ECL developer	Fujifilm, LAS3000
CO2 incubator	Heracell, Heraeus
Magnetic stirrer	Heidolph, Germany

1. Introduction

1.1. Protein trafficking and the endosomal system

The presence of functionally distinct membrane bound organelles is the hallmark of eukaryotic cells. This compartmentalization of the cytoplasm prevents interference between different intracellular pathways. Additionally, it allows the cell to provide appropriate environment for each process to operate most efficiently (Nunnari and Walter 1996; Rothman and Wieland 1996). Every organelle has a distinct composition and is assigned a specialized function. However, in order to maintain the flow of information, the organelles have to interact with each other allowing the exchange of components such as lipids and proteins.

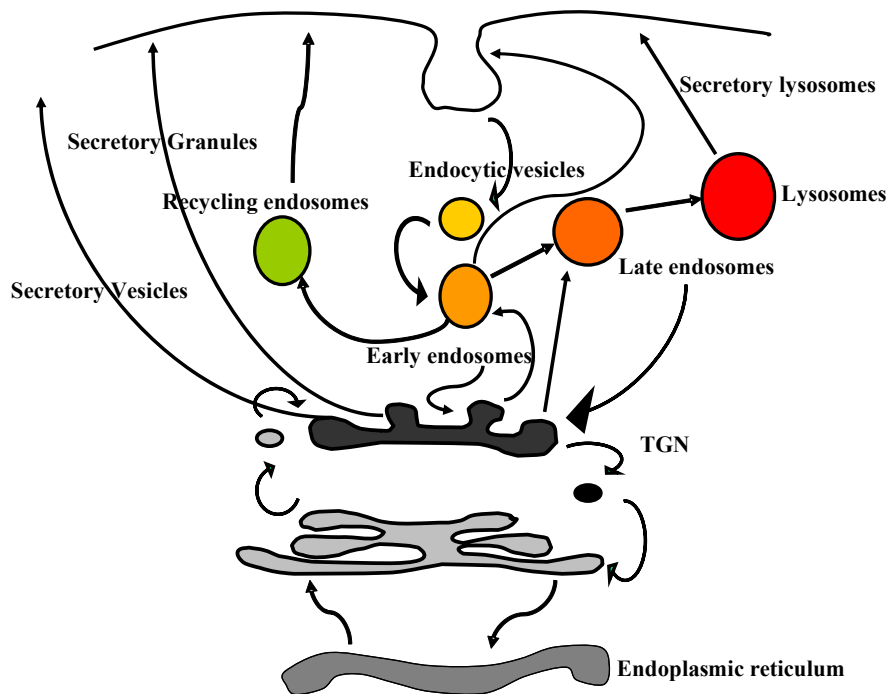


Figure 1.1. A scheme of membrane and protein trafficking through mammalian cells: The proteins are synthesized at the endoplasmic reticulum, modified in the Golgi and transported to their destination. The transport occurs via membrane bound vesicles by retro- and anterograde trafficking. Largely, the endosomal system carries the proteins from the Golgi either to the lysosomes for degradation or to the outside of the cell for secretion. Vesicles can also directly bud off from the trans Golgi network and fuse to the plasma membrane to secrete their contents outside the cells. Substances entering into the cells are also carried to their respective destinations or recycled back to the plasma membrane via the endosomal compartments.

The proteins are synthesized on the ribosomes and are co-translationally transported into the lumen of endoplasmic reticulum (ER). The ER-resident proteins are retained in the organelle while the others are transported via vesicles to the Golgi apparatus. Through the cis-, medial- and trans- Golgi, the proteins undergo massive post translational modifications. At the exit from the Golgi, trafficking pathways get diversified (Figure 1.1) and are discussed later. The final destination of a protein is encoded within the molecule in the form of signal sequences (Blobel 1980). For example, the ER resident proteins carry a KDEL sequence that is recognized by the KDEL receptors. These KDEL receptors are primarily present on the vesicles shuttling between the ER and Golgi and retrieve the escaped ER resident proteins back to the ER (Lodish et al. 2001). Similarly, the soluble lysosomal proteins carry a mannose-6-phosphate (M6P) motif that targets the proteins to the lysosome via binding to the M6P receptors (MPR) (von Figura et al. 1986).

Except a few details that vary between different cell types, the basic flow organization of membranes at the sub-cellular level remains the same and is depicted in Figure 1.1. The different vesicular components and pathways by which a protein can be sorted are described in section 1.1.1 and 1.1.2 respectively.

1.1.1. Compartments of the endosomal system

Transport vesicles can either be formed on the donor membrane at special sites coated with special proteins (clathrin or caveolae) or by alterations of the cytoskeleton (phagocytosis). The Clathrin coated vesicles (CCVs) are the most common means of receptor mediated endocytosis. The CCVs rapidly lose their coat proteins and undergo fusion with the early /sorting endosomes (EE).

Early/sorting endosomes: The early endosomes are complex compartment with both tubulo-vesicular morphology. The vesicular components are typically 250-400 nm in diameter while the tubules radiating from these vesicles are 50-60 nm in diameter and 4-5 μ m in length (Geuze et al. 1983; Gruenberg et al. 1989; Marsh et al. 1986). They are slightly acidic (pH 6.0-6.8) and are primarily responsible for dissociation of the ligand-receptor complex (Kornfeld et al. 1989). This environment of the early endosomes minimizes the risk of damaging the receptors which are intended to be reutilized by the

cells for example by direct recycling to the cell surface (Mellman 1996). In addition, there exists a bidirectional vesicular traffic between the TGN and the early endosomes. Also, the early endosomes can undergo homotypic fusion with other endosomal vesicles and tubules.

Recycling vesicles: The recycling vesicles (RVs) or recycling endosomes arise from the tubular extension of the EEs and are responsible for slower recycling of the freed receptors. Some RVs fuse to the plasma membrane while the others translocate to the perinuclear cytoplasm and accumulate as near the micro tubule organization centre (MTOC) (Hopkins 1983; Yamashiro et al. 1984). The RVs are physically distinct from the sorting endosomes as seen by optical and electron microscopy (Dunn et al. 1989; Ghosh et al. 1994; Marsh et al. 1995; Mayor et al. 1993) and maintain a distinct pH environment. In addition, the perinuclear recycling vesicles act as an intracellular pool of recycling receptors.

Late endosomes and lysosomes: The early endosomal vesicles carrying the ligand /cargo traverse the cytoplasm over the microtubules and fuse with the late endosomes (LEs). The LEs eventually give way to lysosomes. The pH drops to 4.5-5.0 and an array of degradative enzymes leads to degradation of the ligands in the lysosomes. The lysosomes appear as electron dense organelle called 'dense body' surrounded by a single membrane in electron microscopy. The recycling from lysosomes is very slow. This explains why cells are able to accumulate large amount of internalized materials and also the dense appearance of the lysosomes (Mellman 1996)

How does the transport between the EE, LE and lysosomes occurs is still under some debate. Two models were proposed for the passage of material between the compartments of the endosomal system. In the vesicle shuttle model, the EEs were seen as stable structures while the cargo was pinched off from EEs into small transport vesicles that would inturn fuse with the LEs. The maturation model on the other hand suggests that the entire EE moves as a unit and is transformed into the late endosomes (Lodish et al. 2001). There is an increasing evidence that supports the maturation model (Gruenberg et al. 1995). The LEs in thin section electron microscopy appear to have internal vesicles and have been named *multi vesicular bodies* (MVB) or *multi vesicular endosomes* (MVE). These are formed by inward invagination of the limiting endosomal membrane (Vandeurs et al. 1993). The MVBs are proposed to play a role in down regulation of signal transduction by

sequestering the receptors (Di Fiore et al. 1999; Katzmann et al. 2002). Several receptors including the EGF-R have been localized to the internal membranes of the MVBs (Felder et al. 1990). MVBs are also implicated in forming cell specific organelles such as Weible pallad bodies (Blanchard et al. 2002), platelet dense granules (Heijnen et al. 1998) and melanosomes (Huizing et al. 2001).

Secretory lysosomes: The lysosomes were thought to be the end point of endocytic pathways. However, there is an increasing evidence that there of the existence of specialized lysosomes that can act as storage compartments and can exocytose the contents in a regulated fashion. Secretory lysosomes have been studied in specific cell types such as the cytotoxic T lymphocytes which secrete lytic granules (Burkhardt et al. 1990; Griffiths 1996), melanocytes secrete melanosomes that gives rise to pigmentation of skin, eyes and hair (Griffiths 2002). Renal tubular cells secrete lysosomal hydrolases from specialized storage organelles (Gross et al. 1985). Recently it has been shown that the dendritic cells sequester the MHC-II molecules in specialized lysosomes (Mellman and Steinman 2001).

Secretory vesicles and dense core secretory granules: These vesicles carry the proteins to be exported to the outside of the cells. The proteins to be exported are thought to be sorted into these vesicles under specific signals in the TGN. These vesicles bud from the TGN, become mature and are exocytosed either in a constitutive way in secretory vesicles (SVs) or in a regulated manner secretory granules (SG) (Blott and Griffiths. 2002; Bright et al. 1997; Chidgey 1993).

1.1.2. Endosomal pathways and their role in protein sorting

Receptor mediated endocytosis mainly occurs via the formation of clathrin coated vesicles. The receptor-ligand complexes accumulate at specific region on the plasma membrane coated with clathrin molecules and the adaptor complex. Proteins are also trafficked from the golgi via CCVs budding from TGN. These clathrin coated pits invaginate and are pinched off by dynamin protein to form clathrin coated vesicles (Mukherjee et al. 1997). The non-clathrin proteins called adaptor proteins (AP) were found to be essential for CCV formation. It is speculated that AP binding induced membrane curvature and facilitates the attachment of clathrin to the invaginations (Mellman 1996; Mukherjee et al. 1997).

Besides, the APs also recruit membrane proteins that selectively localize to clathrin pits (Pearse 1988; Sorkin et al. 1995). So far four distinct AP complexes have been identified named AP1-4. In addition, AP-1 and AP-3 have cell specific isoforms AP-1B and AP-3B (Ohno 2006). The AP-1 complex is present on clathrin coated buds of the TGN and interacts with proteins that have to exit the golgi in the CCVs. AP-1A regulates the trafficking of mannose 6-phosphate receptor (MPRs) between TGN and endosomes (Ohno et al. 1995; Owen et al. 2004). AP-2 complex is localized to the plasma membrane coated pits and is involved in endocytosis of proteins (Collins et al. 2002; Owen and Luzio 2000). AP-2 also serves as cargo receptor for receptor mediated endocytosis of the transferrin receptor (TfnR) (Ohno 2006). The AP-3 A is believed to traffic cargo from an early endosomal compartment to late endosomes or multivesicular bodies (Nakatsu and Ohno 2003; Owen et al. 2004). AP4 is implicated in traffic of some lysosomal proteins from TGN to lysosomes (Aguilar et al. 2001). In the polarized epithelium cells AP-4 is involved in basolateral transport of the LDL receptor (Simmen et al. 2002).

Besides the clathrin mediated uptake, there are several clathrin independent endocytic pathways. One such route is via small, flask shaped membrane invaginations called caveolae. The molecular machinery that differentiates caveolar endocytosis from clathrin mediated endocytosis is unknown. However, this pathway is important for the entry of bacterial toxins such as cholera toxin B (Orlandi et al. 1998), viruses (Marjomaki et al. 2002) and bacteria as well as some growth factors and hormones (Lobie et al. 1999; Schubert et al. 2001), receptors such as the insulin receptor (Gustavsson et al. 1999) and glycosphingolipids (Singh et al. 2003).

Phagocytosis involves internalization of large particles by binding to cell surface receptors. It is found in leukocytes such as neutrophils and macrophages involved in the uptake of pathogenic microorganisms and antigenic particles. The phagocytic stimulus induces localized polymerization of actin and extension of pseudopod around the particle (Greenberg et al. 1990). The phagosomes fuse rapidly to the endosomes and lysosomes exposing their contents to the hydrolytic enzymes (Desjardins et al. 1994; Rabinowitz et al. 1992).

Cells such as macrophages, dendritic cells exhibit fluid phase endocytosis called macropinocytosis (Steinman and Swanson 1995). Macropinosomes are formed when the membrane folds fuse back into the plasma membrane thereby engulfing the extracellular fluid.

1.2. SNAREs the central component of membrane fusion machinery

Fusion of two lipid membranes in an aqueous medium such as the cytosol of the cell is an energetically unfavorable process due to the presence of repulsive electrostatic forces (Zimmerberg et al. 1993). It was suggested that ‘bridging’ proteins can act as scaffolds to bring the two membranes close together (Monck and Fernandez 1996). The search for such scaffolds led to the identification of a huge number of proteins forming ‘fusion machinery’ and SNARE proteins constitute the core of this machinery.

1.2.1. SNARE proteins: history, discovery and structure

History: Several years of biochemical research led to the discovery of SNARE proteins. The first breakthrough came with the observation that treatment with N-ethylmaleimide (NEM) abolishes the intercisternal transport of the VSV encoded G protein through the Golgi (Rothman et al. 1984). This abolishment was rescued by the addition of cytosol fractions (Block et al. 1988). Eventually, the factor responsible for the rescue was purified from the cytosol and termed NSF for NEM sensitive factor. NSF is a 76 kDa protein with the ability to hydrolyze ATP into ADP (Block et al. 1988).

Following this, three more members of the membrane fusion machinery were identified and termed SNAP for soluble NSF attachment proteins namely, α -SNAP, β -SNAP and γ -SNAP (Clary et al. 1990). Using NSF and SNAP as baits, three interacting proteins were isolated from crude bovine brain membrane fraction. These were termed SNAREs for SNAP-receptors (Sollner et al. 1993b).

Localization of these receptors revealed that all the three were associated with the synapse. VAMP1 (Trimble et al. 1988) also named synaptobrevin (Baumert et al. 1989) was located on the synaptic vesicles and SNAP25 (Oyler et al. 1989) and Syntaxin 1 were found on the pre-synaptic terminals of neurons (Sollner et al. 1993b). The synaptic SNARE complex

comprising of SNAP25 (Oyler et al. 1989), Syntaxin 1 (Bennett et al. 1992) and VAMP1/synaptobrevin is so far the best characterized complex and forms the exemplar for most of the current knowledge of the SNARE proteins (Jahn et al. 2003).

It was found that neurotoxic metalloendoproteases, botulinum toxin B (BoNT/B) and tetanus toxin (TeTx) inhibit exocytosis of synaptic vesicles by cleaving the neuronal SNAREs synaptobrevin (Link et al. 1992; Schiavo et al. 1992) and SNAP25 (Blasi et al. 1993) (Figure 1.2).

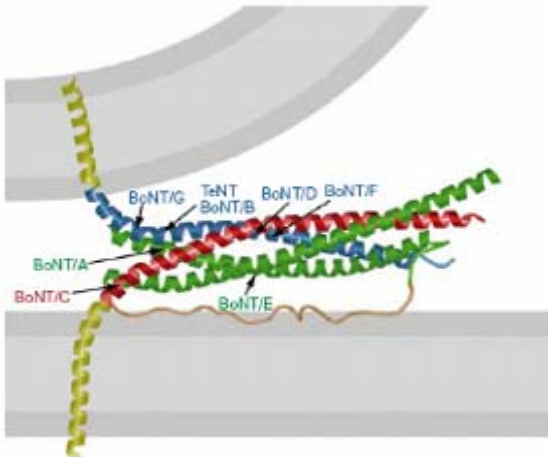


Figure 1.2. A scheme showing assembly of neuronal SNARE proteins to form a core complex: Botulinum and tetanus toxin cleave the SNARE proteins at several cleavage sites (adopted from Sutton et al. 1998).

Structure: All the members of the SNARE family have a characteristic ‘SNARE motif’ which is a stretch of about 60 amino acid residues, located close to the trans-membrane domain. This domain has a highly conserved heptad repeat pattern which forms α helical coil (Jahn et al. 2003; Weimbs et al. 1997). The a and d residues of the heptad are occupied by hydrophobic residues. Most of the SNAREs have a single C terminal trans-membrane domain close to the SNARE motif. While some SNAREs such as SNAP 25 and SNAP23 are attached to the membrane by post translational modification such as palmitoylation of the cystein residues in the spacer region between the two SNARE motifs (Chen et al. 2001; Jahn et al. 2003) (Figure 1.3).

The SNARE motifs are unstructured when the SNAREs are free in solution. However, when the proteins on opposing membranes interact, their SNARE motifs undergo spontaneous restructuring into a highly stable, elongated four helical coiled coil structure called the ‘core complex’ (Hanson et al. 1997; Lin et al. 2000).

Sutton and co-workers crystallized the first core complex of the synaptic SNARE complex comprising of syntaxin 1A, synaptobrevin-II and SNAP 25B at 2.4 Å resolution (Sutton et al. 1998). They observed a highly twisted and parallel bundle of four helices, two contributed by SNAP25 and one each by syntaxin 1 and synaptobrevin. The core bundle could be divided into 16 backbone layers numbered -7 to +8. Basic amino acid residues were found at the membrane proximal end of the core complex, which could interact with the negative charges on the surface of the membranes (Sutton et al. 1998). In addition, the ionic layer at the 0th position of the otherwise hydrophobic bundle comprised an Arginine residue contributed by VAMP and three Glutamine residues, two from SNAP 25 and one from syntaxin 1 (Sutton et al. 1998).

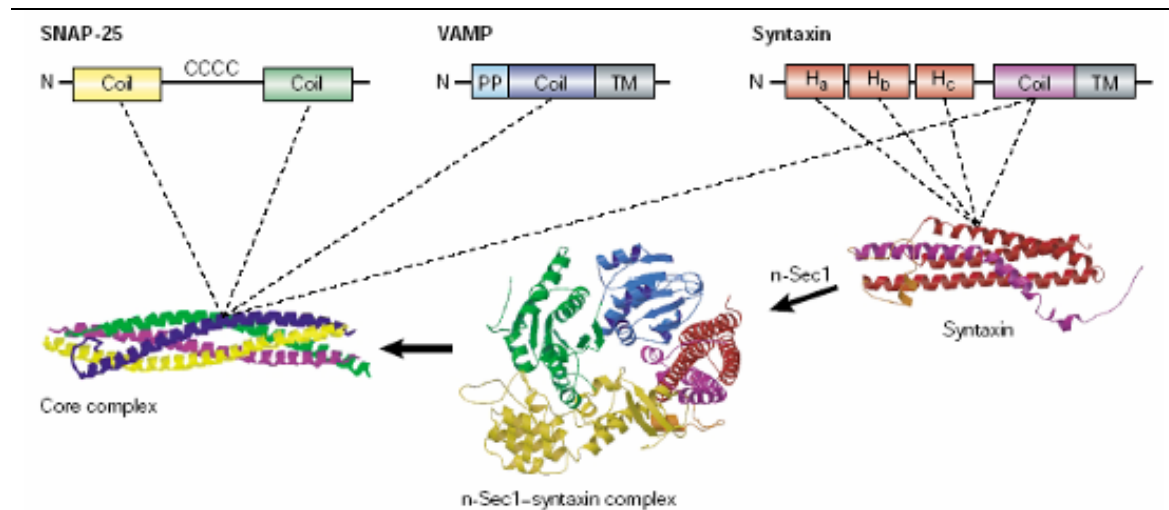


Figure 1.3. The structure of neuronal SNARE proteins: VAMP2 and syntaxin1 have a transmembrane domain that anchors them to the membrane. SNAP25 is associated to the membrane through a stretch of cysteine residues with attached palmitoylate moieties. VAMP and syntaxin have one SNARE motif each while SNAP25 has two coil domains. Syntaxin has an autonomously folding Habc domain at the N terminal. (adopted from Chen and Scheller 2001).

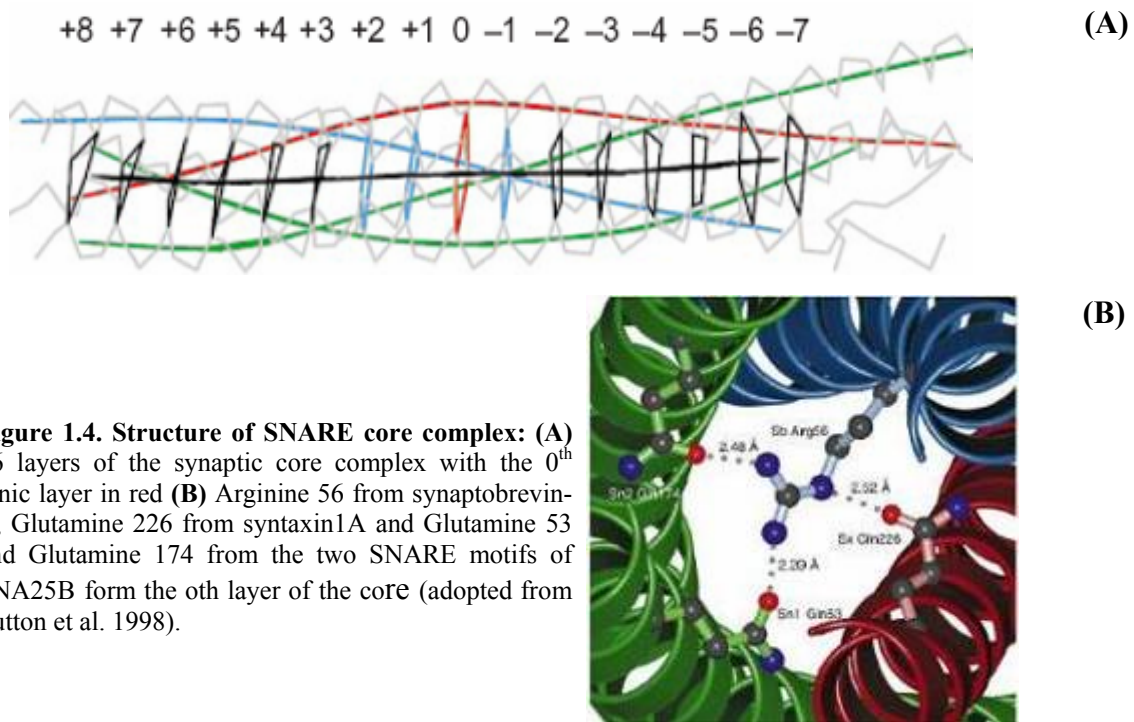
Structural analysis of the core of the late endosomal SNARE complex comprising of syntaxin 7, syntaxin 8, vti1b and VAMP8/endobrevin confirmed the same structure (Antonin et al. 2002). It is therefore thought that the structure of the core complex is evolutionarily conserved and critical to the function of SNARE proteins as members of the fusion machinery.

In addition to the SNARE motif, some of the SNARE proteins have an autonomously folding N terminal domain. These domains are thought to facilitate interaction between

SNAREs and other proteins involved in the fusion machinery. For example, syntaxin 1 has a three helix N-terminal Habc domain (Figure 1.3) that folds back and gives syntaxin a closed confirmation (Dulubova et al. 1999) and facilitate the binding of regulatory proteins such as Munc18 (Ref section. 1.2.3.5) (Hata et al. 1993).

1.2.2. SNARE proteins: Classification

The localization of the neuronal SNAREs syntaxin 1 and SNAP25 on the pre-synaptic membrane and VAMP1 on the synaptic vesicles suggested the existence of two distinct types of SNARE proteins. Based on their localization, SNAREs were classified as v-SNAREs, localized on the vesicles and t-SNAREs on the target membranes (Sollner et al. 1993b).



Subsequently, the involvement of SNARE proteins in many other membrane fusion events was discovered. The v/t classification was confusing for symmetric fusion events such as the homotypic fusion of yeast vacuoles or the fusion of late endosome and lysosome etc. Therefore the SNAREs had to be reclassified into a more comprehensible form. The presence of one Arginine (R) and three Glutamine (G) residues in the 0th ionic layer of the

core of the SNARE complex was a highly conserved feature of the core complexes (Sutton et al. 1998) (Figure 1.4 A and B). Hence it served as a basis to reclassify SNARE proteins into Q SNAREs and R SNAREs depending on the amino acid residue they contribute to the 0th layer of the core.

Further, the three Glutamine contributing SNAREs were sub classified into Qa, Qb and Qc. In reference to the neuronal SNARE complex, Qa SNAREs are located at the position of syntaxin1 of the neuronal complex and Qb and Qc occupy the position of N- and C-terminal motifs of the SNAP25 (Sutton et al. 1998).

So far, most of the known v-SNAREs can be placed in the R SNARE family while most of the t-SNAREs are placed under the Q-SNARE family. There are a few exceptions such as the yeast Bet1p which is a Q SNARE and contributes a serine. Leech synaptobrevin (R SNARE) contributes a lysine to the 0th layer (Sutton et al. 1998). However, the functional classification into v/t SNAREs and structural classification into R/Q SNAREs both are widely used.

1.2.3. Components of fusion machinery and their function

Although SNAREs are central to membrane fusion, they are by no means singularly sufficient. There is a coordinated interplay between several proteins that leads to membrane fusion. Some of these proteins and their functions are discussed in the following section.

1.2.3.1. Rab proteins: The rab cycle

Rab proteins are small GTPases that shuttle between a GDP bound soluble inactive and a GTP bound membrane associated active state. Currently, 10 classical and one atypical Rabs are known in yeast while more than 60 have been identified in the mammalian genome (Pereira-Liel et al. 2001). Rab proteins regulate the assembly of the SNARE complex and mediate membrane attachment by recruiting docking and tethering factors (Pfeffer 1999; Ungar et al. 2003). Additionally, Rabs are present on the specific intracellular localization and can act as the ‘location tags’ (Jahn et al. 2003). Most Rabs are present at the surface of the membranes in a GTP bound active form. As the membranes destined to fuse approach each other, the active rab-GTP forms complexes with docking and tethering factors, thereby bridging the two membranes. Finally, the GTP is cleaved into GDP by GTPase Activating

protein (GAP) and the inactivated Rab protein is removed from the membrane by GDP dissociation inhibitor protein (GDI) (Jahn et al. 2003; Pfeffer 2003). The rab cycle acts in conjunction with SNARE cycle (Ref section 1.2.3.3.) to facilitate membrane fusion.

1.2.3.2. Tethering and docking factors

The donor membrane first recognizes the correct acceptor membrane in a process termed docking or tethering. It is thought to confer specificity to the fusion events. Several tethering and docking proteins have been identified. One of the best studied tethering factor in mammalian cells is a peripheral Golgi membrane protein named p115 (Pfeffer 1999; Waters et al. 1992). The exocyst, a Sec6-Sec8 complex was identified as docking complex for exocytosis in *Saccharomyces cerevisiae* (Hsu et al. 1999; ter Bush et al. 1996), Rabaptin-5 interacts with Rab-5 and is implicated in docking during endocytosis (Stenmark et al. 1995) while EEA-1 is a docking factor during endosomal fusion (Simonsen et al. 1998).

1.2.3.3. The SNARE cycle:

Once the membranes are held together by the docking and tethering factors SNAREs can mediate the actual fusion event. SNARE motifs are unstructured in free SNARE proteins however when the opposing membranes carrying appropriate SNAREs approach each other, the motifs undergo restructuring into helical domains (Hanson et al. 1997). The SNAREs on the opposite membranes ‘zip up’ together from the distal N terminal to the membrane proximal C terminal forming the core complex (Figure 1.5). The orientation of the *trans*-SNARE complex pulls the two membranes close together. (Hanson et al. 1997). The force generated in the process overcomes the energy barrier for facilitating fusion (Hanson et al. 1997).

The irreversible assembly of SNARE core complex is dependent on Ca^{2+} . After the membranes fuse, all the SNAREs are present on one (acceptor) membrane in a so called *cis*-complex. This complex is dissociated by the chaperone ATPase NSF with SNAP as a co-factor thereby freeing the SNARE proteins for another round of membrane fusion (Jahn et al. 2003) (Figure 1.5).

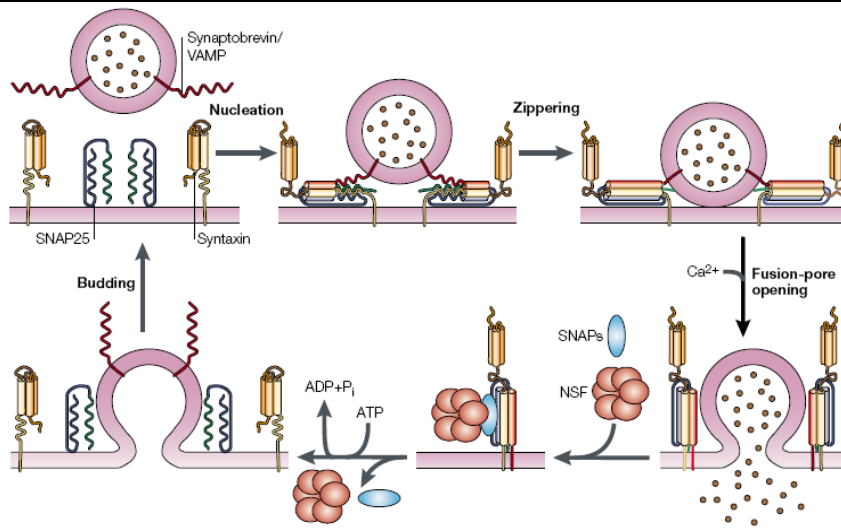


Figure 1.5. The SNARE cycle: showing the assembly of SNARE complex leading to fusion of membranes and eventual dissociation of the complex by ATPase NSF and SNAP (adopted from Rizo and Südhof 2002).

1.2.3.5. *Sec1/Munc18 family of proteins*

The activity of the SNARE proteins is tightly regulated in order to avoid any ‘accidental’ non specific membrane fusion. SM proteins or Sec1/Munc18 family of proteins are small 60-70 kDa hydrophilic proteins (Rizo and Südhof 2002) that act as regulators of SNARE proteins.

Unc18 was the first SM protein to be identified in genetic screen of *C. elegans* for uncoordinated movement (Brenner 1974). The mammalian homologue of Unc18 called Munc18-1 interacts with the Habc domain of syntaxin 1 (Hata et al. 1993). This binding is thought to stabilize the closed conformation of syntaxin 1 and inhibits fusion. The deletion of SM protein Munc18-1 leads to complete abolishment of synaptic vesicle release in the rat brain (Verhage et al. 2000). So far seven SM proteins have been identified in the human genome (Jahn et al. 2003) some of which bind to the SNARE complexes while others bind to the syntaxins. However their exact role has not yet been identified.

1.2.3.6. *Synaptotagmins*

The rapid release of the synaptic vesicles at the synapse was strictly coupled with calcium influx at the synapses. The search for calcium sensors led to Synaptotagmins. These are trans-membrane proteins containing tandem calcium – binding C2 domains (Brose et al. 1992; Yoshihara et al. 2003) and have been implicated in calcium sensing during the SNARE mediated membrane fusion. Synaptotagmin1 was shown to interact with syntaxin1

(Bennett et al. 1992) and the affinity of this interaction increased dramatically upon Ca^{2+} influx. This increase in affinity was proposed to be due to a Calcium induced conformational change in either syntaxin 1 alone or both in synaptotagmin and syntaxin 1 (Chapman et al. 1995). 13 members of synaptotagmin family have been identified (Sudhof 2004) however their physiological role is still under investigation.

1.2.4. Mammalian SNAREs and their complexes

Due to the inherent complexity of the mammalian system, it offers an enormous challenge to understand the fusion mechanism at molecular and functional level. Though several SNAREs have been identified in the mammalian cells, their physiological roles have not been confirmed. The problem is augmented since SNAREs are expressed at different levels in different tissues, some SNAREs show tissue specific expression and some interact with different partners to form different complexes in different tissues. In the following discussion, four mammalian SNARE families and their post Golgi proteins will be discussed in detail: Vesicle associated membrane proteins-VAMPs (R SNAREs), Vti1p homologues (Qb SNAREs), members of the syntaxin family (Qa / Qc SNAREs) and SNAP 25 family (Qb and Qc SNAREs).

1.2.4.1. VAMP Family with special emphasis on VAMP8/Endobrevin

Vesicle Associated Membrane Proteins (VAMPs) are classified as R SNAREs since they contribute an Arginine residue to the 0th layer of the core complex. Till date 7 mammalian VAMPs have been identified and are named VAMP 1-5, 7 and 8. VAMP 1-3 and 5 are toxin sensitive VAMPs while VAMP4, VAMP7 and VAMP8 (Endobrevin) are insensitive to tetanus toxin treatment.

VAMPs 1-5 and 7: The first member of the R-SNARE VAMP family to be known was a 120 amino acid long membrane protein, isolated from the synaptic vesicles of *Torpedo californica* (Trimble et al. 1988). Using cDNA clone of this VAMP, two related genes named VAMP1 and VAMP2 were identified in rat brain (Elferink et al. 1989). Eventually, VAMP1 was identified in bovine brain and was found completely identical to VAMP2 of the rat brain (Sudhof et al. 1989). VAMP1 and VAMP2 are called synaptobrevin 1 and 2

respectively and are highly expressed in neuron and endocrine cells. Synaptobrevins are involved in exocytosis of synaptic vesicles (Jahn and Sudhof 1994).

A non neuronal homologue of synaptobrevins was identified and named VAMP3/Cellubrevin. It was found ubiquitously expressed in all the cells and tissues (hence the name cellubrevin) (Mcmahon et al. 1993a). Several independent studies have been done to assign a physiological role to VAMP3. It has been localized on the membranes of pancreatic secretory vesicles and is implicated in regulating the Ca^{2+} mediated secretion of insulin (Regazzi et al. 1995). VAMP3 was also been localized to platelets and implicated in release of platelet granules (Polgar et al. 2002). In line with these reports, recently VAMP3 has been shown to possibly carry out exocytosis of platelet granules in the absence of the primary platelet v-SNARE VAMP8 (Ren et al. 2006).

VAMP4 was identified in EST database search and has a broad tissue expression profile. It was localized to the Golgi-TGN in the NRK cells (Advani et al. 1998) and tubular and vesicular membranes of the TGN in PC12 cells (Steehmaier et al. 1999a). VAMP4 was shown to function in the SNARE complex that mediates retrograde trafficking from early endosomes to TGN (Ref section 1.2.5) (Kreykenbohm et al. 2002).

VAMP5 was identified in EST database search. It was found to be increased during in vitro myogenesis in C2C12 cells and was preferentially expressed in muscles and heart. VAMP5 was found associated with plasma membrane and intracellular vesicular structures in myotubes (Zeng et al. 1998a).

VAMP7 also called toxin insensitive VAMP (TI-VAMP) was identified in EST database search (Advani et al. 1998). It was found to be abundant on the membranes of the *trans* Golgi network and the late endosomes (Advani et al. 1999) and mediates vesicular transport from the late endosome to the lysosomes (Ref section 1.2.5) (Advani et al. 1999; Ward et al. 2000). VAMP7 was shown to play a critical role in the onset of phagocytosis in macrophages (Braun et al. 2004) and vesicular transport in neurite outgrowth (Martinez-Arca et al. 2000).

VAMP8: VAMP8 also named endobrevin was first identified in EST database search (Wong et al. 1998). Vamp8 gene in mice comprises of four exons. The first exon is non-coding. The second codon contains the 5'UTR and the start codon that encodes the first

amino acid M1 (Methionine). Exon 3 encodes amino acid E2 (Glutamic acid) - T54 (Threonine) and exon 4 encodes S55 (Serine)-T101 (Threonine) and the 3'UTR. The SNARE motif of VAMP8 is encoded in part by exon 3 (aa 13-54) and exon 4 (aa 55-62). The cytoplasmic domain is predicted to be encoded by residues 1-75 (Wong et al. 1998). The mouse Vamp8 gene was found positioned on chromosome 2 while in humans on chromosome 2 (Sikorra et al. 2006).

VAMP8 is a 15kDa, integral membrane protein (Wong et al. 1998) The amino acid sequence of VAMP8 was found to be 32% identical to synaptobrevin/VAMP1, 33% identical to synaptobrevin/VAMP-2 and had 31% identity to VAMP3/cellubrevin. It does not contain the conserved toxin cleavage site and is therefore insensitive to tetanus toxin and botulinum toxin (Wong et al. 1998). By immunogold labeling VAMP8 was found enriched on early endosomes (Wong et al. 1998). Sub cellular fractionation revealed showed VAMP8 to be present in same fractions as asialoglycoprotein receptor corresponding to the early endosomes (hence the name endobrevin) (Wong et al. 1998). In line with these reports, using immunofluorescence staining, VAMP8 was localized abundantly at the membranes of early and late endosomes (Antonin et al. 2000b; Wong et al. 1998). Using two independent approaches, anti-VAMP8 antibody and recombinant VAMP8 protein for inhibiting SNARE assembly, VAMP8 was shown to mediate homotypic fusion of early and late endosomes in PC12 cells (Antonin et al. 2000c). Later, using content mixing assay it was shown that antibody against VAMP8 inhibits only the late endosomal fusion and not the early endosomal fusion. The same result was confirmed by microinjecting Fab fragments of VAMP8 as well as its complex partners syntaxin 8, syntaxin7 and Vti1b. The Fab fragments of each of VAMP8 and other three complex partners resulted in a profound delay in the trafficking of EGF to the lysosomes thereby confirming that VAMP8 is involved in late endosomal fusion (Antonin et al. 2000b).

Besides the late endosomal trafficking, several studies have shown VAMP8 to mediate regulated exocytosis events in several cell types. Using pancreatic acinar cells from VAMP8^{-/-} mice, VAMP8 was shown to be important for regulated exocytosis of zymogen granules in a complex with SNAP23 and syntaxin4 (Wang et al. 2004). VAMP8 was found on the human platelets and was suggested to mediate regulated secretion of platelet

granules (Polgar et al. 2002) and mast cells (Paumet et al. 2000b). In line with these suggestions, using platelets derived from VAMP8^{-/-} mice it was shown that VAMP8 is the primary R-SNAREs involved in the release from dense core granules, alpha granules, and lysosomes from the platelets (Ren et al. 2006). VAMP8 was also shown to be critical for the terminal step of cytokinesis in normal rat kidney (NRK) cells (Low et al. 2003).

1.2.4.2. Mammalian Syntaxins

Syntaxins fall into two distinct protein families depending on their position in the SNARE complex. The first type is the Qa syntaxins also called the ‘true syntaxins’ and occupy the position corresponding to syntaxin1 in the syntaptic SNARE complex. The second type is the Qc syntaxins that occupy the position corresponding to c terminal SNARE motif of SNAP25 in the synaptic complex.

Currently, the Qa syntaxin family has 12 genes in mammals and 7 genes in the yeasts. Syntaxin 1, 2, 3, 5 and 16 also exist in alternatively spliced isoforms (Teng et al. 2001) (Table I). The first syntaxins to be described were 35 kDa neuronal syntaxins 1A and 1B present on the synaptic vesicles bearing 84% identity (Bennett et al. 1992). Among the non neuronal homologs are syntaxin 2, 3, 4 and 5 (Bennett et al. 1993). Syntaxins 6, 8 and 10 are identified as Qc syntaxins. With the exception of syntaxin 11, all the other mammalian syntaxins have the membrane anchoring transmembrane domain (Teng et al. 2001). A summary of post Golgi mammalian syntaxins associated with endosomal pathway and their function is given in Table 1.

Syntaxin 2 was localized to midbody during cytokinesis and was found to be important in the terminal steps of cytokinesis in mammalian cells (Low et al. 2003).

Syntaxin 3 and syntaxin 4 localized to the apical and basolateral surface, respectively, of the polarized epithelial cells and were implicated in conferring specificity to membrane targeting (ter Beest et al. 2005). Syntaxin 4 in a complex with SNAP23 and Munc18c mediates the regulated exocytosis of tumor necrosis factor α during inflammation (Murray et al. 2005; Pagan et al. 2003). Syntaxin 3 and 4 are localized to plasma membrane and secretory granules of mast cells respectively.

Syntaxin 8 functions in late endosomal fusion. It was found to interact physically with cystic fibrosis transmembrane conductance regulator channel (CFTR) and regulate its channel activity (Bilan et al. 2004). Syntaxin 7 was shown to mediate late endosome-lysosome fusion *in vitro* (Mullock et al. 2000).

Table I. Mammalian Syntaxins, their localization and function

Syntaxin	Cellular localization	Tissue distribution	Function assigned
Syntaxin 1A	Presynaptic plasma membrane	Neuronal and secretory cells	Regulated neuronal exocytosis
Syntaxin 1B	Presynaptic plasma membrane	Neuronal and secretory cells	Regulated neuronal exocytosis
Syntaxin 2 (A,B,C and D)	Plasma membrane	Ubiquitous	Exocytosis
Syntaxin 3 (A,B,C and D)	Plasma membrane	Ubiquitous	Apical exocytosis
Syntaxin 4	Plasma membrane	Ubiquitous	Exocytosis, Glut4 translocation
Syntaxin 6 (Qc)	TGN	Ubiquitous	Transport between TGN and endosome, fusion of immature secretory granules
Syntaxin 7	Endosome	Ubiquitous	Late endosome homotypic fusion, late endosome lysosome fusion
Syntaxin 8 (Qc)	Endosome	Ubiquitous	Late endosome homotypic fusion, late endosome lysosome fusion
Syntaxin 11	TGN / late endosome	Ubiquitous	Membrane dynamics in immune system
Syntaxin 12/13	Endosome	Ubiquitous	Recycling of surface proteins, early endosome fusion
Syntaxin 16 (A,B and C)	Golgi/TGN	Ubiquitous	Early endosome-TGN transport

Syntaxin 11 is an atypical member since it lacks the transmembrane domain but has carboxy terminal cystein residues that facilitate attachment to membrane lipids. Syntaxin 11 was identified with maximum expression in lungs, heart and placenta. It is enriched in phagocytic cells of the immune system and is important in membrane fusion in the immune

system (Prekeris et al. 2000). Recent evidences suggest the role of SNARE Syntaxin 11 together with Rab27a and Munc13-4 in the regulated exocytosis of the lytic granules in the activated cytotoxic T lymphocytes (Hong 2005).

Syntaxin 13 had the highest expression in the brain (Advani et al. 1998) and was found to regulate neurite growth from the axons in complex with SNAP25 (Hirling et al. 2000).

1.2.4.3. Mammalian Vti1 homologs: Vti1a and Vti1b

In their efforts to identify the interacting partner for Vps10p, a sorting receptor for vacuolar proteases in yeast, Fischer von Mollard and colleagues identified v-SNARE Vti1p (Vps10p tail interacting protein). Vti1p is involved in four different SNARE complexes and mediates the following transport steps: Traffic from the *trans* Golgi network (TGN) to late endosomes, fusion with vacuole (vacuole in yeast is equivalent to lysosomes in mammalian cells), early endosomes to TGN and homotypic TGN fusion and retrograde traffic to *cis*-Golgi (von Mollard et al. 1997).

Using EST database searches, a 232 residue long, human homolog (hVti1) of the yeast Vti1p was found. The protein displayed 29% homology with the yeast Vti1p and could functionally replace it in Vti1p deficient yeast cells. Additionally, two mouse homologues mVti1a and mVti1b were found that exhibited 31% amino acid identity with each other (Lupashin et al. 1997; von Mollard et al. 1998). Due to their low identity, Vti1a and Vti1b were thought to take part in distinct fusion events. In line with this, antibody against Vti1a specifically blocked the fusion of early endosomes while anti Vti1b antibody blocked late endosomal fusion (Antonin et al. 2000b). Vti1a and Vti1b are Qb SNAREs occupying position corresponding to the N terminal SNARE motif of SNAP25 in the neuronal SNARE complex.

Vti1a also called Vti1-rp2 (Vti1p related protein 2) is a 29 kD integral membrane protein with 217 amino acid residues. Vti1a localizes to perinuclear structures (Kreykenbohm et al. 2002) and is particularly enriched in Golgi stacks and *trans*-Golgi network (Kreykenbohm et al. 2002; Xu et al. 1998). Additionally, a brain specific variant of Vti1a called Vti1a- β was identified which was enriched on the synaptic vesicles. Vti1a- β does not interact with synaptobrevin, syntaxin 1 and SNAP25 (Antonin et al. 2000d).

Vti1b also called Vti1-rp1 is 233 amino acid residues long. Vti1b was found on early endosomes, multivesicular bodies and tubules and vesicles not associated with *trans*-Golgi network or plasma membrane (Kreykenbohm et al. 2002).

1.2.4.4. Mammalian SNAP25 family members

SNAP25 a 25kD protein was the first member of the synaptosomal associated protein family (therefore the name SNAP25) to be identified from mouse hippocampus (Oyler et al. 1989). It contributes two SNARE motifs Qb and Qc to the neuronal exocytic SNARE complex (Sollner et al. 1993b). SNAP25 lacks a transmembrane domain but is attached to the membrane by palmitoylation of the cystein residues in the spacer region between the two SNARE motifs (Chen et al. 2001; Jahn et al. 2003). Recently, it has been assigned a second function as an endosomal Q-SNARE regulating the traffic between sorting endosome and recycling endosome (Aikawa et al. 2006). SNAP25 important for the regulated exocytosis of secretory vesicles in the neuroendocrine cells and for neurite outgrowth (Aikawa et al. 2006).

Using yeast two hybrid screening, SNAP23, a 23 kD homolog of the SNAP25 was identified from the human B lymphocytes. It has 211 amino acid residues and bears 59% identity with SNAP25 (Ravichandran et al. 1996). It is ubiquitously expressed and there is increasing evidence of it being involved in exocytosis. The relocation of SNAP23 was found to be important for exocytosis of mast cell granules (Guo et al. 1998) (Puri et al. 2003). SNAP23 was also shown to be involved regulated exocytosis of zymogen granules from pancreatic acinar cells (Holt et al. 2006).

SNAP29 was identified as a Syntaxin3 interacting protein. It bears 26% identity with SNAP25 and co-localizes with endosomal, lysosomal and Golgi markers. It does not have a cystein rich domain that anchors SNAP25 and SNAP23 to the membranes and is therefore implicated to participate in several trafficking events (Steggmaier et al. 1998).

Recently, a 47 kD Qab SNARE named SNAP47 was identified from purified rat brain synaptic vesicles. SNAP47, like SNAP29 does not have a cystein rich anchoring region and has a rather ubiquitous tissue expression profile. In *in-vitro* liposome fusion experiments

SNAP47 was shown to replace SNAP25 and interact with the neuronal SNAREs Syntaxin1 and synaptobrevin although less efficiently (Holt et al. 2006).

1.2.5. Mammalian SNARE complexes: emphasis on VAMP8 complexes

The first SNARE complex to be identified was the neuronal SNARE complex involved in the fusion of synaptic vesicles to the pre-synaptic plasma membrane. It comprises of synaptobrevin (R), syntaxin 1A (Qa) and SNAP25 (Qb and Qc) SNAREs (Sollner et al. 1993a). This complex is so far the best studied and is often used as a model for several SNARE related studies. In addition, five endosomal SNARE complexes have been described so far (Figure 1.6).

By co-immunoprecipitation experiments from rat liver homogenates, Antonin and co-workers identified the endosomal SNARE complex of VAMP8/endobrevin (R), syntaxin 7 (Qa), syntaxin 8 (Qc), Vti1b (Qb). Fab fragments of antibodies against each of the SNAREs and exogenous recombinant proteins were shown to inhibit homotypic late endosomal fusion in content mixing assay. Hence VAMP8 in a complex with syntaxin8, syntaxin 7 and Vti1b mediates the homotypic fusion of late endosomes (Antonin et al. 2000b).

Recently using co-immunoprecipitation VAMP8 (R) was shown to form a complex with syntaxin 4 (Qa) and SNAP23 (Qb and Qc) in the pancreatic acinar cells of mice. VAMP8 in this complex was implicated in mediating secretagogue stimulated exocytosis of zymogen granules (Holt et al. 2006) and exocytosis of secretory lysosomes (Polgar et al. 2002).

Additionally, VAMP8 was proposed to exist in a complex with syntaxin 4 and SNAP23 and possibly mediates the secretory exocytosis in mast cells (Paumet et al. 2000b).

VAMP7 forms a complex with syntaxin 7 in the alveolar macrophages and was implicated in the late endocytic fusion events (Ward et al. 2000). Eventually, a complex of VAMP7 (R), syntaxin 7 (Qa), syntaxin 8 (Qc) and Vti1b (Qb) was identified that mediates the heterotypic fusion between late endosomes and lysosomes (Pryor et al. 2004).

A complex between Vti1a- β (Qb), Syntaxin 6 (Qc), Syntaxin 16 (Qa) and VAMP4 (R) was identified in the synaptosomes from rat brain (Kreykenbohm et al. 2002). This complex was implicated in the retrograde trafficking from the early endosomes to the *trans*-Golgi (Mallard et al. 2002).

Recently a complex between syntaxin 13 (Qa), Vti1a (Qb), syntaxin 6(Qc) and VAMP4(R) has been characterized that mediates homotypic early endosomal fusion (Brandhorst et al. 2006).

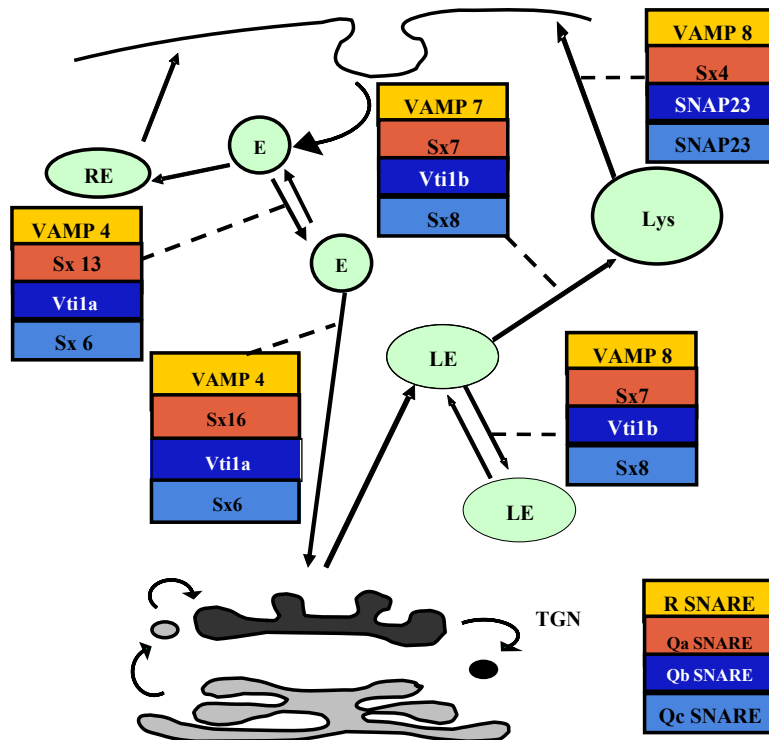


Figure 1.6. Mammalian endosomal SNARE complexes identified till date. Lys: lysosomes, RE: Recycling endosomes, E: early endosome, LE: Late endosome and TGN: *trans*-Golgi network

1.3. Thymus and its role in development of T-lymphocytes

1.3.1. Thymus: structure and function

Thymus is a primary lymphoid organ located in the upper anterior thorax just above the heart. It comprises of two lobes that are further divided into numerous lobules. The lobes are surrounded by a capsule and are structurally and functionally compartmentalized. The outer compartment is the cortex and the inner compartment is called medulla. The region close to the capsule is known as the sub capsular zone while the region between medulla and cortex is called the cortico-medullary junction (Figure 1.7). Both, the cortex and the medulla have a three dimensional stromal cell network made up of epithelial cells. The macrophages and dendritic cells are primarily present in the cortico-medullary junction and

the medulla. Developing T lymphocytes, macrophages and dendritic cells are embedded in the stromal matrix and physically interact with the epithelial cells.

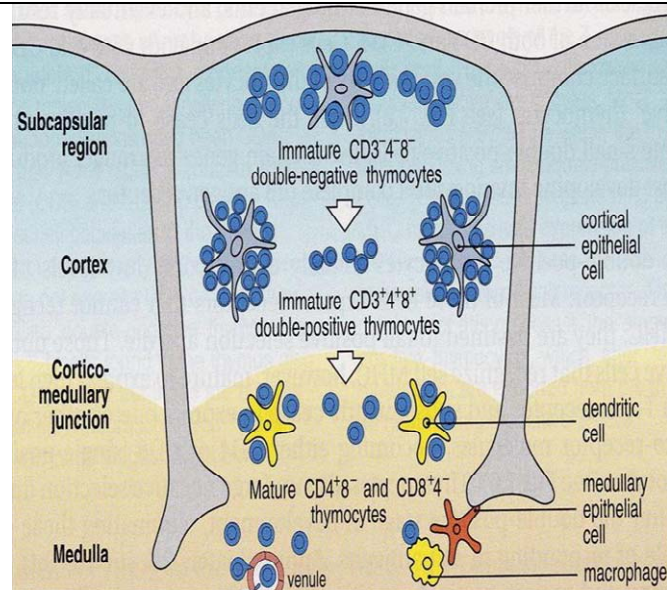


Figure 1.7. Structural organization of thymus. Differential localization of T-lymphocytes in the thymus during different stages of development. (adopted from Immunology by Janeway et al. 2001).

The T-lymphocytes arise from common lymphoid progenitor cells that in turn differentiate from the pluripotent hematopoietic stem cells in the bone marrow. The T-cell precursors migrate from the bone marrow into the subcapsular region of the thymus (Lind et al. 2001) and undergo several stages of development (therefore the name Thymus dependent or T lymphocytes). Consequently, the thymic cortex is thickly packed with immature T-lymphocytes. As the cells undergo selection and maturation, they move towards the medulla and finally exit into the systemic lymph circulation via lymphatic vesicles. Therefore, the medulla has a thin population of mature T-lymphocytes (Goldsby et al. 2000; Janeway et al. 2001b).

The role of thymus in the immune system was discovered with studies conducted on mouse models. The surgical removal of thymus in neonatal mice lead to immune deficiency with almost no circulating T-lymphocytes and reduced cell-mediated immunity (Miller and Osoba 1967). The importance of thymus is exemplified in a condition called DiGeorge's Syndrome. It is a congenital birth defect in humans and occurs due to developmental failure of the third and fourth pharyngeal pouches. It leads to an abnormal thymus besides other symptoms. Most of the affected infants die within the first two years of life, primarily due to infections in the absence of T-lymphocytes (Goldsby et al. 2000; Janeway et al. 2001b).

1.3.2. T-cell development

1.3.2.1. Developmental stages of T-lymphocytes

The development of T-lymphocytes and thymic stroma is mutually interdependent (Shores et al. 2005). On one hand, the stromal cells create the right microenvironment for the sequential stages of maturation of the T-lymphocytes (Anderson et al. 1996). On the other hand, the presence of T-lymphocytes is critical for the developing medullary and cortical epithelial cells (Hollander et al. 1995; Shores et al. 2005). Each developmental stage of the T lymphocytes is marked by the expression of distinct cell surface molecules and rearrangement of T-cell receptor genes. The markers that characterize the mature T-lymphocytes are the CD4 or CD8 antigens, and the T-cell receptor (TCR):CD3 complex.

The lymphoid progenitor cells are devoid of CD4, CD8 and most other markers present on mature T-lymphocytes, therefore they are called 'double negative' cells (CD4⁻CD8⁻). Additionally, their TCR genes are not rearranged and they do not express TCR on the cell surface.

The development of the cells through the double negative stage can be further divided depending upon the expression of surface adhesion molecules CD44, CD25 and c-Kit (receptor for the hematopoietic cytokine, stem cell factor). The T lymphocyte progenitors that arrive in the thymus do not bear the surface markers CD44 and CD25. In the first stage, also known as DN1 (double negative stage 1), the cells express CD44 but not CD25 (CD44⁺CD25⁻). In the second stage called DN2, the cells express CD44 and c-Kit and CD25 (CD44⁺CD25⁺). In the DN3 stage, the expression of CD25 is maintained while CD44 expression becomes low (CD44^{low}CD25⁺). Gradually, the expression of both CD44 and CD25 is lost at the fourth stage, DN4 (CD44⁻CD25⁻). At this point, the β chain of the TCR is rearranged and expressed to the surface of the cells.

The cells that express a correctly rearranged β chain are positively selected and lose the expression of CD25. The ones that fail to rearrange the β chain undergo programmed cell death.

The β chain is expressed at the surface together with a surrogate α chain called pre-T-cell α chain (pT α) to form pre-T cell receptor (pre-TCR). The pre-TCR is expressed together

with CD3 signaling complex that stimulates proliferation of the cells. CD3 complex comprises of five subunits namely gamma chain (γ), delta chain (δ), 2 epsilon chains (ϵ), and 2 zeta (ξ) chains that are physically associated with the TCR. (Janeway et al. 2001a).

The pre-TCR also stimulates the expression of the co-receptor molecules, CD4 and CD8 on the cell surface. At this stage the pre-TCR bearing cells are called double positives (DP) due to the presence of both CD4 and CD8 together on the surface (pre-TCR: CD4⁺CD8⁺). At this stage, the α chain of the TCR rearranges and is expressed together with the β chain to form the α : β TCR. Eventually, the big double positive T lymphocytes loose the expression of either CD4 or CD8 and become single positive (CD4⁺CD8⁻ or CD4⁻CD8⁺). The cells bearing α : β TCR: CD3 together with either CD4 or CD8 molecules are the mature T-lymphocytes (Janeway et al. 2001a). In addition, these cells also express several other surface molecules some of which are involved in signaling while others are involved in cell adhesion.

Besides the α : β TCR, there exists a minor population of T-lymphocytes bearing an alternative receptor. This TCR receptor is a heterodimer of γ and δ chains. Very less is known about the structure of the γ : δ TCR and function of this cell repertoire in the immune system (Goldsby et al. 2000; Janeway et al. 2001a).

1.3.2.2. Thymic selection of the T cells

The T-lymphocytes are subjected to selection at several stages of development. Thymic stroma plays a critical role in the positive and negative selection of the maturing T-lymphocytes. It provides the right microenvironment for interaction between the lymphocytes and the epithelial and antigen presenting cells (van Ewijk 1991). Only the cells that successfully cross each selection stage survive while the others are subjected to apoptosis. More than 95% of the cells generated in the immune system undergo cell death during maturation.

Positive selection: The first step of selection occurs soon after the expression of the β -chain and formation of pre-TCR (von Boehmer 1994). Positive selection by correctly rearranged TCR- β chain is essential for progression of the T cell development. The cells that successfully rearrange the β chain are selected for maturation. Additionally, further

rearrangement of the β chain loci is suppressed in these cells in a process called 'allelic exclusion'. The pre-TCR signals the accelerated rearrangement of the α chain of TCR. Only the cells that produce a functional α chain and express $\alpha:\beta$ TCR on the surface are allowed to survive, while the others are subjected to programmed cell death (von Boehmer 1994).

MHC restriction: In addition to the expression of a functional TCR it is important that the T-lymphocytes can distinguish between the 'self' and 'non-self' antigens. This occurs via a process called MHC (Major Histocompatibility Complex) restriction (Miller and Osoba 1967). The thymic stromal cells express MHC class I molecules and the antigen presenting cells of the thymus also express MHC II on their surface. The presentation of 'self' antigens by a MHC molecule serves as the basis of MHC restriction. The $\alpha:\beta$ TCR bearing $CD4^+CD8^+$ cells that recognize the 'self' antigens on the MHC molecule with low affinity are positively selected. These cells eventually become single positive mature T-lymphocytes while the others undergo apoptosis.

Additionally, positive selection is also thought to coordinate the selective expression of either CD4 or CD8 on the cell surface. During MHC restriction the cells are double positives, $CD4^+CD8^+$ while at the end of the selection, they lose the expression of either one of the markers. The cells that bear CD4 receptor recognize the peptides presented by MHC II molecules and become cytokine secreting T_H cells. While the cells with CD8 receptor recognize MHC I presented peptides and become cytotoxic T killer cells (T_C cells).

Negative selection: The process of negative selection essentially eliminates self reactive T-lymphocytes from the T cell repertoire. The cells that either recognize the self MHC molecule or the self antigen presented by the MHC molecule with very high affinity or do not recognize the MHC molecules are clonally deleted (Goldsby et al. 2000; Nossal 1994). The removal of such cells is very important since they can become autoreactive and cause autoimmune disorders. According to a suggested model, strong TCR activation triggers calcium dependent activation of protein kinase C (PKC). This in turn upregulates the expression of Bcl-2 interacting mediator of cell death (Bim) (Cante-Barrett et al. 2006). Bim was shown to play a central role in the negative selection of T-lymphocytes (Bouillet et al. 2001).

1.4. Background information and objective of the project

1.4.1. Creation and analysis of Vti1b knock out mice

(The creation and analysis of Vti1b deficient mice was done by Vadim Atlashkin. Zentrum Biochemie und Molekular Zellbiologie, Abteilung Biochemie II, Universität Göttingen).

Vti1b is a Qc SNARE that forms a complex with VAMP8, syntaxin 7 and syntaxin 8 and mediates the homotypic fusion of late endosomes. Previously in our laboratory, Vti1b knock out mice were created in order to study the physiological role of vti1b and its role in late endosomal trafficking. Exon 4 of the Vti1b gene encodes most of the SNARE motif. This exon was disrupted by targeted insertion of a neomycin resistance gene. The targeting construct was electroporated into the mouse embryonic stem cell line 129/SvJ and clone with homologous recombination were injected into blastocysts (Atlashkin et al. 2003). The chimeric mice so obtained were crossed with C57BL/6 female mice. Heterozygous mice were detected by PCR and crossed to get Vti1b homozygous null mice. Vti1b protein was completely absent in tissue extracts of knock out mice and the Vti1b heterozygous (+/-) mice had a reduced level of Vti1b protein (Atlashkin et al. 2003)

Level of syntaxin 8 was reduced in all the tested tissues of the Vti1b knock out mice. However, northern blot analysis showed comparable expression of syntaxin 8 mRNA in the wild type and the knockout mice. The low level of protein was found to be due to increased degradation of the protein in the lysosomes of the knock out mice (Atlashkin et al. 2003).

The mice showed heterogeneous phenotype with some of the mice being smaller than their littermates. Large amount PAS positive globules, containing glycogen, were found in the hepatocytes of the small vti1b knockouts. Some small mice showed enlargement of gall bladder and some mice, older than 15 months, showed liver cysts.

Pulse chase experiments using Cathepsin D showed that there was no delay or blockage in the transport from Golgi to lysosomes. However, there was a slight delay in the lysosomal degradation of asialofetuin endocytosed by receptor mediated endocytosis in hepatocytes of small Vti1b deficient mice (Atlashkin et al. 2003).

1.4.2. VAMP8 knock out mice

VAMP8^{-/-} mice were created by gene trapping by lexicon genetics, USA and were bought from Jackson Laboratory, USA. The SNARE motif of VAMP8 is encoded in part by exon 3 (aa 13 to 54) and in part by exon 4 (55 to 62) of the Vamp8 gene. Random insertional mutagenesis into intron between exon 3 and 4 was done using gene trap vector VICTR20 (Figure 1.8) (Zambrowicz et al. 1998).

The gene trap vector VICTR20 used consists of a splice acceptor site, followed by an internal ribosome entry site, a galactosidase/neomycin phosphotransferase fusion gene and a polyadenylation signal yielding a first mRNA. The second part of VICTR20 contains a phosphoglycerate kinase-1 promoter, a puromycin N-acetyltransferase gene and a splice acceptor sequence generating a second mRNA, which was used to determine the point of insertion (Figure 1.8). This means that both mRNAs transcribed from the mutant locus encode only partial and non functional SNARE motif.

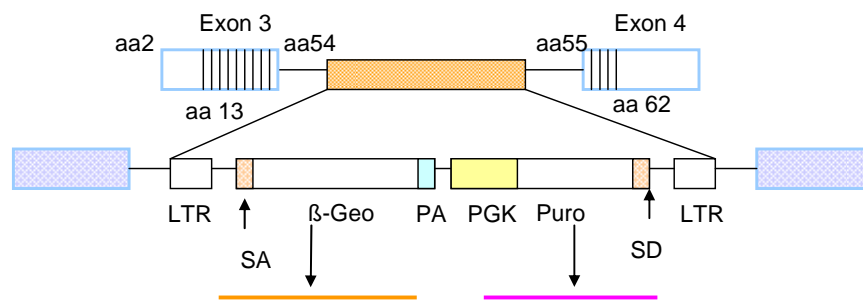


Figure 1.8. A scheme showing vector design for 3' trapping of the VAMP8 gene: SA, Splice Acceptor, fused to reporter gene β -Geo, β -galactosidase/neomycin phosphotransferase fusion gene; PA, Poly Adenylation sequence; PGK Phosphoglycerate Kinase-1 promoter; Puro, Puromycin N-acetyltransferase gene; SD, Splice Donor site.

In order to create double knockout mice for Vti1b and VAMP8, various crosses were made between VAMP8^{-/+} Vti1b^{-/-} or Vti1b^{-/+} VAMP8^{-/-} mice.

1.4.3. Initial findings

(By Dr. Ralf Dressel, Department for Immunogenetics, Georg-August Universität Göttingen and Dr. Fayyazi, the Department of Pathology, Georg-August Universität Göttingen.)

VAMP8^{-/-} Vti1b^{-/-} mice were generated and analyzed with an aim to study the effect of deleting two SNAREs of the same complex on endosomal trafficking. These mice showed a

phenotypic onset in the early post natal life. 66% of the VAMP8^{-/-} Vti1b^{-/-} mice became sick and died before reaching one month of age. Several organs from a VAMP8^{-/-} Vti1b^{-/-} small and sick 16 day old mouse were excised examined by histochemistry. Liver, kidney, spleen, intestine and brain from this mouse showed no defects. However there was a major defect in the morphology of the thymus (Figure 1.9). The thymus from the age matched control showed two clearly distinguishable areas: the medulla and the cortex (Figure A, B, C). In the thymus from VAMP8^{-/-} Vti1b^{-/-} mouse however, the cortico medullary boundary was completely disrupted with medullary cells scattered within the cortex (Figure D, E, F).

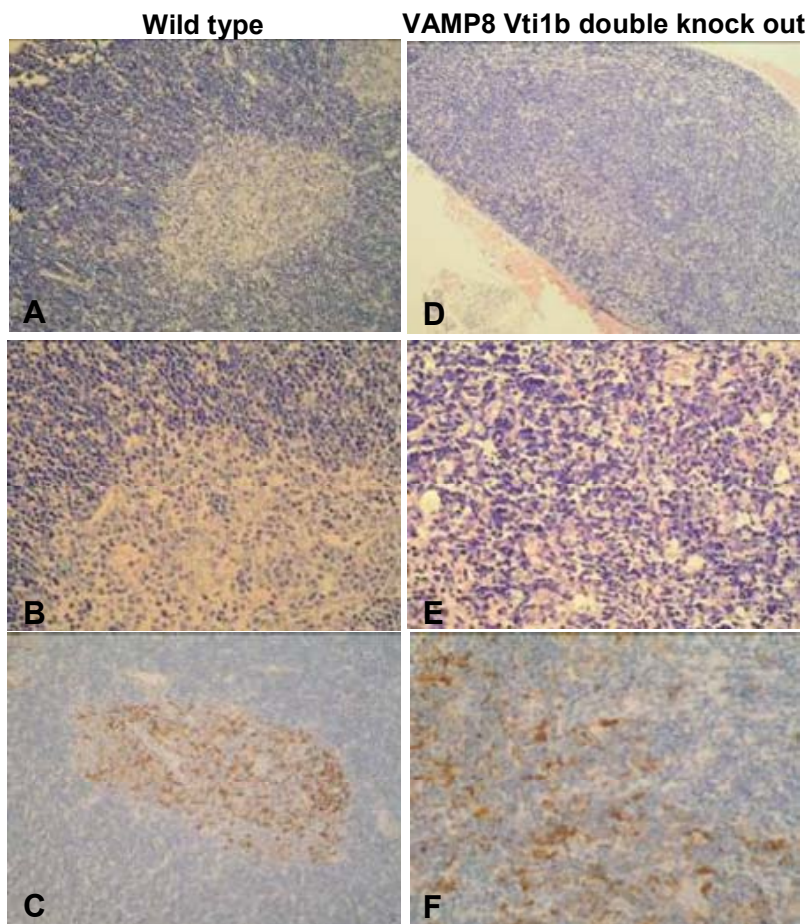
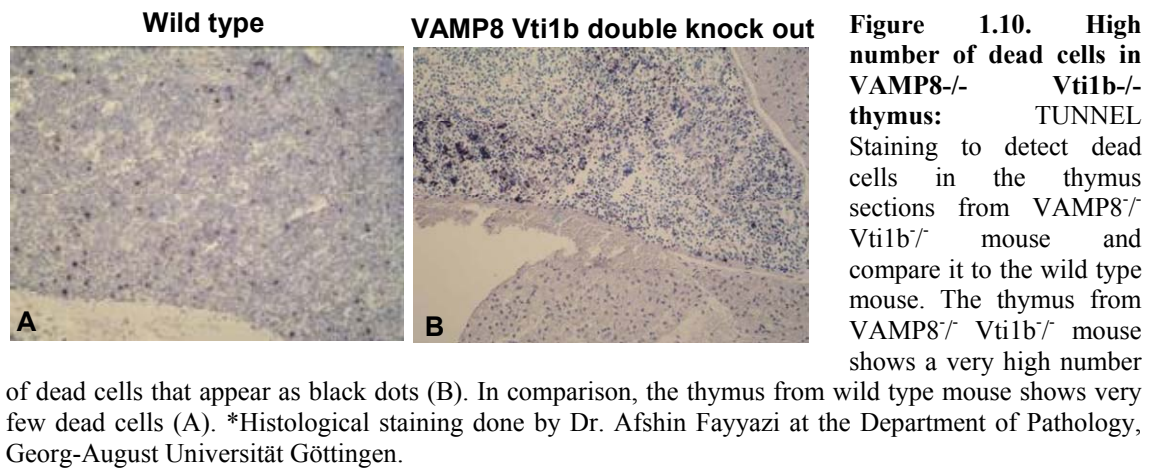


Figure 1.9. Morphological Defect in thymus from VAMP8^{-/-} Vti1b^{-/-} mice: Histological staining of thymus sections from a VAMP8^{-/-} Vti1b^{-/-} small and sick mouse shows a gross defect in the thymus morphology compared to the wild type control. The thymus from the wild type mouse showed distinct areas: the lightly stained medulla and a darkly stained cortex (A) with a distinct boundary between the two areas (B). This demarcation was also seen in the fascein staining that specifically stains the dendritic cells (brown) present in the medulla (C). In the VAMP8^{-/-} Vti1b^{-/-} small and sick mouse there was no boundary between the cortex and medulla (D) and light pink stained medullary cells appear scattered between the purple stained cortex cells (E). This disruption was also observed in fascein stained sections. The medullary dendritic cells (brown) appear scattered

between the cortex (blue) cells (F). (*Histological staining done by Dr. Afshin Fayyazi at the Department of Pathology, Georg-August Universität Göttingen.

In addition, the thymus of this small and sick VAMP8^{-/-} Vti1b^{-/-} mouse also showed a very high apoptosis compared to the wild type control (Figure 1.10).



To study if the disruption in thymus morphology effects the maturation of the T lymphocyte, thymocytes from VAMP8^{-/-} Vti1b^{-/-} mice were stained with antibodies against CD4 and CD 8 surface antigens. The cells were analyzed by FACS analysis. Out of three independent experiments, two experiments showed a high count for CD4⁻CD8⁻ cells while the third experiment did not show this defect. Additionally it was noticed that the two mice that showed a difference in the CD4⁻CD8⁻ cells also were much lighter than the mouse used in the third experiment.

1.4.4. Initial findings

(Masters Thesis submitted by Namita Kanwar to the Faculty of Biology at Georg August Universität Göttingen)

In the initial work, live births and deaths of VAMP8^{-/-} Vti1b^{-/-} and VAMP8^{-/-} Vti1b^{+/-} mice were recorded. It was observed that VAMP8^{-/-} Vti1b^{-/-} and VAMP8^{-/-} Vti1b^{+/-} pups had high early post-natal mortality. First postnatal month resulted in the loss of nearly 67% of VAMP8^{-/-} Vti1b^{-/-} and 59% of VAMP8^{-/-} Vti1b^{+/-} mice. All the mice were born in normal Mendelian ratios and were normal at birth. However a large population of these mice started to loose weight between 12-29 days of age and after 2-3 days of constant weight loss, eventually died. At the time of death, these mice were very small (weighed 35-50% of the littermates) and looked very sick. The surviving mice were fertile but lighter than their littermates.

In this study, three ~one month old sick VAMP8^{-/-} Vti1b^{-/-} mice were analyzed just before death and compared to VAMP8^{+/-} Vti1b^{+/-} controls. The thymus from these sick mice showed a disruption in morphology as seen before and described in section 1.5.3. There was no cortico-medullary boundary in the thymii of these mice and the medullary region was reduced to remnants. The thymus from these sick VAMP8^{-/-} Vti1b^{-/-} mice were smaller in size and the cell count was reduced by around 10 folds compared to VAMP8^{+/-} Vti1b^{+/-} controls. FACS analysis showed a disturbance in the developing thymocyte subsets. There was upto 3 folds increase in the percentage of CD4⁺ cells while CD4⁺CD8⁺ cells were reduced by 2 folds the thymus from sick VAMP8^{-/-} Vti1b^{-/-} mice. However, unlike the findings of the first experiment by Dr. Dressel, there was no increase in the CD4⁻CD8⁻ cells. The analysis of DN1-4 subsets showed a decrease in CD44⁺CD25⁻ (DN1) and CD44⁻CD25⁺ (DN3) cells in VAMP8^{+/-} Vti1b^{+/-} mice. In addition, these thymii also showed increased annexinV positive cells.

The development of thymocytes was also analyzed in four 2 months adult VAMP8^{-/-} Vti1b^{-/-} mice. However, there was no difference in the developing DN1-4 subsets as well as the more mature CD4/CD8 subsets in the thymii from the adult VAMP8^{-/-} Vti1b^{-/-} mice.

In addition, three experiments were done to analyze the peripheral repertoire of T and B lymphocytes from adult VAMP8^{-/-} Vti1b^{-/-} mice. There was no defect in the populations of mature CD4⁺ and CD8⁺ T lymphocytes and B lymphocytes in the VAMP8^{-/-} Vti1b^{-/-} mice compared to VAMP8^{+/-} Vti1b^{+/-} controls.

The activity of several lysosomal enzymes was checked in the liver and kidney of adult VAMP8^{-/-} Vti1b^{-/-} mice. There was no difference in the activities of β -hexosaminidase, β -galactosidase, β -mannosidase and β -glucuronidase enzymes in either the liver or the kidney of VAMP8^{-/-} Vti1b^{-/-} mice compared to the VAMP8^{+/-} Vti1b^{+/-} controls.

1.4.5. Objective of the study

The main objective of this study was to understand the physiological role of the late endosomal SNARE protein VAMP8/endobrevin. The first experiments already gave an indication that VAMP8^{-/-} Vti1b^{-/-} mice had a developmental defect in the thymus and T lymphocyte maturation. However, there were some discrepancies and a high standard error

in the data obtained from different experiments. This study was focused on understanding the underlying mechanism that causes a defect in the thymus in the absence of VAMP8. The first aim of this study was to ascertain the defect in the thymus morphology and to study which populations of T lymphocytes are affected due to the loss of VAMP8^{-/-} and Vti1b^{-/-} in the VAMP8^{-/-}Vti1b^{-/-} mice. Several experiments were done on VAMP8^{-/-} Vti1b^{-/-} thymocytes adult and sick mice to get statistically significant data and establish that the defect is actually due to the knock out and not just by mere chance.

The second aim was to know whether the thymus defect is a consequence of the simultaneous loss of both VAMP8 and Vti1b or is primarily caused by the loss of either one of the two SNAREs. Thymus and thymocyte development in the VAMP8^{-/-} Vti1b^{+/+} and Vti1b^{-/-} VAMP8^{+/+} mice were studied in detail and compared to the data from VAMP8^{-/-} /Vti1b^{-/-} mice.

The initial experiments showed an increased cell death in the thymus of VAMP8^{-/-}Vti1b^{-/-} mice. Therefore the third aim of this study was to understand the reason for the increased death and the massive reduction in the thymus of the VAMP8^{-/-}Vti1b^{-/-} mice. Thymus and thymocytes from VAMP8 and Vti1b single knock out mice were also analyzed for cell death and the sensitivity to apoptotic stimuli.

Additionally, it is known that ablation of some SNAREs such as Vti1b specifically destabilize other SNARE partners example syntaxin 8 and subject them to increased degradation. We wanted to study if the ablation of VAMP8 effects the expression or stability of other SNARE proteins especially in the thymus.

Since VAMP8 is implicated in late endosomal homotypic fusion as well as in the regulated exocytosis of secretory granules in the acinar cells, mast cells and platelets. It was interesting to know whether deleting VAMP8 and Vti1b causes any defect in endosomal vesicular trafficking. Endocytosis, endosomal trafficking and phagocytosis were studied in cells derived from VAMP8^{-/-} Vti1b^{-/-}, VAMP8^{-/-} and Vti1b^{-/-} mice.

2. Materials and Methods

2.1 DNA Techniques

2.1.1. DNA extraction from mouse tail biopsy

To 0.5 cm long freshly excised tail tips, 500 μ l NET buffer, 50 μ l 10% SDS and 50 μ l of 10 mg/ml of Proteinase K were added with vigorous mixing after each addition. Tissue was digested by incubating at 56°C overnight with constant shaking at 800 rpm (Thermomixer, Eppendorf). The samples were centrifuged at 13,000 rpm for 10 minutes to pellet down the hair and other insoluble debris and the supernatant was transferred to fresh tubes. DNA was precipitated with 500 μ l Isopropanol and isolated either by fishing out with a molded pasteur pipette hook or by centrifuging the sample at 13,000 rpm for 5 minutes at room temperature. The DNA pellet was washed two times with 70% ethanol, air dried and finally resuspended in 100 μ l of 10mM Tris-HCL pH 8.5. The DNA sample was stored at 4°C and further used for PCR amplification to determine the genotype of the mice.

NET Buffer

NaCl	100mM
Tris/HCl	10mM
EDTA	25mM

2.1.2. PCR amplification of genomic DNA to determine genotype

In order to determine the genotype, DNA from mouse tail biopsy was subjected to PCR amplification. Approximately 400 ng of DNA sample was mixed with PCR mix (Ref. Table II) to a final volume of 20 μ l. Amplification was carried out by placing the tubes in thermocycler, master cycler – gradient or personal Eppendorf. VAMP8H and VAMP8M were used as the forward and reverse primers for amplification of intact gene *Vamp8* and PuroF and PuroR primers for amplification of the β -geo cassette. While for *vt11b*, we used primer set Seq5 and Seq 50 for determining the wild type gene fragment and Seq5 and

AK30 for amplification of the *neo^f* disrupted gene fragment (for primer sequences ref. Table III).

Table II. PCR mix composition and conditions for PCR amplification

PCR Mix Components	Volume/Sample
dd H ₂ O	15.5 µl
10X PCR reaction buffer	2.0 µl
dNTP mix	0.4 µl
Forward primer	0.5 µl
Reverse primer	0.5 µl
Taq polymerase	0.1 µl

* for amplification of the *Puro^f* disrupted fragment, 14.5µl of dd H₂O and 1µl of DMSO was added to the mix.

Conditions for VAMP8 wild type PCR	
Temperature	Time
95°C	40 seconds
61.4°C	30 seconds
72°C	30 seconds
35 cycles	

Conditions for VAMP8 puro PCR	
Temperature	Time
95°C	40 seconds
52°C	40 seconds
72°C	50 seconds
30 cycles	

Conditions for <i>vt1b</i> wild type and <i>vt1b neo^f</i> PCR	
Temperature	Time
95°C	40 seconds
52°C	40 seconds
72°C	50 seconds
30 cycles	

All the primers were bought from Iba GmbH, Göttingen and dissolved 1:20 with VS water. The primers were stored at -20°C.

Table III. Primers used for genotyping

Primer	PCR	Sequence
VAMP8 H	VAMP8 wild type	CCGAAACAAGACAGAGGACTTG
VAMP8 M	VAMP8 wild type	CGTTAGGAATGGAGCAGTTGAC

Puro F	VAMP8 puro	CCGAGTACAAGCCCACGGTG
Puro R	VAMP8 puro	CGCTGCCCAGACCCTTGCCC
Seq 5	Vti1b wild type, neo	CTCTTCTATGATTTCTGTACC
Seq 50	Vti1b wild type	GAGGGATCCAATACCTTCTC
AK 30	Vti1b neo	CGGATCAAGCGTATGCAGCCG

2.1.3. Agarose gel electrophoresis for DNA separation

Depending upon the size of the DNA fragment to be amplified, 1% or 2% agarose gels were used. The required amount of agarose was weighed out and dissolved in 1xTAE buffer by boiling and stored at 60°C incubator. The gels were casted by pouring the agarose solution in the casting chamber with comb and allowing it to solidify. 6x DNA loading buffer was added to the PCR amplified products to an end concentration of 1x and the samples and DNA marker were loaded in the wells. The gels were run in 1x TAE buffer at 90-95 volts (3-4V/cm²).

In case of Vamp8 wild type PCR, the amplified products were run on gel containing ethidium bromide while for the puro PCR products, the gels were kept in ethidium bromide chamber for 10 minutes and the bands were visualized under UV.

50 ml of 6X Sample buffer

0,15% xylene cyanol FF	75 mg
40% (w/v) Sucrose	20 g
Make up volume to 50ml with 1x TAE buffer	

2.1.4. Determination of DNA concentration

The DNA samples were diluted 1:10 in VS water and the DNA concentration was spectrometrically measured in a Quartz cuvette at 260 nm against VS water as blank in Gene QuantII (DNA / RNA calculator from Pharmacia Biotech).

2.2. Protein Techniques

2.2.1. Tissue homogenate preparation

Freshly cut organs were placed in cold pre-weighed tubes on ice. For every 100 mg of tissue 900 μ l of 1x TBS was added. The tissues were then homogenized in Ultra-Turrax homogenizer. Around half of this 10% homogenate was aliquoted into eppendorf tubes. The remaining half was further divided. 1:10 and 1:100 dilutions were made with 0.05% (w/v) TritonX-100 and the remaining homogenate was supplemented with 1% Triton X-100 and 1X protease inhibitors. All samples were aliquoted and stored at -20°C .

50 μ l of 100x protease inhibitor cocktail

PMSF (17.4mg/ml in ethanol stock)	25 μ l
Leupeptin (10mg/ml in water stock)	0.5 μ l
Pepstatin (1mg/ml in methanol stock)	5.0 μ l
Methanol	19.5 μ l

2.2.2. Determination of protein concentration

0.1mg/ml BSA was used to get a standard curve. 1, 2, 5, 10 and 20 μ g of BSA solution was pipetted into eppendorf tubes and made up to a volume of 200 μ l with water. Similarly, 2 and 5 μ l of homogenates were made up to a volume of 200 μ l with water. Bradford reagent $\text{\textcircled{R}}$ BIORAD stock solution was diluted 1:4 (200 μ l in 600 μ l VS water). 800 μ l of 1X reagent was added to each tube and samples incubated at room temperature for 20 minutes. Absorbance was measured at 595nm wavelength. A standard curve was plotted from the values of the BSA standards and the protein concentration of samples was determined by extrapolation from the standard curve.

2.2.3. Measurement of lysosomal enzyme activities in tissue homogenates

Three 2ml tubes per sample were prepared. In two tubes, appropriate amount of 10% homogenate (enzyme source) was pipetted and the volume was made up to 10 μ l (Ref. Table IV). 50 μ l of substrate (Ref. table V) was then added to the two sample tubes. The third tube was used as a control, it contained only the homogenate (same volume as test tubes) and substrate buffer to a total volume of 60 μ l without any substrate. The samples were incubated in 37°C water bath for the appropriate amount of time (Ref. table IV). After

incubation, the enzymatic reaction was terminated with addition of 2 ml of Stop solution (0.2 M glycine /NaOH pH 10.8). The readings were taken at extinction 365nm and emission 410 nm (Koster et al. 1993).

Substrate buffer	
Sodium citrate	0.1M, pH 4.6
Sodium Azide	0.08 %
BSA	0.4 % (w/v)

Table IV: Scheme of sample preparation for assaying the lysosomal enzyme activities

Enzyme	Treatment
β -Hexosaminidase	5 μ l of 1:100 diluted homogenate, 30mins at 37°C
β -Galactosidase	10 μ l of 1:100 diluted homogenate, 120mins at 37°C
β -Mannosidase	10 μ l of 1:100 diluted homogenate, 120mins at 37°C

Table V: lysosomal enzymes and their substrates

Lysosomal Enzyme	Substrate
β -Hexosaminidase (β -Hex)	1mM 4-Methyl-Umbelliferyl-2Acetamido-deoxy- β -D-glucopyranosid
β -Galactosidase (β -Gal)	1mM 4-Methyl-Umbelliferyl- β -D-galactopyranosid
β -Glucuronidase(β -Glu)	1mM 4-Methyl-Umbelliferyl- β -D-glucopyranosid
β -Mannosidase(β -Mann)	1mM 4-Methyl-Umbelliferyl- β -D-mannopyranosid

2.2.4. Triton X-114 extraction of proteins

Protein concentration of the homogenate samples was determined (Ref. 2.2.2). Sample volume equal to 400 μ g of protein was transferred to fresh tubes. 1X PBS was added to make up the final volume to 720 μ l (end protein concentration of 0.5mg/ml). 80 μ l of 10% TritonX-114 was added and the samples incubated at 4°C for 15 minutes. The samples were then centrifuged at 4°C for 5 minutes at 13,000rpm. Supernatant was transferred to fresh tubes and incubated at 30°C with shaking. 500-800 μ l Saccharose solution was pipetted in fresh 2 ml tubes and the supernatant was carefully layered on top of the saccharose bed. The samples were centrifuged for 5 minutes at 13,000rpm at room temperature. The upper hydrophilic protein layer and the saccharose bed were removed. The drop of detergent containing the hydrophobic proteins was resuspended in 800 μ l of ice cold 1X PBS.

The detergent was removed from the sample by acetone treatment: The 800 μ l of protein sample was transferred to glass centrifugation (® Corex tubes) tubes. 8 times the volume of

acetone was added and samples incubated for 2 hours (or overnight) at -20°C . Later centrifugation was done for 10 minutes at 10,000rpm and the supernatant was removed. The pellet was washed with 80% acetone and dried. The dry pellet was resuspended in 70 μl of 1X stop buffer with β -mercaptoethanol (Bordier 1981).

Saccharose solution

Saccharose	6 %
Triton X 114	0.6 %

2.2.5. Preparation of protein samples for SDS page separation

Protein concentration of the samples of interest was determined using Bradford assay (Ref. 2.2.2) and the amount of proteins to be separated was calculated (between 30-60 μg). The samples were mixed with 3x sample loading buffer containing bromophenol blue to a final concentration of 1X. The samples were boiled at 95°C for 5 minutes and then loaded on the wells of SDS gels.

3x Sample buffer

1 M Tris/HCl pH 6.8	18.8 ml
Sucrose	15 g
Bromophenol blue	5 mg
SDS	4.5 g
Dissolve in 45 ml of VS water, add 1:10 β -mercaptoethanol before use	

2.2.6. SDS polyacrylamide gel separation of proteins

Gel assembly was prepared by aligning two glass plates with spacers in between them. The sides of the plates were sealed off with 1% agarose. Freshly prepared separating gel was poured between the two plates (Ref. Table VI). The gel was layered with 1ml of water and allowed to set for around 30 minutes at room temperature. Later water was removed and stacking gel solution was poured (Ref. Table VII) and the comb was fitted in between the plates. The gel was left undisturbed till the stacking gel was set. Later the wells were washed with water. Samples were prepared (Ref. 2.2.5) loaded in the wells on the gel. The gel was run at 30 mA for around 2-3 hours in 1X SDS PAGE running buffer.

10 x running buffer (Dissolve in 1 liter of VS water)

Tris	30.2 g
Glycine	144 g
SDS	10 g

Ammonium Peroxidisulfate (APS) solution

10% w/v APS in VS water

Table VI: Composition of resolving SDS gel

Resolving gel			
Components	15ml of 11%	15ml of 12.5%	15ml of 15 %
1.5 M Tris/HCl pH 8.8	3.75ml	3.75ml	3,75ml
Bis acrylamide	5.5ml	6.25ml	7,5ml
ddH ₂ O	5.45ml	4,65ml	3,4ml
10% SDS	150µl	150µl	150µl
10% APS	150µl	150µl	150µl
TEMED	7.5µl	7.5µl	7,5µl

Table VII: Composition of stacking SDS gel

Stacking gel	
Components	7.5 ml of 5.5 %
1.5 M Tris/HCl pH 8.8	936µl
Bis acrylamide	1.39ml
ddH ₂ O	4.95ml
10% SDS	75µl
10% APS	150µl
TEMED	7.5µl

2.2.7. Semi dry protein transfer

Nitrocellulose membrane was cut to the required size and soaked in 1X semidry buffer for 2-3 minutes.

10x Semi dry buffer

Tris	58 g
Glycine	29.2 g
10% SDS	37 ml

Make up volume to 1 liter with VS water

1x buffer: 80ml 10x buffer in 200 ml methanol and 720ml VS water

Six pieces Whattman paper, cut to size, were also soaked in 1X semidry buffer for around 5 minutes. The gel was carefully removed from between the gel assembly and soaked in 1X semidry for 1-2 minutes. The western blot transfer assembly was then made by placing 3 pieces of wet Whattman paper followed by the membrane, then the gel and finally the

remaining 3 pieces of paper were placed over it. Any air bubbles were removed by gently rolling a roller over the paper stack. The assembly was closed and transfer was allowed to occur at 116 mAmps for 1 hour. After transfer, the blot was transferred to a chamber for antibody staining.

2.2.8. Western blotting

The membrane was blocked with botto solution for 30 minutes at room temperature with slight rocking. Appropriate primary antibody dilution was made in blotto (Ref Table XII). The membrane was incubated in primary antibody solution for 2 hrs at room temperature or at 4°C overnight, depending upon the antibody used. Washing was done with 1X PBS+1%Tween three times for 5 minutes each. HRP-labeled secondary antibody was dilution in 1X PBS+1%Tween (1:10,000-1:20,000). Membranes were incubated with the secondary antibody solution for around 1hour 30 minutes with gentle rocking. The membranes were then washed 5 times with 1X PBS+1% Tween and 2 times with 1X PBS for 5 minutes each. The blot was developed using ECL Super Signal kit from PIERCE. The chemiluminescence substrates were mixed in equal amounts just before use. The membrane was incubated in this solution for 1-2 minutes and exposed to luminescence image analyzer for varying lengths of time depending upon the intensity of the signal.

2% Blotto solution

Dissolve 2g of milk powder in 100 ml of 1x PBS-1% TritonX-100 solution

2.3 Tissue culture techniques

The cells were cultivated in a 5% CO₂ incubator (Heracell, Heraeus) at 37°C in DMEM supplemented with 10% Fetal Calf Serum and 100U/ml penicillin/streptomycin unless otherwise mentioned.

2.3.1. Isolation of Primary fibroblasts from mouse embryos

A female mouse in around 12.5-14.5 day of pregnancy was killed by spinal dislocation and the abdomen was carefully cut open. The uterus carrying the fetus was excised and washed in 1X PBS. The amnion layer was carefully removed and the released embryos were separated from each other and washed in sterile 1XPBS. The embryos were kept under

sterile conditions. The head of each of the embryos was removed and stored at 4°C for genotyping. The liver and heart of the embryos was removed carefully. The remaining embryo was teased with a pair of forceps to break it into small sections. For each embryo, one 25 ml Erlenmeyer flask was prepared with sterile glass beads at the bottom and filled with 5 ml of trypsin solution. The pieces of each embryo were put into one sterile Erlenmeyer flask and placed at 37°C for 15 minutes on a shaking platform, for digestion.

After the tissue was digested, 10 ml of DMEM medium was added to nullify trypsin and the cells were pipetted up and down to get single cell suspension. The cells from each embryo were collected in a sterile 15 ml falcon tube and centrifuged for 5 minutes at 1200 rpm. The supernatant was discarded and the cell pellet was suspended in 10 ml of DMEM and plated out on 6 cm diameter petri dish. The cells were cultivated overnight at 37°C, 5% CO₂ incubator. The next day, the medium was replaced with 10 ml of fresh DMEM and the cells were cultivated over night. The cells were allowed to grow till confluent. The primary cells were trypsinized and half the cells were frozen (Ref. 2.3.5) while the other half were cultivated to get immortalized cell lines (Ref. 2.3.3).

Trypsin EDTA solution (from Gibco)

Trypsin	0.05% w/v
EDTA	0.02 %
Dissolved in Puck's modified salt solution	

2.3.2. Maintenance of cells

Once the cells reached 80-90% confluence in the flasks, they were passaged. The old medium was removed and the cells washed once in pre-warmed sterile PBS. The cells were then trypsinized with 0.5 ml of Trypsin-EDTA solution at 37°C for 5 minutes or till all the cells had detached from the surface of the flask. Following this, trypsin was neutralized with the addition of DMEM medium containing 10% fetal calf serum. The cells were resuspended well by pipetting them up and down several times. Finally, the desired number of cells was plated on to the cell culture flasks and cultivated at 37°C, 5% CO₂.

2.3.3. Immortalization of primary fibroblasts by passaging

The primary mouse embryonic fibroblasts were cultivated in 25ml flasks and passaged (Ref. 2.3.2). Most of the primary fibroblasts died out after first few passages. However, a

few cells overcame the cell cycle block and started to divide in a rather uncontrolled fashion i.e. they became immortalized. They were then maintained in desired confluence as described in 2.3.2.

2.3.4. Isolation of murine peritoneal macrophages

Mice were killed by asphyxiation followed by spinal dislocation and fixed to the dissection board to stretch out the abdomen well. The skin over the abdomen was carefully removed. A small cut, just enough to let in the tip of a pasteur pipette, was made in the peritoneal membrane. A pasteur pipette was filled with ice cold sterile PBS and was inserted into the peritoneal cavity through the cut. PBS was released into the cavity with great care not to injure any internal organ. The abdomen was lightly massaged and the PBS with macrophages was retrieved into the Pasteur pipette. Several such rounds of PBS injection and recovery were done till around 10mls of PBS with cells were recovered from the abdominal cavity. PBS with cells was collected in 15ml polypropylene, non-pyrogenic, sterile tubes (red cap, from Sarstedt AG and Co. Nümbrecht Germany) and always kept on ice. It was important to use this tube since the isolated macrophages have a tendency to adhere strongly to the surface of any other plastic tubes. It was also important to keep the cells on ice since it circumvents the cells from attaching themselves to the tubes. The cells were pelleted by centrifugation at 900 rpm for 4 minutes at 4°C. The pellet was resuspended in 500µl of cold DMEM medium. Cells were counted in a Neubauer chamber and 2×10^5 cells were seeded on coverslips in a 24 well plate and supplemented with 1 ml of pre-warmed DMEM+10% FCS. After 2-3 hours, the medium was replaced with fresh DMEM+10% FCS to remove the non-sticking cells (which are not macrophages). The cells were left over night in 37°C, 5% CO₂ incubator.

2.3.5. Cryoconservation of cells

The cells to be preserved were cultivated till they were around 70%-80% confluent. The cells were trypsinised and the detached cells were collected in 10 ml of DMEM medium. The cells were collected by centrifugation at 1000rpm for 7 minutes. The cell pellet was resuspended in cold cryo-medium (10% v/v DMSO in DMEM supplemented with 10%

FCS and penicillin/ streptomycin). The cells were immediately divided into 1 ml aliquots and frozen at -80°C. After 1-3 days, the cells were transferred to liquid nitrogen storage tanks or -170°C freezer for long term storage.

2.3.6. Histological analysis

Tissue samples were fixed in 4% formaldehyde and embedded in paraffin. 5 to 10µM thick sections were obtained as described (Fayyazi et al. 2000). Deparaffinized sections were stained by haematoxylin and eosin (H&E). In situ end labeling (ISEL) was done to visualize the dead cells as described in Fayyazi et al. 2000.

For the detection of dendritic cells, fascein staining was performed. The deparaffinized sections were incubated three times for 5 minutes each in 0.01 mol/L citrate buffer (pH 6.0) at high power (600-700 Watt) in a microwave. The sections were incubated with 1:50 diluted anti-fascein antibody (DAKO, Hamburg, Germany) for 1 hour and visualized a biotinylated secondary antibody, a peroxidase conjugated streptavidin, and diaminobenzidine as chromogen (Biogenex, Hamburg, Germany) according to manufacturer's instructions. The sections were counterstained in Super Mount Medium (Biogenex) and analyzed by light microscopy.

2.4. FACS techniques

2.4.1. Preparation of T- lymphocytes from thymus

Mice were killed by asphyxiation followed by spinal dislocation. Thymus was excised and lymph nodes were carefully removed. The organ was homogenized in 10ml of complete RPMI-1640 medium supplemented with 10% FCS, 2mM L-glutamine and 100U/ml penicillin and streptomycin, in Tenbroek glass homogenizer with 10 strokes to obtain a single cell suspension. 10µl of single cell suspension was diluted in 90µl of 1% acetic acid (1:10 dilution). The thymocytes were counted in a Neubauer chamber (Fortuna W.G. Co).

2.4.2. Preparation of T- lymphocytes from spleen

Mice were killed by asphyxiation followed by spinal dislocation. Spleen was excised and homogenized in 10ml of complete RPMI-1640 medium supplemented with 10% FCS,

2mM L-glutamine and 100U/ml penicillin and streptomycin, in Tenbroek homogenizer with 10 strokes to obtain a single cell suspension. The cells were treated with erythrocyte lysis buffer for 5-7 minutes at room temperature to lyse the erythrocytes. Later the cells were centrifuged at 1200 rpm for 7 minutes (Multifuge 1_L, Heraeus). The supernatant (lysed erythrocytes) was drained and the pellet containing the T-lymphocytes was resuspended in 5 ml of RPMI-1640 supplemented medium. 10µl of single cell suspension was diluted in 90µl of 1% acetic acid (1:10 dilution). The T-lymphocytes were counted in a Neubauer chamber.

Erythrocyte lysis buffer

Ammonium chloride (NH ₄ Cl)	155mM
Potassium hydrogen carbonate (KHCO ₃)	10mM
EDTA	0.1mM
Adjust the pH to 7.4-7.8	

2.4.3. Phenotyping of primary T- lymphocytes from Thymus or Spleen

1x 10⁶ Thymocytes were transferred to FACS tubes (BD Falcon) and washed once with 1x PBS. The cells were collected at the bottom of the FACS tube by centrifugation (Multifuge 1_L, Heraeus) at 1200 rpm for 7 minutes. 1µl of chromophore (Fluorescein isothiocyanate-FITC, Phycoerythrin-PE or Tricolor-TC) conjugated antibodies against T-lymphocyte surface antigens were added to the samples and incubated for 1 hour at 4°C (Ref. Table VIII for staining scheme, Table X for antibody source and concentrations). Anti CD44 and anti CD4 antibodies were conjugated with biotin, therefore we used a two step detection method. Following staining with these antibodies, the cells were washed in PBS and incubated with TC labeled streptavidin for 45 minutes at 4°C. After staining, the cells were washed with 1x PBS and finally resuspended in 200µl of 1x PBS. The cells were counted in fluorescence assisted cell counter (Becton Dickinson-FACScan) and evaluated using CELLQuest software (Becton Dickinson).

For staining with anti Annexin V antibody, the cells were washed in 1x Binding buffer (10x Binding buffer, BD pharmingen) and at the end resuspended in 200µl of 1x Binding buffer instead of 1x PBS.

Isotype control staining and quadrant setting: For each antibody staining for a surface marker, a parallel sample was stained with isotype control specific for that surface marker antibody. Isotype controls are monoclonal antibodies not directed against any antigen normally expressed on the cells of the test organism but they belong to the same immunoglobulin subclass and are conjugated with the same fluorochrome as the monoclonal antibody against the marker. An isotype control antibodies for mouse should therefore not bind to any specific antigens on mouse derived cells. This staining with isotype control is used for two purposes: First for detection of any non-specific staining from the immunoglobulin. Any signal obtained from isotype control staining was subtracted from the corresponding anti-marker antibody staining. Second, for setting up the quadrant locations on dot plots. The cells not stained with the isotype control appear in the lower left region of the dot plot. Thus the lower left (LL), upper left (UL), upper right (UR) and lower right (LR) quadrants were set in reference to the isotype control staining.

Compensation: Since the excitation-emission spectra of FITC (em 525nm), PE (em 576nm) and TC (em 665nm) chromophores are close it is possible that a single laser could excite more than one chromophore. Compensation is the process by which this fluorescence ‘spillover’ originating from a fluorochrome other than the one specified is subtracted as a percentage of the signal from specific chromophore. For example, spectral overlap between FITC and PE produces light which is detected by both the FL1 and FL2 detectors. The amount of FITC fluorescence being detected by the FL2 detector (i.e. PE detector) can be regarded as excess fluorescence and is therefore compensated out.

For doing compensation, one sample of cells was stained only with anti CD8a-FITC, anti CD4-TC or anti CD4-PE antibody. Each chromophore was excited using all the three excitation wavelengths and the spillover from one fluorescence channel to the adjacent was subtracted by observing the dot plot while the sample was running.

Gating: 10,000-30,000 cells were counted for each staining. Of all the counted cells, specific cells of interest were selected in a process called ‘gating’. Gating is based on usage of antibodies tagged with different chromophores (FITC, PE or TC). For example, cells stained with anti-FITC conjugated antibody can be specifically chosen or gated on, leaving out the cells that fluoresce in the PE or TC channel.

For CD4/CD8 phenotyping, the cells were gated according to their light scattering properties. The larger and more granulated cells like the granulocytes and smaller cells like

erythrocytes have light scattering properties different from medium sized thymocytes. Thus from the forward scatter (FSC) and side scatter (SSC) plots it is possible to specifically gate on the region of thymocytes. The thymocytes were then analyzed on the basis of signal intensity for CD4 (anti-CD4-PE) and CD8 (anti-CD8-FITC) staining in the PE and FITC channels respectively. The CD8 cells in FITC fluorescence channel were plotted on X axis while the CD4-PE on the Y axis. Therefore, CD4⁺ cells appeared on lower right quadrant of the dot plot, CD8⁺ appeared on upper left quadrant while CD4⁺CD8⁺ cells appeared in the upper right quadrant of the dot plot. The unstained CD4⁻CD8⁻ cells appeared in the lower right quadrant (Ref section 3.3.2 for representation picture).

For CD4⁻CD8⁻ DN cells, two step gating strategy was used. In the first step, the cells were gated according to their light scattering properties just as for the CD4/CD8 cells. In the second gating step, all the cells except the DN1-4 were excluded. The cells bearing the CD4 and CD8 markers (mature T lymphocytes), B220 (marker for B lymphocytes), NK1.1 and DX5 (markers for natural killer cells) were stained with specific antibodies conjugated with Phycoerythrin (PE). The anti CD44 antibody was conjugated with tricolor (TC) and CD25 antibody to fluoro-isothio cyanin (FITC). Therefore we could specifically gate on the DN cells labeled with FITC (CD25) and TC (CD44) and exclude the cells bearing PE label. The DN1-4 subsets were then analyzed for CD44 and CD25 expression depending on the signal intensity for FITC and TC fluorescence similar to CD4/CD8 analysis.

Table VIII: Scheme for FACS staining with chromophore conjugated antibodies for phenotyping of T lymphocytes

Staining	Fluorescent Channel I : FITC	Fluorescent Channel II : PE	Fluorescent Channel III : TC
1	Blank control		
2	rIgM	rIgG2a	rIgG2b
3	mIgM	mIgG2a	
4	CD8a	CD4	
5	CD25	CD4, CD8a, CD3, B220, NK1.1, DX5	CD44* Biotin
6	MHC-II	CD8b	CD4
7	Annexin V		PI
8	Annexin V	CD8a	CD4
9	TCR αβ	CD3	
10	Hamster IgG		

* Primary antibody against CD44 was biotin labelled. Therefore, Tricolor (TC) labelled streptavidin was used for detection. Streptavidin binds to biotin and enables the detection of CD44 surface marker.

2.4.4. Induction of apoptosis by dexamethasone treatment

1x 10⁶ T-lymphocytes were transferred to FACS tubes, one test and one control tube for each time point (0hr, 3hr, 6hr, 24hr). The control (un-induced) samples were resuspended in 200µl of RPMI-1640 (Gibco BRL) medium while the test (induced) samples were resuspended in 200µl of 0.1µM dexamethasone (Sigma Aldrich) diluted in RPMI-1640 medium. Both the test and control sample tubes were placed at 37°C, in 5% CO₂ incubator for the respective time points. For the 0hr time point, we had only untreated samples which were immediately washed in 1x PBS and stained to visualize dead cells. After each time point, the dead cells were counted either by Annexin-V/ propidium iodide staining (Ref. 2.4.5) or by Sub-G1 peak assay (Ref. 2.4.6) in both the test and control samples.

Preparation of 1mM dexamethasone stock solution

Dexamethasone	3.92 mg
100% Ethanol	1.0 ml
DMEM culture medium	9.0 ml
Dilute 1mM stock to 0.1µM with RPMI-1640 medium freshly before the experiment.	

2.4.5. Annexin V and propidium Iodide co-staining to visualize dead cells

After incubation for appropriate time, the cells were washed with 1x Binding buffer (BP Pharmingen) and incubated with 1µl of FITC labeled annexin V and 10 µl of 1µg/ml propidium iodide diluted in 1x PBS for 1 hour at 4°C. The cells were washed in 1x Binding buffer (BD Pharmingen) and collected by centrifugation at 1200 rpm for 7 minutes. Finally the cells were resuspended in 200µl of 1x binding buffer and counted in FACS SCAN (Becton Dickinson) and evaluated using CELL Quest software (®Becton Dickinson).

2.4.6. Sub G1 peak assay to determine dead cells

After incubation for appropriate time, the cells were transferred very quickly into a 15ml falcon tube with 10 ml ice cold 99% ethanol. The cells were left overnight at -20°C for fixation. After fixation, the cells were centrifuged at 1200 rpm, 10 minutes at room temperature, transferred to FACS tubes and washed once with 1x PBS. The cells were stained for 1 hour with 200 µl of 1µg/ml propidium iodide at 37°C. The cells in Sub G1 region (G₀ /G₁ peak) were counted with Doublet Discrimination mode in FACScan

(Becton Dickinson) and evaluated using CELL Quest software (Becton Dickinson). Doublet discrimination mode is used to rule out the possibility that two attached G1 cells passing through the laser beam will create fluorescent peak with height and pulse areas similar to a single G2 cell.

2.4.7. Induction of apoptosis by plate bound anti CD3 ϵ and CD28 antibodies.

2.4.7.1. Preparation of ELISA plates:

The assay was done as described by Thien and co-workers (Thien et al. 2005b). An antibody mix was prepared with 10 μ g/ml each of anti CD3 ϵ (Purified, clone 145-2C11, BD Pharmingen) and CD 28 (Biotinylated, clone 37.51, BD Pharmingen) antibodies or 10 μ g/ml anti CD3 ϵ alone in filter sterilized coating buffer. 50 μ l of the antibody mix (i.e. 0.5 μ g of each antibody / well) was pipetted into the wells of a 96-well ELISA plates (F96 Maxisorp, Nunc, Roskilde, Denmark). The plates were left overnight at 4°C. The wells for unstimulated control samples were incubated with 50 μ l of coating buffer. Just before the experiment, the wells were washed once with sterile PBS.

2.4.7.2. Induction of apoptosis:

The freshly excised thymii were homogenized with sterile homogenizer in 10ml of supplemented RPMI-1640 medium. The cells were counted in Neubauer chamber. 2 x 10⁶ cells were transferred to the ELISA plates: in the uncoated well for unstimulated controls and in the antibody coated wells to induce apoptosis. The plates were incubated for 3, 6 and 24 hours at 37°C in 5% CO₂ incubator. The 0 hour sample was immediately washed and stained with annexin-V and propidium iodide to visualize the initial apoptosis. After each time point, the cells were washed and stained with annexin V and propidium Iodide (Ref.2.4.5).

ELISA Plate Coating Buffer

Solution A	0.2 M Na ₂ CO ₃
Solution B	0.2M NaHCO ₃
Mix 85 ml solution A and 40 ml of solution B in 500 ml of H ₂ O	

2.4.8. Induction of apoptosis using Anti-FAS (CD95) antibody

The freshly excised thymii were homogenized in RPMI-1640 medium and the cells were counted. 1×10^6 cells were transferred to FACS tubes in duplicates for every time point. One tube of cells was treated with the antibody to induce apoptosis, while the cells in the other tube were left un-induced in order to study spontaneous apoptosis with time. $1 \mu\text{g}$ of anti FAS antibody (Jo2 BD Pharmingen, Cat no. 554254) was added to the cells for induction and $200 \mu\text{l}$ of RPMI-1640 was added to tubes with untreated control samples. Both, the test and control tubes for each time point were placed in 37°C incubator with 5% CO_2 . After the end of each time point, the cells were washed once in the annexin V binding buffer and incubated with $1 \mu\text{l}$ of FITC conjugated annexin V and propidium iodide for 1 hour at 4°C . The cells were counted in FACS Scan (®Becton Dickinson) and evaluated using Cell Quest software (Becton Dickinson).

2.4.9. Preparation of cells for bone marrow and transplantation

The mice were killed by spinal cord dislocation and the both the femur bones (thigh bones) was carefully removed. With the help of syringe and needle, 5-10 mls of DMEM (supplemented with 10% FCS and penicillin/ streptomycin) was flushed through the shaft of the bone. The medium containing cells was collected under sterile conditions. The cells were counted in a Neubauer chamber and frozen in 1 ml of cryomedium (10% v/v DMSO in DMEM supplemented with 10% FCS and penicillin/ streptomycin). 1×10^6 bone marrow derived pluripotent cells were transplanted into irradiated (5psi) $\text{RAG2}^{-/-} \gamma\text{c}^{-/-}$ mice. Transplantation was done at the central animal facility and irradiation of the $\text{RAG}^{-/-}$ mice was carried out at Strahlentherapie und Radionkologie by Dr. Mirko Nitsche. Development of lymphocytes derived from the transplanted bone marrow in the $\text{RAG}^{-/-}$ mice was studied for 4, 7 and 9 weeks after transplantation.

2.4.10. Analysis of transplanted $\text{RAG2}^{-/-} \gamma\text{c}^{-/-}$ mice

($\text{RAG2}^{-/-} \gamma\text{c}^{-/-}$ mice were obtained from Professor Dr. Rodewald, from the Institute of Immunology, University of Ulm)

After 4, 7 and 9 weeks of transplantation, $\sim 50\text{-}100 \mu\text{l}$ blood was collected from the transplanted $\text{RAG2}^{-/-} \gamma\text{c}^{-/-}$ mice and erythrocytes were lysed as described in 2.4.2. The remaining lymphocytes were washed once with PBS and centrifuged at 1200 rpm for 7

minutes. The cells were stained with 1µl of chromophore conjugated antibodies against markers: CD3, CD4, CD8, B220, NK1.1, DX1.5 and CD19 (Ref. Table X) for 1 hour at 4°C. The cells were washed in PBS and resuspended in 100µl of PBS. The cells were counted in FACScan (Becton Dickinson) and analyzed using CellQuest software.

2.5. Immunofluorescence techniques

2.5.1. Growing cells for immunofluorescence

Cover slips were sterilized at 180°C for 4 hours and placed in a 24 or 4 well plate with a flame sterilized forceps. Mouse embryonic fibroblasts were trypsinized (or freshly obtained macrophages), collected and counted. Required number of cells were pipetted on to the coverslips and supplemented with 200µl of pre-warmed DMEM medium. The plates were swirled around to avoid clustering of the cells on the coverslips. The cells were allowed to seed on the coverslips for 1-2 days at 37°C, 5% CO₂ incubator, till the right confluence was achieved.

2.5.2. Uptake of fluorescently labeled LDL

The VAMP8^{-/-} and VAMP8^{+/+} control immortalized mouse embryonic fibroblasts were grown on coverslips till they were 70% confluent. Cells were washed twice with PBS and starved in serum free DMEM + 1% BSA for 2h at 37°C to allow maximal recycling of the LDL receptors to the cell surface. The medium was then replaced with cold DMEM+ 1% BSA with 200µl of 10µg/ml fluorescently labeled low-density-lipoprotein (BODIPY® FL LDL, Invitrogen™ Molecular Probes™, Eugene, Oregon, USA). The cells were immediately placed on ice in dark for 1 hour to allow receptor binding. The cells were washed with sterile PBS twice at room temperature and incubated at 37°C in DMEM + 1% BSA for different chase times: 0min, 15min, 30min, 1hour and 3 hours. After the chase period, the cells on the coverslips were washed twice with PBS at room temperature and fixed in 3% PFA in PBS for 30 min at room temperature. The cells were washed twice with PBS and rinsed with water. Finally, the coverslips were mounted on glass slides with DAKO® mounting medium. The cells were viewed under Leica DM5000B fluorescence microscope (Leica microsystems) at the excitation wavelength of BODIPY® 488 nm.

2.5.3. Uptake of fluorescently labelled beads by peritoneal macrophages

Peritoneal macrophages were isolated (Ref. 2.3.4.) and seeded at a concentration of 2×10^5 cells / coverslip and cultivated in DMEM+ 10% FCS at 37°C, 5% CO₂ overnight. 1µM diameter fluorescent beads (Flouresbrite® BB carboxylate microspheres Polysciences Inc.) were coated in 10% goat serum for better uptake into the cells. The beads, at a concentration 50 beads per cell, were pipetted in an eppendorf tube, supplemented with ~ 500µl of 10% goat serum and held on a rotating wheel for half an hour. Before the experiment, the cells were starved in DMEM-FCS for 2 hours at 37°C. The cells were then fed with the pre-coated beads (50 beads/cell) and incubated for several periods of pulse (10, 15, 20 and 30 minutes). After pulsing, the medium was replaced by fresh DMEM medium and chased at 37°C for 30 minutes and 60 minutes (Ref. table IX). After the respective pulse and chase times, the cells were washed with ice cold 1x PBS. The cells were fixed with methanol (Ref. 2.5.4) and stained with anti lamp2 antibody (Ref.2.5.6). The cells were viewed under Leica confocal laser scanning microscope TCS SP5 (Leica microsystems) at the excitation wavelength of 360nm.

Table IX. Pulse chase times to study uptake of BB fluoresbrite beads(® Polysciences Inc.)

Pulse time	Chase time	Following treatment
10 minutes	-	Fix and immunofluorescence
15 minutes	-	Fix and immunofluorescence
20 minutes	-	Fix and immunofluorescence
30 minutes	-	Fix and immunofluorescence
30 minutes	30 minutes	Fix and immunofluorescence
30 minutes	60 minutes	Fix and immunofluorescence

2.5.4. Methanol fixation

Cells, seeded on the coverslips, were washed once with 1x PBS at room temperature. 1ml of methanol (-20°C) was added to each of the wells and left for 5 minutes at room temperature. After fixation, methanol was removed and immediately replaced with 1 ml of PBS. It is important not to let the cells dry out. The cells were washed twice with 1x PBS and immunofluorescence was performed as described in section 2.5.6.

2.5.5. PFA fixation

Cells seeded on the coverslips were washed once with PBS at RT and incubated for 30 minutes with 3% PFA in PBS. After this, the cells were washed twice with PBS and once

with dd H₂O and the coverslips mounted on glass slides or immunofluorescence was performed as described in section 2.5.6.

2.5.6. Immunofluorescence for lamp1/2 and DAPI staining

After fixation, either with methanol or PFA, the cells were washed twice with PBS and blocked with 50mM NH₄Cl solution in PBS for 10 min. Then cells were permeabilized with 0,05% Triton X-100 in PBS 2 times 5 minutes each and blocked with 1% BSA in PBS solution for 20 minutes. Following this, the cells were stained with primary antibody. The primary anti lamp1/2 antibody was diluted 1:100 in 1% BSA PBS solution. 20 µl of the antibody solution was pipetted onto a parafilm. Coverslips were placed with cell side down on the drop of antibody solution in a dark humid chamber. Cells were incubated with the antibodies for 1h in a humid dark chamber. After incubation, the coverslips were placed back into the wells with the cell side up. The cells were washed 3 times for 5 minutes each with 1x PBS and incubated with 10% goat serum in PBS for 20 min. Secondary antibody anti-rat Cy3 was diluted 1:200 in 10% goat serum solution and 20 µl was pipetted on fresh parafilm. The cells were again placed upside down on the drop of antibody solution for 45 minutes at room temperature in a dark humid chamber. Cells were then washed 5 times for 5 minutes each with 1xPBS and rinsed twice times with water. The coverslips mounted in DAKO mounting medium containing DAPI stain (DAKO®, Carpinteria, CA) and allowed to dry overnight at room temperature.

Table X: List of antibodies used for FACS analysis

Surface staining of T-lymphocytes				
Antibody	Conjugate	Concentration	Source	Marker for
Primary antibodies				
Anti Mouse CD 4	PE	50µg/500µl	Caltag	T lymphocyte
Anti Mouse CD 4	TC	100µg/500µl	Caltag	T lymphocyte
Anti Mouse CD8a	FITC	100µg/1ml	Caltag	T lymphocyte
Anti Mouse CD8a	PE	50µg/500µl	Caltag	T lymphocyte
Anti Mouse CD8b	PE	50µg/500µl	Caltag	T lymphocyte
Anti Mouse CD3	PE	50µg/500µl	Caltag	T lymphocyte
Anti Mouse CD25	FITC	0.5 mg/ml	BD Pharmingen	Immature thymocyte
Anti Mouse CD44	Biotin	100µg/1.0ml	Caltag	Immature thymocyte
Anti Mouse B220	PE	50µg/500µl	Caltag	B lymphocyte
Anti Mouse DX5	PE	0.5 mg/ml	BD Pharmingen	Natural killer cells
Anti Mouse MHCI	FITC	100µg/1.0ml	Caltag	MHC I ⁺ cells
Anti Mouse TCRαβ	FITC	100µg/1.0ml	Caltag	TCRαβ ⁺ mature T-lymphocytes
Anti Mouse Annexin V	FITC	50µg/500µl	BD Pharmingen	Apoptotic cells
Anti Mouse CD19	FITC	100µg/1.0ml	Caltag	B lymphocyte
Anti Mouse NK1.1	FITC	100µg/1.0ml	Caltag	Natural killer cells
Anti Mouse MHCII	FITC	100µg/1.0ml	Caltag	MHCII ⁺ dendritic cells
Isotype controls				Control for
Anti Rat IgG2a	PE	50µg/500µl	Caltag	CD8a (FITC and PE), CD4 (PE and TC), B220 (PE), CD3(PE)
Anti Rat IgG2b	Biotin	50µg/500µl	Caltag	CD44 (Biotin)
Anti Rat IgM	FITC	50µg/500µl	Caltag	CD25(FITC),DX5 (PE)
Anti Mouse IgG2a	PE	50µg/500µl	Caltag	NK1.1 (PE)
Anti Mouse IgM	FITC	50µg/500µl	Caltag	MHCII (FITC)
Hamster anti Mouse IgG	FITC	50µg/500µl	Caltag	TCRαβ (FITC)
Secondary antibody for Biotin conjugated anti-CD44 antibody and its isotype control rIgG2b				
Streptavidin	TC	50µg/500µl	Caltag	

Table XI: List of antibodies used for apoptosis induction assays

Plate bound CD3ϵ and CD28 induced apoptosis assay			
Antibody	Concentration		Source
	Stock	Working	
Purified hamster anti-mouse CD3 ϵ (145-2C11)	31.25 μ g/ml	10 μ g/ml	BD Pharmingen
Biotnylated anti-mouse CD28 (37.51)	500 μ g/ml	10 μ g/ml	BD Pharmingen

Anti FAS antibody induced apoptosis assay		
Antibody	Concentration	Source
Purified anti mouse Fas monoclonal Clone Jo2 (Cat no 554254)	1.0mg/ml	BD Pharmingen

Table XII: List of antibodies used for western blot analysis and immuno fluorescence

Antibodies against SNARE proteins for western blotting					
Protein	Name	Mol. weight	Type	Dilution	Source
Vti1a	56	27	Polyclonal (Rabbit serum)	1:3000	Antonin et al. 2000c
Vti1b	55	29	Polyclonal (Rabbit serum)	1:3000	Antonin et al. 2000c
Endobrevin /VAMP8		16	Polyclonal (Rabbit serum)	1:1000	Synaptic Systems GmbH, Göttingen
Syntaxin 6		31	Monoclonal (Mouse)	1:5000	Transduction Laboratories.
Syntaxin 8	60	27	Polyclonal (Rabbit serum)	1:1000	Antonin et al. 2000b
Syntaxin 7	Sx7/8	30	Polyclonal (Rabbit serum)	1:1000	Antonin et al. 2000b
SNAP 29	Sn29/1	29	Polyclonal (Rabbit serum)	1:1000	Antonin et al. 2000b
Syntaxin16	ODTH	37	Polyclonal (Rabbit serum)	1:1000	Kreykenbohm et al. 2002
VAMP4	136	19	Polyclonal (Rabbit serum)	1:1000	Kreykenbohm et al. 2002

Antibodies for immunofluorescence		
Antibody	Dilution	Source
Lamp1 (Rat monoclonal ID4B)	1:200	Hybridoma Bank, Iowa, USA
Lamp2 (Rat monoclonal ABL93)	1:200	Hybridoma Bank, Iowa, USA
Anti rat - Cy3	1:200	Dianova

List of commonly used buffers

Buffer	Composition
NET Buffer	100mM NaCl, 10mM Tris/HCl pH8.0, 25mM EDTA
TBS	150mM NaCl, 50mM Tris/HCl pH7.4
TE	1mM EDTA, 10mM Tris/HCl pH 7.4
10x PBS	1.5M NaCl, 160mM Na ₂ HPO ₄ , 40mM NaH ₂ PO ₄
1M Tris/HCl (1000ml)	121g Tris base dissolved in 800 ml bidistilled H ₂ O, pH adjusted with HCl and volume was made up till 1000 ml
50x TAE	2M Tris-base, 0.1M EDTA, adjust pH 8,0 with acetic acid
1x TAE	50x stock solution dissolved 1:50 in VS water

List of media used for cell culture**Dulbeccos Modified Eagle Medium - DMEM**

Component	Source	Volume/Concentration
DMEM	PAN biotech, GmBH	1000ml
Fetal calf serum	Gibco BRL, Eggenstein	10%
L-glutamine	Gibco BRL, Eggenstein	2mM
Penicillin/streptomycin	Gibco BRL, Eggenstein	100 U/ml
Mix the components and pre warm the medium before use		

Starvation Medium

Component	Source	Volume/Concentration
DMEM	PAN biotech, GmBH	1000ml
L-glutamine	Gibco BRL, Eggenstein	2mM
Penicillin/streptomycin	Gibco BRL, Eggenstein	100 U/ml
Mix the components and pre warm the medium before use		

Medium for cryoconservation of cells

Component	Volume (for 10ml medium)
DMEM complete (ref table)	7 ml
Fetal calf serum	2 ml
DMSO	1 ml
1ml of cryo preservation medium for each cryo tube.	

Roswell Park Memorial Institute medium - RPMI 1640

Component	Source	Volume/Concentration
RPMI 1640	Gibco BRL, Eggenstein	1000ml
Fetal calf serum	Gibco BRL, Eggenstein	10%
L-glutamine	Gibco BRL, Eggenstein	2mM
Penicillin/streptomycin	Gibco BRL, Eggenstein	100 U/ml
Mix the components and pre warm the medium before use		

3. Results

3.1 Ablation of VAMP8/endobrevin causes partial early mortality

3.1.1. Progressively degenerating health and early death in VAMP8^{-/-} mice

The birth and death of VAMP8^{-/-} Vti1b^{-/-}, VAMP8^{-/-} Vti1b^{+/-}, VAMP8^{-/-} and VAMP8^{+/-} Vti1b^{-/-} pups was recorded. It was seen that all the VAMP8^{-/-} genotypes had a high rate of mortality before the age of one month. During the initial work (Ref. section 1.4.4) 30 out of 45 (66%) VAMP8^{-/-} Vti1b^{-/-} and 20 out of 34 (58%) VAMP8^{-/-} Vti1b^{+/-} were reported dead before the age of one month (Figure 3.1). In this work, similar recording of births and death for VAMP8^{-/-} showed that 20 out of 55 i.e. 36% VAMP8^{-/-} mice were dead before one month of age (Figure 3.1). In comparison only 2.2% deaths were observed in VAMP8^{+/-} Vti1b^{-/-} mice (Figure 3.1).

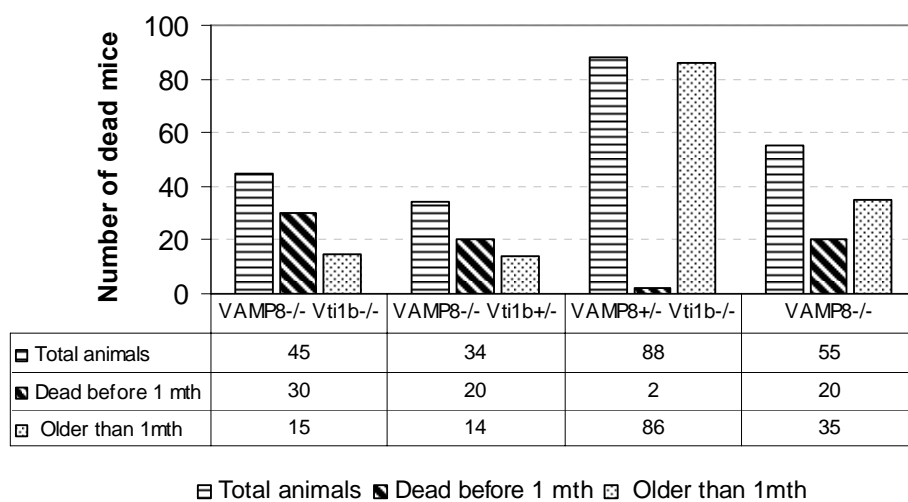


Figure 3.1. High early mortality in VAMP8/endobrevin^{-/-} genotypes: There was a high early mortality in VAMP8^{-/-} mice compared to the VAMP8^{+/-} mice. While 30 out of 45 VAMP8^{-/-} Vti1b^{-/-} and 20 out of 34 VAMP8^{-/-} Vti1b^{+/-} mice died before reaching the age of 1 month. The VAMP8 single knock out mice had an early onset of death and 20 out of 55 mice died before the age of weaning. VAMP8^{+/-} mice however were more like the wild type mice with a very low rate of mortality (less than 2%).

VAMP8^{-/-} and VAMP8^{-/-}Vti1b^{-/-} mice were born in expected Mendelian ratios indicating a normal pre-natal development. The mice also showed a normal post natal development up to day 7. After the 8th day, 36% of the VAMP8^{-/-} mice began to lose weight and became smaller than the littermates. Loss of weight was observed till up to 2-3 days accompanied by progressively degenerating health, following which these mice died (Figure 3.2).

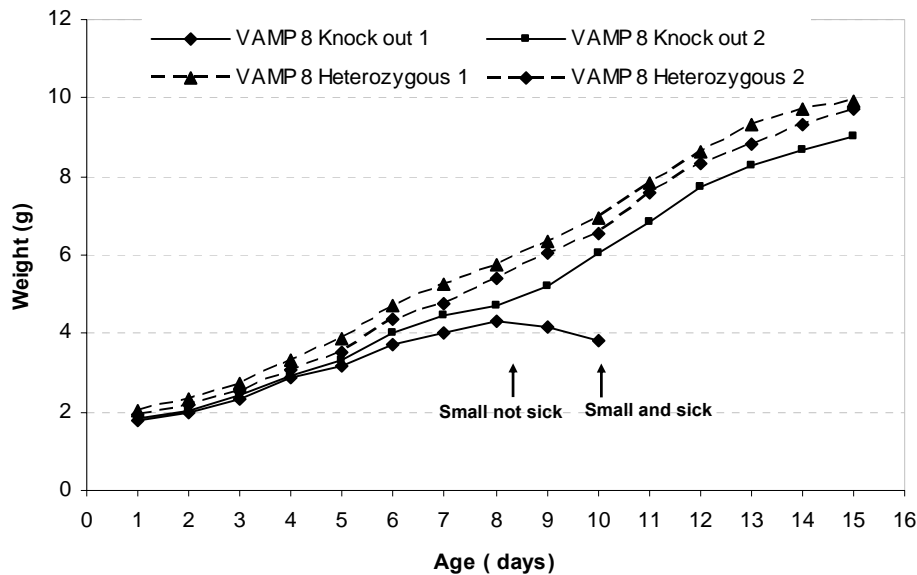


Figure 3.2. Weight gain pattern in $VAMP8^{-/-}$ mice: Characteristic pattern of weight gain of a representative litter shows heterogeneity in the phenotype of $VAMP8^{-/-}$ mice. One out of the two $VAMP8^{-/-}$ pups lost weight starting post natal day 8 for 2-3 consecutive days, became sick and eventually died. While the other $VAMP8^{-/-}$ pup survived the weaning and became adults. At the first day of weight loss, the mice were smaller than their littermates but were apparently active and did not look sick. This stage is called small not sick. While after 2-3 days of weight loss, the mice looked very weak and sick and this stage is described as small and sick.

After the first day of weight loss, the mice were smaller than their littermates by around 1.5 folds.

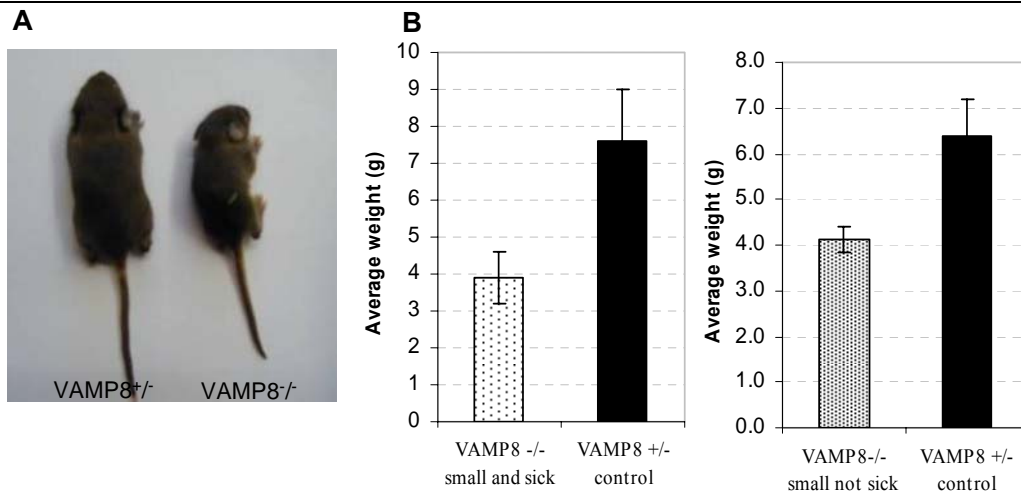


Figure 3.3. Massive weight loss in small $VAMP8^{-/-}$ mice : A 11 day old $VAMP8^{-/-}$ mouse (right) weighing 3.6 grams on the day of death compared to a $VAMP8^{+/-}$ littermate (left) weighing 6.3 grams on the same day (A). The average weight of small and sick mice is reduced at an average by 1.9 folds ($n=7$, age 8-12 days, left graph) while the mice at the preceding small not sick were lighter by 1.5 folds ($n=4$, age 8-12 days, right graph) compared to littermate controls (B).

Following this, there was a progressive decrease in weight such that at the time of death, the VAMP8^{-/-} small and sick mice weighed almost half (average 1.9 fold decrease) that of the heterozygous littermates (Figure 3.3 A, B). The mice were very weak with a shivery and unstable gait

Similar pattern of weight loss and early mortality was previously observed in the VAMP8^{-/-} Vti1b^{-/-} and VAMP8^{-/-}Vti1b^{+/-} (Ref. section 1.4.4). However in contrast to VAMP8^{-/-} mice that had a much early and sudden onset of the phenotypic manifestation and most of the VAMP8^{-/-} Vti1b^{-/-} mice died between post natal day 15-30. At the end of one month, just about 33% of the VAMP8^{-/-}Vti1b^{-/-} and 41% of VAMP8^{-/-}Vti1b^{+/-} mice were alive (Ref. section 1.4.4).

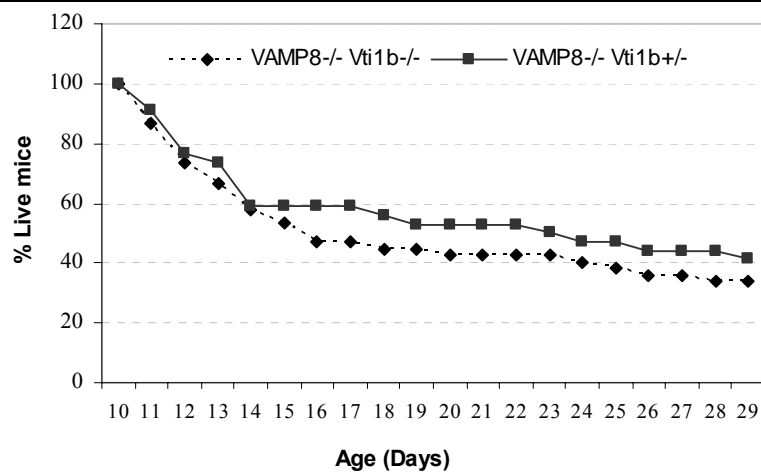


Figure 3.4. VAMP8^{-/-} Vti1b^{-/-} mice show high early mortality:

Record of birth and death of VAMP8^{-/-} Vti1b^{-/-} double knock out and VAMP8^{-/-} Vti1b^{+/-} mice. The VAMP8^{-/-} Vti1b^{-/-} knock out mice showed the highest number of deaths with just about 33% surviving mice at the end of one month. The VAMP8^{-/-} Vti1b^{+/-} mice also had a high death rate with about 41% survivors after one month.

The VAMP8^{-/-} and VAMP8^{-/-} Vti1b^{-/-} mice that survived past the initial one month of post natal life, reached adulthood and were fertile. However, they were in most cases lighter and smaller than their heterozygous littermates.

3.1.2. Heterogeneity in the VAMP8^{-/-} phenotype

There was heterogeneity in the phenotype among the VAMP8^{-/-} mice. For further reference, the mice have been divided into three categories based on their health status.

The first stage is called 'small not sick' stage. This stage marked the beginning of health degeneration when the mice just started to loose weight but they looked active and were healthy.

The second category is 'small and sick' stage, when the mice had lost weight for 2-3 days consecutively and looked very weak and small and eventually died.

The third category comprises of the 'adult' VAMP8^{-/-} that did not loose weight and became adults that were fertile and healthy. In all the experiments, VAMP8^{+/-} littermate mice were used as controls for the VAMP8^{-/-} test mice.

3.2. Ablation of VAMP8 causes defects in Thymus

3.2.1. Morphological defect

*Histological staining done by Dr. Afshin Fayyazi at the Department of Pathology, Georg-August Universität Göttingen.

Several organs from a small and sick VAMP8^{-/-} Vti1b^{-/-} mouse were examined histologically. While kidney, intestine, brain, spinal cord, spleen and heart appeared normal, the thymus showed a morphological defect. The pancreas of VAMP8^{-/-} Vti1b^{-/-} mice also showed a defect. The pancreas of small as well as adult VAMP8^{-/-} Vti1b^{-/-} mice looked enlarged and creamy. This defect was probably due to the loss of VAMP8 similar to what was previously described by Wang and co-workers in their VAMP8^{-/-} mice. (Wang et al. 2003). However we concentrated on studying the thymus

During the initial work (Ref. section 1.4.3, 1.4.4), thymus of a few VAMP8^{-/-} Vti1b^{-/-} mice was studied by histochemistry and compared to the wild type mice. The normal morphology of thymus section from an adult wild type mouse is depicted in Figure 3.5A. The cortex (C) and medulla (M) appear as distinct compartments in Giemsa staining (Figure 3.5A). On higher magnification, a clear boundary defining the thymic cortex and the medulla was observed (Figure 3.5B). Dendritic cells are strictly confined to the medulla and the cortico-medullary junction and can be seen by Fascadein staining of thymus sections. As seen in Figure 3.5C, the yellow stained dendritic cells are present only in the medulla within a well defined boundary and are excluded from the cortex. In addition, thymus from 2 months old adult VAMP8^{-/-} Vti1b^{-/-} mouse showed a normal morphology (analysed during master's thesis) with a clearly defined medullary and cortical boundary (Figure 3.5D and E) and dendritic cells strictly confined to the medullary region (Figure 3.5F). However, thymus from small and sick VAMP8^{-/-} Vti1b^{-/-} mice showed no distinction into cortex and medullary compartments (Figure 3.5G).

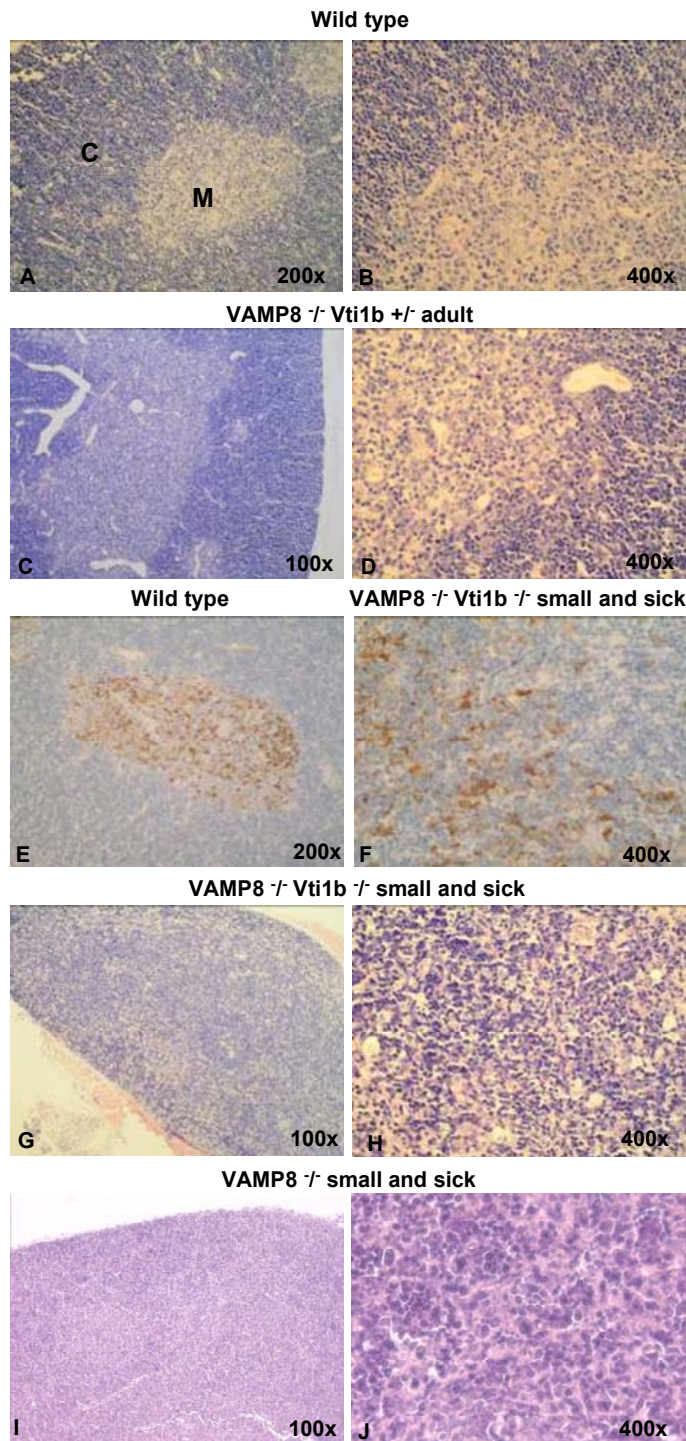


Figure 3.5. Morphology of thymus is disrupted in VAMP8^{-/-} small and sick mice: HE stained sections from the thymus of a wild type mouse showed a distinction into two compartments, the cortex (C) and the medulla (M) (A,B). Fascein stained thymus sections from wild type mouse showed the dendritic cells strictly confined to the medullary region (brown E). Thymus from a healthy adult VAMP8^{-/-} mouse also showed a clear distinction into cortex and the medulla (C-D). In contrast, the thymus section from small and sick VAMP8^{-/-} Vti1b^{-/-} (G-H) and from a 8 day old VAMP8^{-/-} (I,J) mice did not show the characteristic compartmentalization into cortex and medulla with medullary cells (pink) scattered through the thymic cortex (blue). Fascein stained thymus sections from a small and sick VAMP8^{-/-} Vti1b^{-/-} mouse showed a scattered pattern of dendritic cells (brown F). The pictures were taken by Leica-DM IRB microscope at the indicated magnifications.

*Histological staining done by Dr. Afshin Fayyazi at the Department of Pathology, Georg-August Universität Göttingen.

On higher magnification, complete disruption of the cortico-medullary boundary was more prominent. There were few pink stained medullary cells randomly scattered between the

cortical cells (Figure 3.5H). Dendritic cells were also scattered in these thymii, as seen by fascein staining (Figure 3.5I).

During this work, the disruption of thymus morphology in VAMP8^{-/-} Vti1b^{-/-} mice was confirmed by analysis of thymii from several small and sick and adult VAMP8^{-/-} Vti1b^{-/-} mice. In addition the thymus from small and sick VAMP8^{-/-} mice were also analyzed. Thymii from small and sick VAMP8^{-/-} mouse showed a morphological defect similar to the VAMP8^{-/-} Vti1b^{-/-} mice. There was no distinct compartmentalization into cortex and medulla and a few medullary cells appeared scattered throughout the cortex (Figure 3.5J).

In addition, thymus from a 9 day old small not sick VAMP8^{-/-} mouse was analyzed histologically. There was a no disruption of the cortico-medullary boundary in the thymus of this mouse and the two regions were clearly demarcated. Hence, it was confirmed that the disruption of thymus morphology was a characteristic feature of the small and sick stage of both VAMP8^{-/-} and VAMP8^{-/-} Vti1b^{-/-} mice, while the thymus is normal at the small not sick stage.

3.2.2. Reduction in thymus size and total cell count

Total cell count of thymus was analyzed from several VAMP8^{-/-} small and sick, small not sick and adult mice. The thymii were homogenized in 10ml of RPMI-1640 supplemented medium and the cells counted in a Neubauer chamber. It was seen that the thymus cellularity in the VAMP8^{-/-} mice was reduced quite rapidly with the progression of phenotypic manifestation. While the small not sick mice already showed a signs of reduction in thymic cellularity, the most severe reduction was seen in the thymii from the small and sick mice.

The VAMP8^{-/-} small not sick mice had an average of 140 million cells compared to 260 million in the VAMP8^{+/+} controls i.e. a reduction by around 1.8 fold (Figure 3.6). The cell count in the small and sick VAMP8^{-/-} mice rapidly reduced by upto 10 folds. There were just about 26 million cells in the thymus of the small and sick mice compared to 260 million in the controls (Figure 3.6). Thymus from the adult VAMP8^{-/-} mice also showed a slight reduction by around 1.4 folds compared to littermate controls (Figure 3.6).

As previously observed, similar reduction was observed in the total thymus cell count of VAMP8^{-/-} Vti1b^{-/-} mice at the small and sick stage. On an average, the small and sick VAMP8^{-/-} Vti1b^{-/-} mice had around 40 million cells compared to around 510 million in the

littermate controls i.e. a reduction of up to 13 fold in the total cell count (Ref. section 1.4.4 and Figure 3.7A).

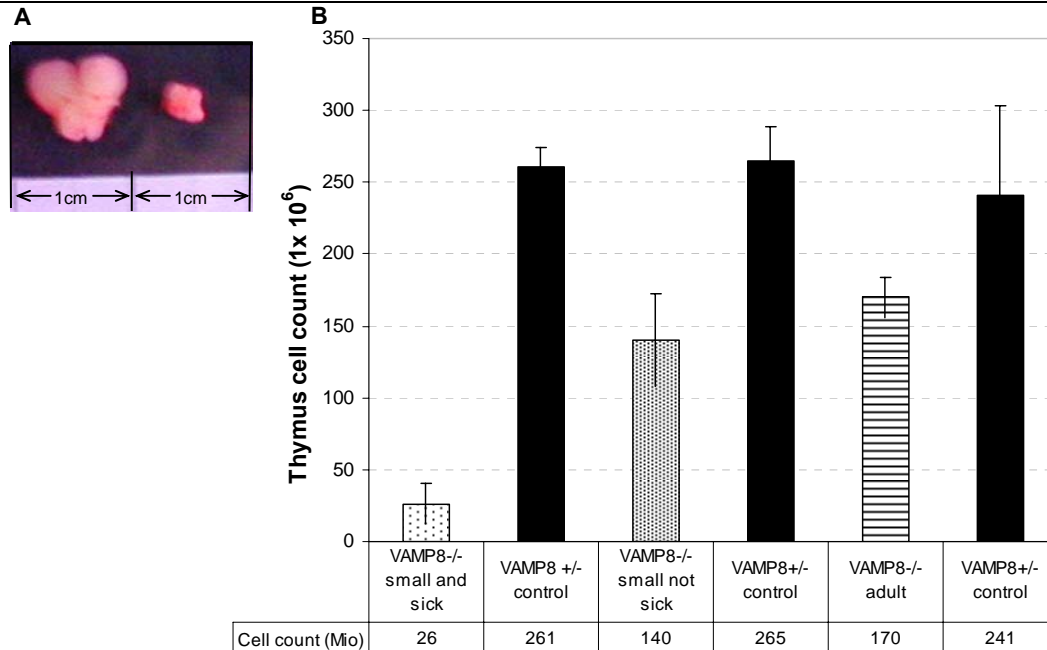


Figure 3.6. Thymus cellularity is progressively reduced in VAMP8^{-/-} small and sick mice: The size of the thymus is highly reduced in the VAMP8^{-/-} small and sick mice (A). The total cell count is also reduced by around 10 folds in the VAMP8^{-/-} mice (n=7 age 8-12 days) at the small and sick stage. The reduction in cell number can also be seen in the small but not so sick stage (n=5 age 8-12 days) and in the adults (n=3 age 1.5-2 months), (1.8 fold, 1.4 fold respectively) (B).

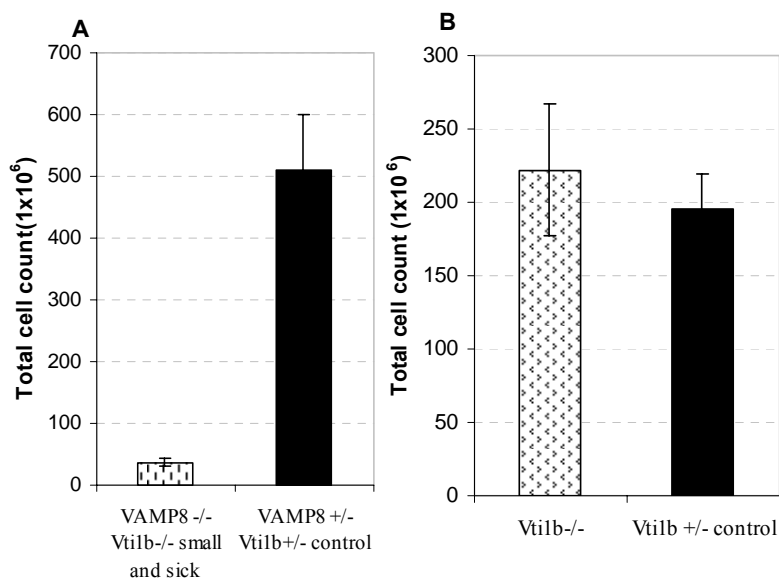


Figure 3.7. The cellularity of thymus is reduced in small and sick VAMP8^{-/-} Vti1b^{-/-} but not in Vti1b^{-/-} mice: Small and sick VAMP8^{-/-} Vti1b^{-/-} mice (n=5, 12-25 days) show up to 13 fold reduction in total cell count (A). *Onset of phenotype was spread over first 1 month of age in VAMP8^{-/-} Vti1b^{-/-} mice compared to 7 days in the VAMP8^{-/-} mice. The data shown here is from VAMP8^{-/-} Vti1b^{-/-} mice between days 12-25. Hence the control VAMP8^{+/-} Vti1b^{+/-} have a higher number of total cell count compared to VAMP8^{-/-} controls. Vti1b small mice (10-12 days, n=4) do not show any reduction in the thymus cellularity (B).

However in *Vti1b*^{-/-} mice aged day 10-12, there was no reduction in the thymus cellularity compared to littermate *Vti1b*^{+/-} control mice (Figure 3.7B). The control mice had an average of 220 million cells compared to average 200 million cells in the *Vti1b*^{-/-} mice.

Table XIII: A summary of reduction in total cell count in different studied genotypes.

Test Genotype	Test Thymocytes (Mio)	Control Thymocytes* (Mio)	Fold decrease
VAMP8 ^{-/-} small and sick	26	260	10 x
VAMP8 ^{-/-} small not sick	140	266	1.8 x
VAMP8 ^{-/-} adult	170	242	1.4x
**VAMP8 ^{-/-} <i>Vti1b</i> ^{-/-} small and sick	40	510	13x
<i>Vti1b</i> ^{-/-}	200	220	-

*Vamp8^{+/-} littermates were used as controls for the *Vamp8*^{-/-} mice, *Vamp8*^{+/-} *Vti1b*^{+/-} littermates for the *Vamp8*^{-/-} *Vti1b*^{-/-} and *Vti1b*^{+/-} littermates for the *Vti1b*^{-/-} mice. The same number of control and test mice was used. ** The window of phenotypic onset is extended over post natal days 11 to 29 in the *Vamp8*^{-/-} *Vti1b*^{-/-} small and sick mice. The mice analyzed were aged 12-25 days and therefore the corresponding controls have a higher total cell count compared to the *Vamp8*^{+/-} aged between 8-12 days.

Additionally, the spleen was severely reduced in the VAMP8^{-/-} *Vti1b*^{-/-} and VAMP8^{-/-} small and sick mice. The total count of T lymphocytes in the spleen of VAMP8^{-/-} *Vti1b*^{-/-} small and sick mice was 13.8 million compared to 135 million in the controls i.e. a reduction by 10 folds. However there was no reduction in the T lymphocytes cell count in the spleen of VAMP8^{-/-} adult mice (263 million) compared to the controls (266 million).

The above data indicates that VAMP8 is important for development of the thymus in mice and possibly for early postnatal survival. It was also confirmed that the previously observed phenotype in the VAMP8^{-/-} *Vti1b*^{-/-} mice is contributed entirely by the loss of VAMP8 while the loss of *Vti1b* does not affect thymus development.

3.2.3. SNARE proteins in the thymus

In order to confirm that the VAMP8^{tm1Lex} mice do not have VAMP8 protein, protein levels in the VAMP8^{+/+}, VAMP8^{+/-} and VAMP8^{-/-} mice were checked by western blot. VAMP8 was present in thymus of VAMP8^{+/+} and VAMP8^{+/-} mice while VAMP8 was not detect in thymii from the VAMP8^{-/-} mice (Figure 3.8A). From previous work in our lab it was known that syntaxin8 is degraded in the absence of *Vti1b* in the *Vti1b*^{-/-} mice (Atlashkin et

al. 2003). Therefore, we wanted to know if levels any of the SNARE proteins are changed due to the loss of VAMP8.

Deficiency of VAMP8 did not have a considerable effect on the amount of its complex partners syntaxin7, syntaxin8 and Vti1b nor of the early endosomal Vti1a or SNAP-29. Western blot analysis showed a reduced amount of syntaxin 8 in the thymus from VAMP8^{-/-} Vti1b^{-/-} mice (Fig. 3.8B) as expected for Vti1b-deficient tissue (Atlashkin et al. 2003). The loss of the late endosomal SNARE complex could possibly be compensated for by the early endosomal SNARE complex. However, there was no major change in the amounts of the early endosomal SNAREs VAMP4, Vti1a or syntaxin16.

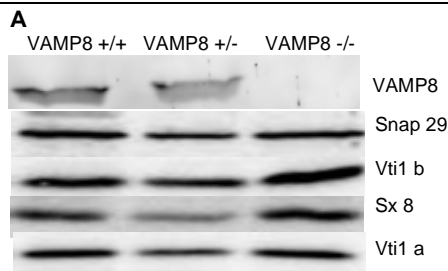


Figure 3.8A. SNARE profile of the thymus from healthy VAMP8^{-/-} mouse aged ≥ 1.5 months in comparison to the VAMP8^{+/-} and wild type mice. There was no difference in the expression level of SNAP29, Vti1b, syntaxin 8 and Vti1a in thymii of control and test mice.

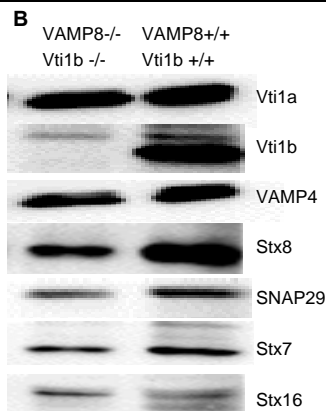


Figure 3.8B. SNARE profile of thymus from VAMP8^{-/-} Vti1b^{-/-} mouse (≥ 1.5 months) and littermate wild type mouse. There was no difference in the expression of Vti1a, VAMP4, SNAP29, syntaxin 7 and syntaxin 16 between the two samples. There was no Vti1b detected in the double knock out thymus while syntaxin 8 was reduced due to the deficiency of Vti1b in the VAMP8^{-/-} Vti1b^{-/-} mouse.

3.3. Deficiency of VAMP8 leads to defective T-cell maturation

The compartmentalization of thymus into functionally distinct areas: the cortex and the medulla, is critical for the development of the T-lymphocytes. The developmental stages of T lymphocytes can be divided on the basis of sequential expression of markers CD44, CD25, CD4 and CD8. The T cell progenitors that arrive in the thymus are devoid of most of the Thymocyte markers especially CD4 and CD8 and are therefore called double negative (DN) cells. These DN cells express CD44 and CD25 molecules in a specific

sequence and are divided into four stages of development DN1-4 as: $CD44^+CD25^-$ (DN1) $CD44^+CD25^+$ (DN2) $\longrightarrow CD44^-CD25^+$ (DN3) $\longrightarrow CD44^-CD25^-$ (DN4).

The DN4 cells start expressing both the CD4 and CD8 molecules called $CD4^+CD8^+$ (DP) stage. This is followed by the loss of expression of either CD4 or CD8 thereby maturing into $CD4^+$ (SP) or $CD8^+$ (SP) cells. The progression of each subset to the next one is under strict selection mediated by a constant crosstalk between the T lymphocytes and the stromal cells. We wanted to know if the observed disruption of the thymus morphology affects the T-lymphocyte development adversely in the small $VAMP8^{-/-}$ mice.

Freshly excised thymus from $VAMP8^{-/-}$ small and sick, $VAMP8^{-/-}$ small not sick and adult mice were homogenized. Thymocytes were stained with antibodies (linked with fluorescent conjugates) against T cell surface markers CD4, CD8, CD44, CD25 and T cell receptor (TCR). The labeled cells were counted in cell sorter (BD FACScan) and the expression of these markers on the surface was analyzed. The percentage of cells counted in the isotype controls was subtracted from the samples to avoid errors due to non-specific staining and auto-fluorescence.

3.3.1. Development of $CD4^-CD8^-$ DN1-4 subsets is disturbed in sick $VAMP8^{-/-}$ mice

At first, detailed phenotyping of the $CD44/CD25$ thymic precursor subsets was performed on $CD4^-CD8^-(DN)$ cells. The objective was to analyze the $CD44^+CD25^-$ (DN1), $CD44^+CD25^+$ (DN2), $CD44^-CD25^+$ (DN3) and $CD44^-CD25^-$ (DN4) subsets in the thymus from $VAMP8^{-/-}$ mice and compare to the $VAMP8^{+/+}$ controls. Two step gating strategy was used to analyze just the DN thymocytes (Figure 3.9). In the first step, the cells were gated according to their light scattering properties. The larger and more granulated cells like the granulocytes and smaller cells like erythrocytes scatter light differently when compared to the medium sized thymocytes. Thus from the forward (FSC) and side scatter (SSC) dot plot it is possible to specifically gate on the region of thymocytes (Figure 3.9A). In the second gating step, the cells bearing the CD4 and CD8 markers (mature T lymphocytes), B220 (marker for B lymphocytes), NK1.1 and DX5 (markers for natural killer cells) were stained with specific antibodies conjugated with Phycoerythrin (PE).

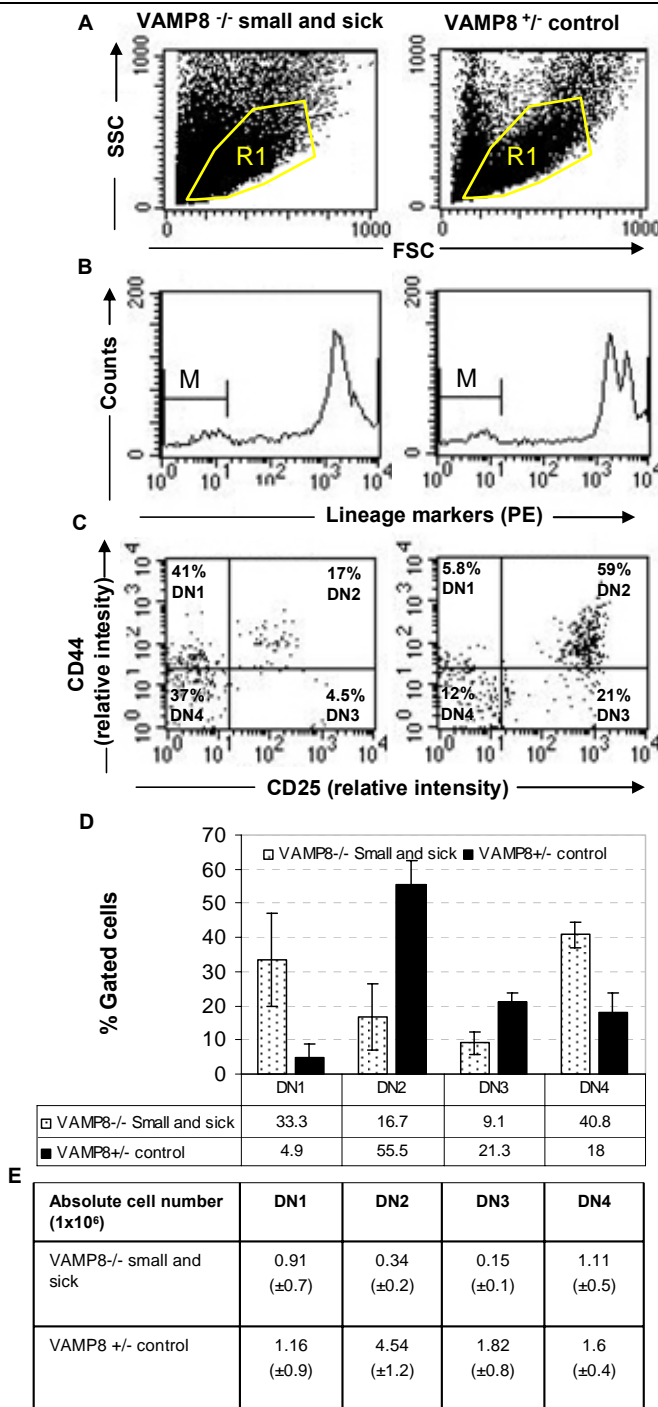


Figure 3.9. Analysis of DN1-4 thymocyte precursor subsets in small and sick VAMP8^{-/-} mice: Single cell suspension from thymus of VAMP8^{-/-} small and sick mice were stained with antibodies against CD44 and CD25 markers to visualize DN1-4 subsets. Two step gating strategy was used for analysis of DN subsets. At first, the cells were gated according to their light scattering characteristics. Very large and granular cells such as granulocytes and very small cells such as leukocytes as well as debris are excluded out. While the cells in the size range of thymocytes are included in the region of interest R1 shown in yellow FSC: Forward scatter, SSC: Side scatter (A). Further, the mature T lymphocytes bearing lineage markers CD4, CD8; natural killer cells with DX5, NK1.1 and B lymphocytes bearing B220 marker were excluded. These cells show high signal intensity in the PE channel and appear as large peaks seen in the right corner of the area plots in figure B. While the cells with low or no signal for these markers are the DN cells and are gated under marker M. Relative intensity of fluorescence are plotted along the X and Y axis. While the area under the curve shows the cell count (B). These DN cells were further analyzed for the distribution of DN1-DN4 subsets. A representative dot plot data from a 10 day old small and sick VAMP8^{-/-} mouse compared to a VAMP8^{+/-} mouse. The X and Y axis show the relative intensities of signal in the fluorescence channels plotted on log scale (C). Each dot represents a cell. The number of cells in the DN1 and DN4 stage was massively increased while the DN2 and DN3 cells were reduced (C). A histogram plot of six experiments (age 10-12 day) comparing the DN1-4 subsets on VAMP8^{-/-} small and sick mice to VAMP8^{+/-} littermate controls (D) There was a massive decrease in the absolute cell number of DN subsets with DN2 and DN3 being most severely reduced (E).

The anti CD44 antibody was conjugated with tricolor (TC) and CD25 antibody to fluorescein isothiocyanate (FITC). Therefore we could specifically count the DN cells labeled with FITC (CD25) and TC (CD44) and exclude the cells bearing PE label (Figure 3.9B). The

DN1-4 subsets were then analyzed for CD44 and CD25 expression depending on the signal intensity for FITC and TC fluorescence (Figure 3.9C).

Although we could detect all the DN subpopulations (DN1-DN4), there was a considerable difference in the percentage of these cells in the VAMP8^{-/-} small and sick mice compared to the VAMP8^{+/-} controls (Figure 3.9C, D). The absolute cell count of all the DN subsets was massively reduced with DN2 and DN3 cells being reduced by upto 13 and 12 folds respectively. DN1 and DN4 subsets were reduced by 1.2 and 1.4 folds respectively (Figure 3.9 E). The percentage of DN1 and DN4 cells progressively increased by 6.8 fold (33% compared to 5% in controls) and 2.3 fold (40% compared to 18% in controls) respectively in the VAMP8^{-/-} small and sick mice (9-12 days of age n=6) compared to the littermate VAMP8^{+/-} controls. The DN2 cells were reduced on an average by 3.3 (17% compared to 55% in controls) and DN3 by 2.3 folds (9% compared to 21% in controls) (Figure 3.9D). By contrast, the VAMP8^{-/-} small not sick mice did not show any difference in the DN subsets (Figure 3.10).

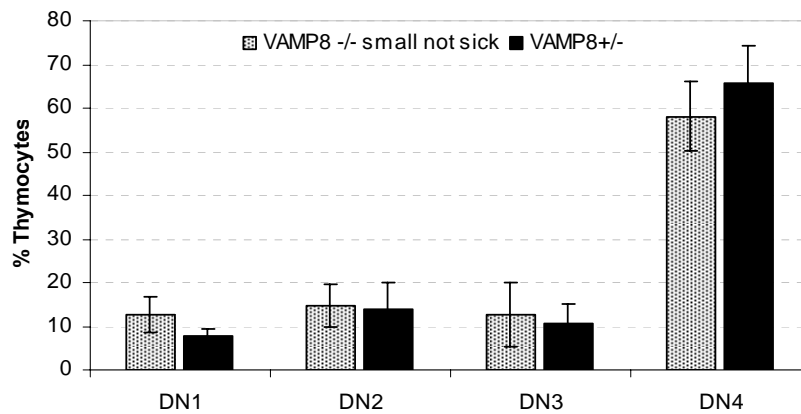


Figure 3.10. Analysis of DN1-4 thymocyte precursor subsets in small not sick VAMP8^{-/-} mice aged 10-12 days n=3. There was no difference in the distribution of the DN1-4 subsets in the thymus of VAMP8^{-/-} small not sick mice compared to VAMP8^{+/-} controls.

These results indicate that the ablation of VAMP8 causes a maturational defect in the thymocytes. There seems to be a transitional block at the DN1 and DN4 stages leading to an increased percentage of these cells. This could also explain the reduced percentage of cells in the DN2 and DN3 stages. The defect is characteristic of the very late stage of the phenotypic development i.e. in the small and sick mice.

3.3.2. Development of CD4/CD8 subsets is disturbed in sick VAMP8^{-/-} mice

Since the DN4 cells progress to CD4⁺CD8⁺ (DP) and eventually into CD8⁺ or CD4⁺, the observed disturbance DN subsets could result in an abnormal maturation of the CD4/CD8

cells. Therefore, we checked the distribution of the $CD4^+CD8^+$ and $CD4^+/CD8^+$ cells in the thymii of $VAMP8^{-/-}$ small and sick, $VAMP8^{-/-}$ small not sick and $VAMP8^{-/-}$ adult mice. Anti CD4 antibody was conjugated with PE and anti CD8 antibody with FITC. Therefore we could study the developmental stages of CD4/CD8 subsets depending on the signal intensity in the FITC and PE channel. The reduction in thymus cellularity (mentioned before) reflected in a reduced absolute cell number of all the CD4/CD8 subsets Table XIV.

Table XIV: Despite the increase in the percentages, the absolute number of thymocyte subsets was reduced in the small and sick mice (n=5) compared to the littermate controls

	CD4 CD8 DN (10^6)	CD4 CD8 DP (10^6)	CD4 SP (10^6)	CD8 SP (10^6)
$VAMP8^{-/-}$ small and sick	2.4 (± 1.4)	17.4 (± 18.4)	7.9 (± 2.0)	1.7 (± 0.4)
$VAMP8^{+/+}$ Control	9.5 (± 1.7)	225.2 (± 4.3)	21.7 (± 3.7)	6.8 (± 1.7)

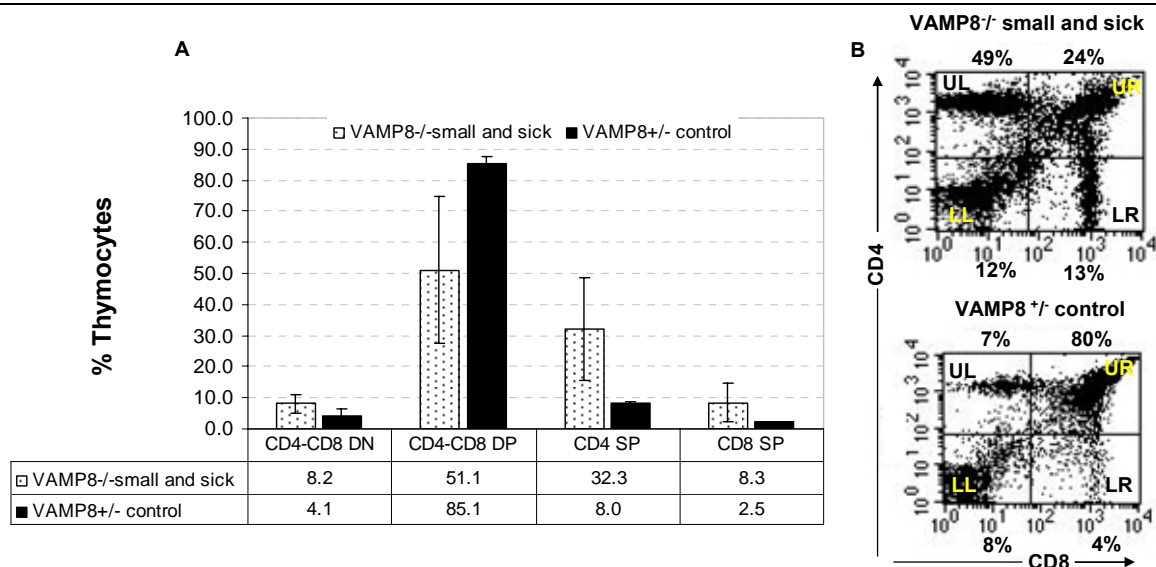


Figure 3.11. CD4/CD8 phenotyping of developing T lymphocytes from small and sick $VAMP8^{-/-}$ mice
Thymus from $VAMP8^{-/-}$ small and sick mice were stained with antibodies against CD4 and CD8 surface markers and analyzed for the CD4/CD8 expressing subsets. (n=5, 8-11 days) There was a massive decrease in the $CD4^+CD8^+$ (CD4 CD8 DP) and increase in the $CD4^+$ (CD4 SP) and $CD8^+$ (CD8 SP) cells in the $VAMP8^{-/-}$ thymus of small and sick mice compared to the controls (A). A representative dot plot data shows the distribution of the CD4/CD8 subsets. The $CD4^+$ cells appear in the upper left quadrant (UL), the $CD8^+$ cells appear in the lower right quadrant (LR), the $CD4^+CD8^+$ cells appear in the upper right quadrant (UR) while the $CD4^-CD8^-$ cells can be seen in the lower left quadrant (LL). The $VAMP8^{-/-}$ small and sick mice clearly have an increased number of cells in the UL ($CD4^+$), LR ($CD8^+$) and LL ($CD4^-CD8^-$) quadrants while there is reduced number of cells in the UR ($CD4^+CD8^+$) (lower dot plot) compared to the respective quadrants in the control (top dot plot) (B).

As seen from Figure 3.11, we could detect CD4/CD8 populations in the $VAMP8^{-/-}$ small and sick mice, however, there was a marked disturbance in all the developing subsets

(Figure 3.11). The percentage of CD4⁺ and CD8⁺ and CD4⁻ CD8⁻ cells showed a progressive increase. There were around 32% CD4⁺ cells in the thymus of small and sick VAMP8^{-/-} mice compared to 8% cells in the controls i.e. a 4 fold increase (Figure 3.11). VAMP8^{-/-} small and sick mice had 8% CD8⁺ cells compared to 2.5 % in VAMP8^{+/-} (3.3 fold increase). There were 8% CD4⁻CD8⁻ in the sick mice compared to 4% in the controls (2 fold increase). The CD4⁺CD8⁺ cells were drastically reduced. The VAMP8^{-/-} small and sick mice (n=5, 8-11 days) had 51% CD4⁺CD8⁺ cells while the control mice had 85% of these cells i.e. a decrease of upto 1.6 fold (Figure 3.11).

This disturbance in the CD4/CD8 bearing subsets of the developing T lymphocytes was found to be characteristic for the small and sick stage. The VAMP8^{-/-} small not sick mice (Figure 3.12) and the adult mice (Figure 3.13) showed a normal percentage of developing CD4/CD8 cells.

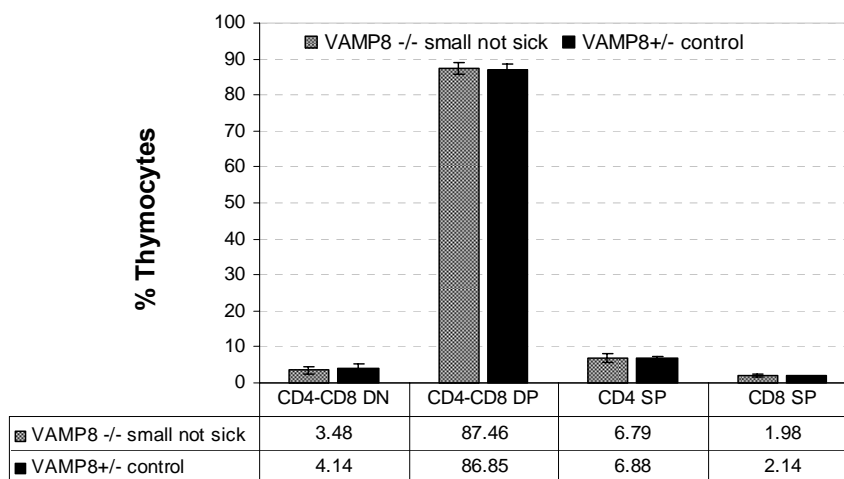


Figure 3.12. CD4/CD8 phenotyping from small not sick VAMP8^{-/-} mice (n= 3, age 8-12 days). There is no difference in the percentage of CD4/CD8 subsets between the test and the control mice

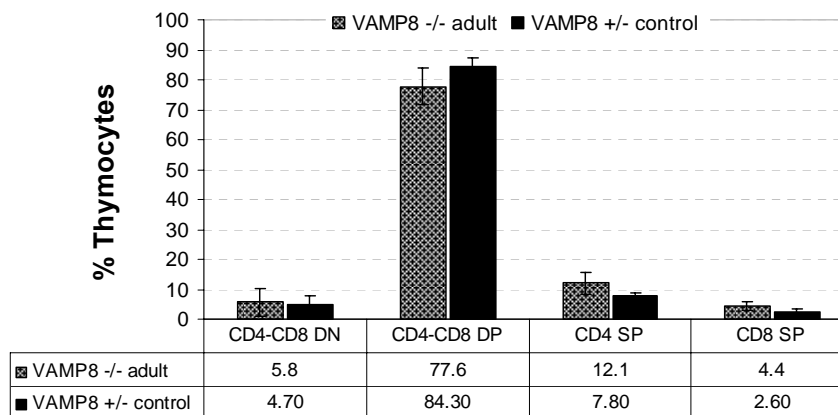


Figure 3.13. CD4/CD8 phenotyping from adult VAMP8^{-/-} mice (n= 5, age ≥ 1.5 months). There is no difference in the percentage of CD4/CD8 subsets between the test and the control mice

3.3.3. Development of CD4/CD8 subsets is disturbed in sick VAMP8^{-/-} Vti1b^{-/-} mice

Initial experiments on small and sick VAMP8^{-/-} Vti1b^{-/-} mice showed a similar disturbance in T lymphocytes development as the small and sick VAMP8^{-/-} mice (Ref. section 1.4.4). Further experiments were done on the thymus from small and sick as well as small not sick VAMP8^{-/-} Vti1b^{-/-} to confirm the results and generate statistically significant data sets. In this study it was confirmed that the small and sick VAMP8^{-/-} Vti1b^{-/-} mice also showed a disturbance in development similar to the small and sick VAMP8^{-/-} mice. There was a massive increase in the percentage of CD4⁺ cells in the small and sick VAMP8^{-/-} Vti1b^{-/-} mice. There were around 49% CD4⁺ cells in the sick mice compared to 20% in the control mice i.e. an increase by 2.5 fold (Figure 3.14A).

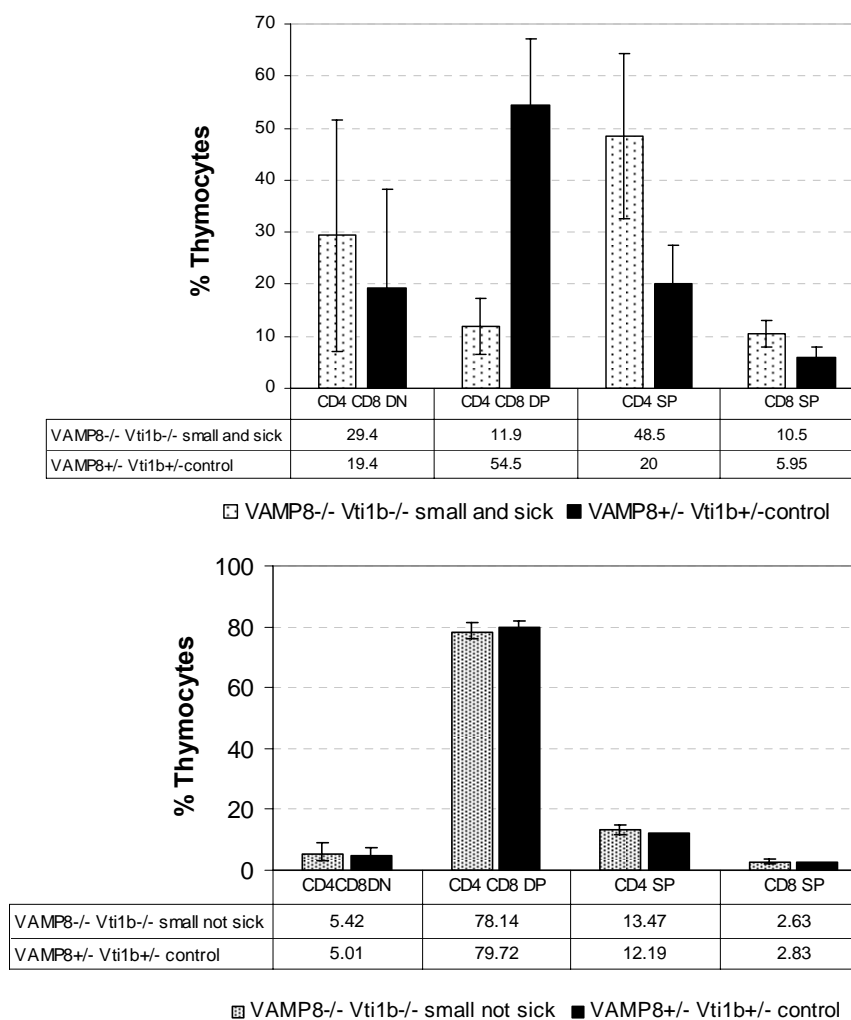


Figure 3.14. CD4/CD8 phenotyping of thymocytes from small not sick VAMP8^{-/-} Vti1b^{-/-} mice. CD4⁻CD8⁻ (CD4 CD8 DN), CD4⁺ (CD4 SP) and CD8⁺ (CD8 SP) were highly increased in the small and sick VAMP8^{-/-} Vti1b^{-/-} mice (n=5, aged 12-25 days) compared to the controls. CD4⁺CD8⁺ cells were reduced in these mice (A). This defect was not observed in the VAMP8^{-/-} Vti1b^{-/-} mice at the small but not sick stage (n=3, age 12-25 days) (B).

A similar two fold increase was seen in the CD8⁺ cells. The CD4⁺CD8⁺ cells were reduced by around 5 folds. The small and sick mice had 12% double positive cells (CD4⁺CD8⁺) compared to 55% in the control mice. However, no such difference was seen in the small but not sick stage of the VAMP8^{-/-} Vti1b^{-/-} mice (Figure 3.14B).

3.3.4. Vti1b^{-/-} mice do not show defect in T lymphocyte maturation

Further, it was interesting to know whether the loss of Vti1b in Vti1b^{-/-} mice also causes disturbance in T cell maturation. Thymocytes from 10-12 day old Vti1b^{-/-} mice were stained with antibodies against CD4 and CD8 surface markers (Figure 3.15). There was no difference in the percentage of CD4/CD8 bearing immature and mature T-lymphocytes between the Vti1b^{-/-} mice and the Vti1b^{+/+} controls.

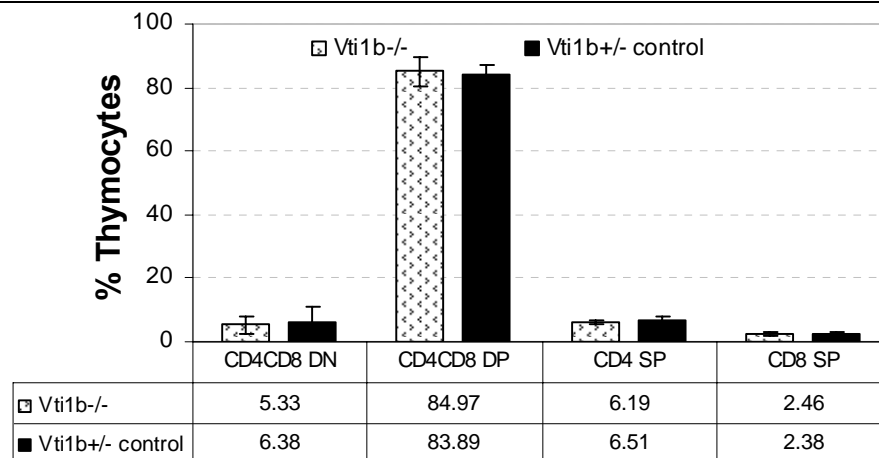


Figure 3.15.
CD4/CD8 phenotyping of thymocytes from Vti1b^{-/-} mice: Single cell suspension of thymii from Vti1b^{-/-} mice (n=3, age 10-12 days) stained for CD4 and CD8 surface markers. There is no difference in the distribution of CD4⁺ (CD4 SP),

CD8⁺ (CD8 SP), CD4⁻ CD8⁻ (CD4 CD8 DN) and CD4⁺ CD8⁺ (CD4 CD8 DP) cells in the Vti1b deficient thymii compared to Vti1b^{+/+} thymii.

3.3.5. T cell receptor expression unaltered in VAMP8^{-/-} small and sick mice

T cell receptor (TCR) is essential for signal transduction during T-cell development. It was interesting to study whether the loss of VAMP8^{-/-} causes any defect in the expression of the TCR molecules on the surface of cells derived from small and sick mice. Thymocytes from test and control mice were stained with FITC labeled antibodies against αβTCR. At first, the percentage of TCR positive cells was analyzed in both the VAMP8^{-/-} and VAMP8^{+/-} control mice. FACS analysis showed an increase in the percentage of TCR^{high} cells in the

VAMP8^{-/-} small and sick mice. This could be explained due to the massive increase in the percentage of $\alpha\beta$ TCR^{high}CD4⁺ and $\alpha\beta$ TCR^{high}CD8⁺ cells in the thymii of these mice as discussed previously (Figure 3.16A, B).

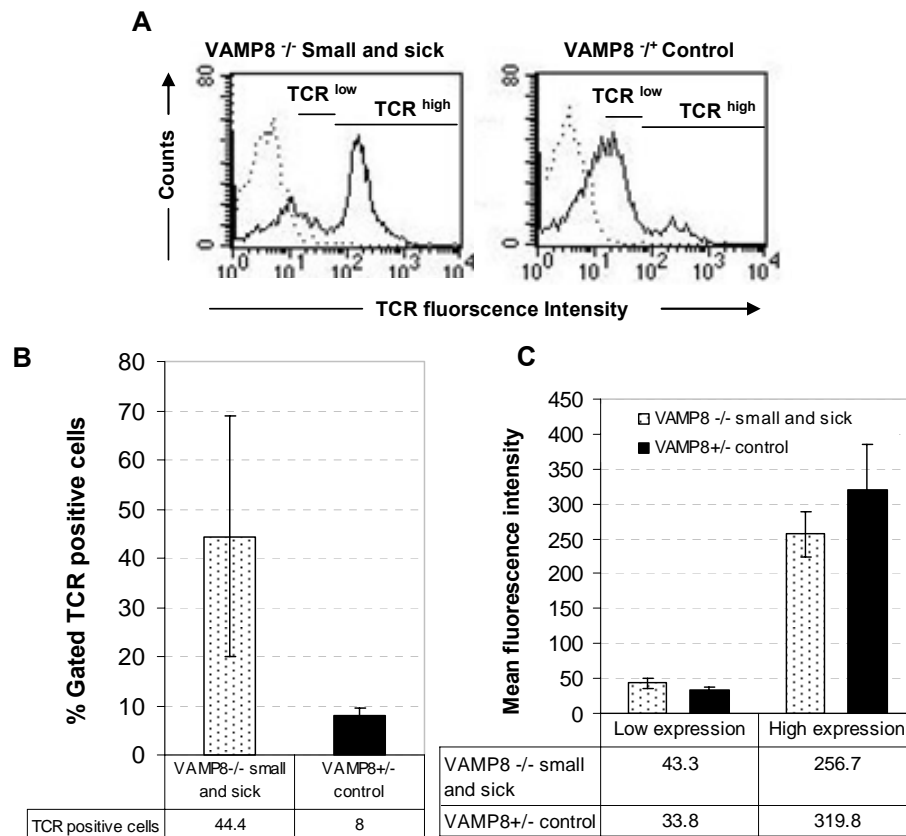


Figure 3.16. Analysis of TCR expression on the thymocytes from small and sick VAMP8^{-/-} mice: A representative area plot. (—) line depicts intensity signal from samples while (---) depicts signals from isotype control staining. The area under the — line curve shows the percentage of cells stained for TCR while the fluorescence intensity is depicted along the X axis. As seen from the area plot on left, the percentage of TCR^{high} cells is higher in the

VAMP8^{-/-} small and sick mice compared to the control. However, the intensity of signal as seen along the X axis is similar for the VAMP8^{-/-} small and sick mice and test mice (A). Graphical depiction of data from n=3 VAMP8^{-/-} small and sick mice aged 9-12 days showing an increase in the percentage of $\alpha\beta$ TCR^{high} cells (B). However, the mean intensity of TCR on the surface of the TCR positive cells is not significantly altered in the VAMP8^{-/-} small and sick mice compared to the VAMP8^{+/-} control mice (C).

Secondly, in order to study the surface expression of the TCR to the surface of the developing T lymphocytes, the intensity of TCR was quantified on the TCR⁺ T lymphocytes (Figure 3.16C). The reason behind these experiments was that if the trafficking of TCR to the surface of the thymocytes was blocked due to the lack of the late endosomal SNARE VAMP8, it could reflect as an altered intensity of TCR signal on cells. However, the mean intensity of TCR signal on high and low TCR expressing cells was found unaltered between thymii from VAMP8^{-/-} small and sick and the control mice (Figure

3.16C). Hence, the lack of VAMP8 does not cause a defect in the surface expression of TCR on the T-lymphocytes.

3.3.6. VAMP8 deficiency does not cause defect in adult peripheral T-cell reservoir

In order to know whether the peripheral repertoire of mature T lymphocytes was affected in the adult VAMP8^{-/-} mice, lymphocytes from the spleen of several adult (≥ 3.0 months) VAMP8^{-/-} mice were analyzed. The spleens were excised, homogenized and the erythrocytes were lysed. The remaining cells were stained with fluorescently labeled antibodies against CD4, CD8, CD3 surface markers for mature T lymphocytes, B220 marker for the B-lymphocytes and DX5 marker for the natural killer (NK) cells. Cells were also stained with annexinV and propidium iodide to visualize the extent of apoptosis in the cells from adult VAMP8^{-/-} spleens. We observed no significant difference in the repertoire of peripheral mature CD4⁺CD3⁺ and CD8⁺ CD3⁺ T lymphocytes, B-lymphocytes and NK cells in the adult VAMP8^{-/-} mice and the controls. The extent of annexin V and PI stained dead cells was also comparable between the adult VAMP8^{-/-} mice and the littermate VAMP8^{+/+} control mice (Figure 3.17).

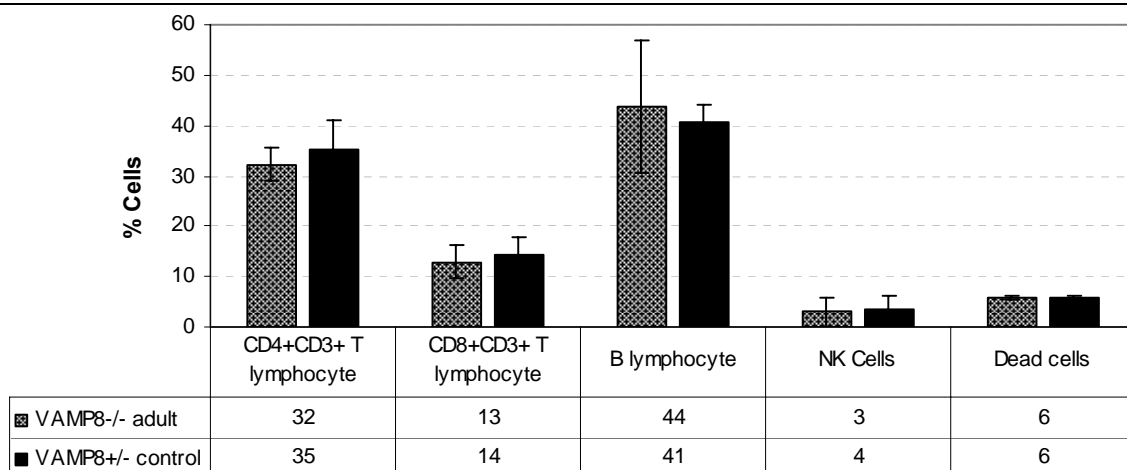


Figure 3.17. Analysis of peripheral repertoire of lymphocytes and natural killer cells from adult VAMP8^{-/-} mice: Adult VAMP8^{-/-} mice (n=4, age ≥ 3 months) show no difference in the distribution of mature T-lymphocyte populations CD4⁺ CD3⁺ and CD8⁺ CD3⁺, B lymphocytes stained with B220 surface marker, natural killer (NK) cells stained DX5 marker and dead cells co-stained with annexinV and propidium iodide (PI) in the spleen compared to VAMP8^{+/+} control mice.

3.4. Thymocytes show high cell death

3.4.1. Thymus from small and sick mice have high cell death *in vivo*

The initial analysis of VAMP8^{-/-} Vti1b^{-/-} mice showed a high number of dead cells in the thymus. Figure 3.18A is a TUNNEL stained thymus section from a 2 month old wild type mouse showing basal level of apoptosis present in the thymus at any point of time (Ref. section 1.4.4 and Figure 3.18A, black spots represent dead cells). The thymus from 2 months old VAMP8^{-/-} Vti1b^{-/-} adult mouse appeared very similar to the wild type, with a few scattered dead cells (Ref. section 1.4.3 and Figure 3.18B). However, the thymus of ~1 month old small and sick VAMP8^{-/-} Vti1b^{-/-} mouse showed a massive number of dead cells either localized to the periphery or scattered out in the lobe in TUNNEL staining (Ref. section 1.4.3 and Figure 3.18D).

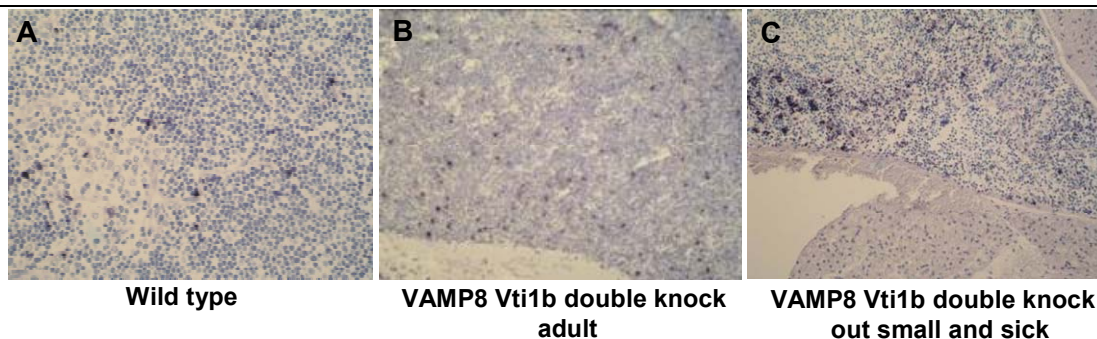


Figure 3.18. Thymus from small and sick VAMP8^{-/-} Vti1b^{-/-} mice show high number of dead cells: Histological staining of thymus sections to detect dead cells. TUNNEL staining of thymus sections from a 2 months old wild type (A) and VAMP8^{-/-} Vti1b^{-/-} (B) mouse show a few dead cells stained in black. TUNNEL staining of sections from small and sick VAMP8^{-/-} Vti1b^{-/-} mouse also shows a massive amount of dead cells (C). *Histological staining done by Dr. Afshin Fayyazi at the Department of Pathology, Georg August Universität Göttingen.

In this work, apoptosis was studied in thymus from small and sick VAMP8^{-/-} mice. Freshly prepared single cell suspensions of thymus were stained with annexinV and propidium iodide (PI) (Figure 3.19). Under normal conditions, phosphatidylserine (PS) is almost completely confined to the inner leaflet of the plasma membrane by ATP dependent translocases called flippases. However, as one of the first hallmarks of apoptosis, the activity of flippases is down regulated resulting in exposure of PS residues to the outer leaflet of the plasma membrane. Annexin V is a calcium dependent phospholipid binding

protein that can bind to the exposed PS. Therefore, chromophore (FITC) conjugated annexinV is used to detect early apoptotic cells (Figure 3.19, dot plot: upper left UL quadrant).

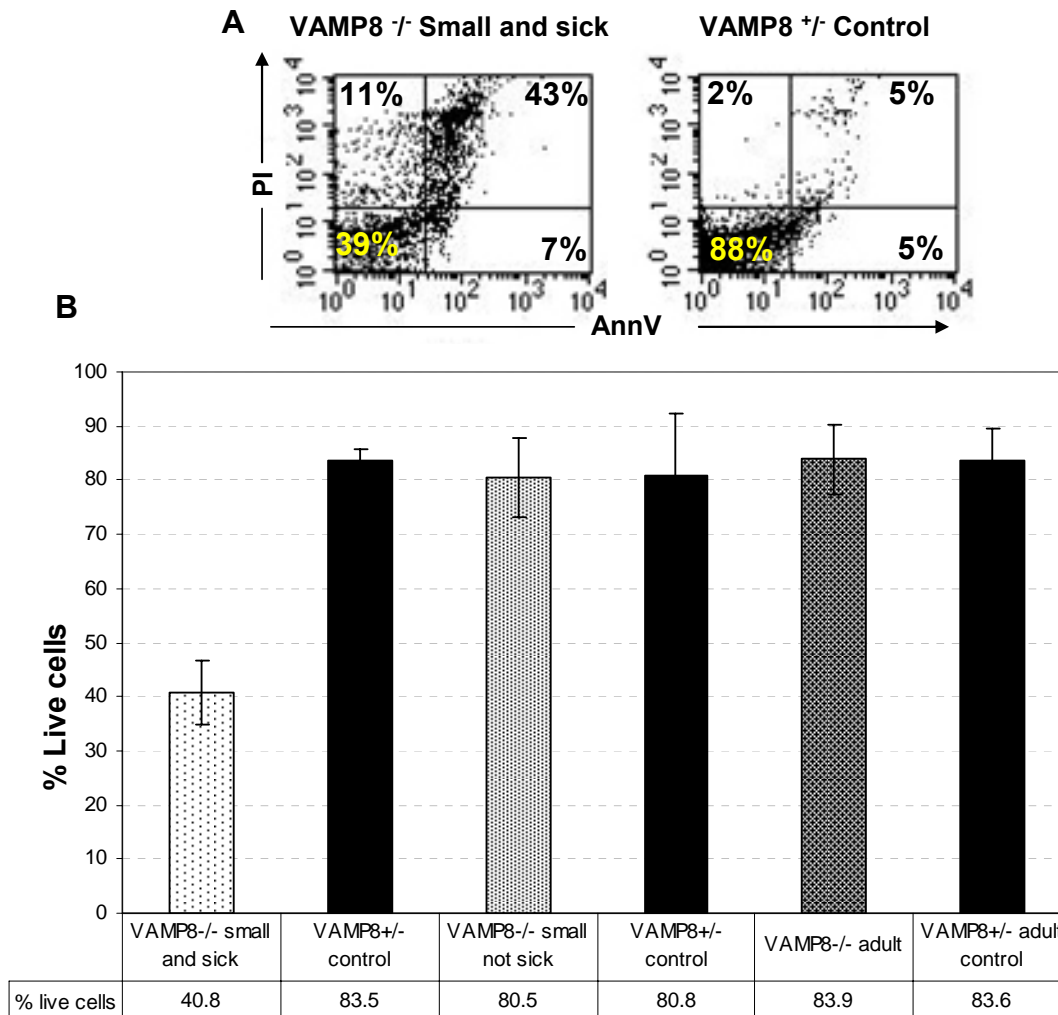


Figure 3.19. Analysis of dead cells in the thymus of small and sick VAMP8^{-/-} mice: A representative dot plot data showing dead cells stained with annexinV (LR Quadrant), propidium iodide (UL), annexinV and propidium iodide (UR) and live cells in the LL quadrant. The VAMP8^{-/-}/small and sick mice clearly have an increased number of dead cells in the UL, UR and LR quadrants and massively reduced live cells (right dot plot) compared to the control (left dot plot (B)) Thymocytes from small and sick mice (n=4, age 8-13 days) show a much lower number of live cells compared to heterozygous littermate controls. This high cell death was not seen in the thymocytes from VAMP8^{-/-} small but not sick (n=3, age 10-12 days) and the adult mice (n=6, age 1.5-2.5 months).

Secondly, in the intact cells, the plasma membrane is impermeable to dyes that can intercalate and stain the DNA. In advanced apoptosis, however, the plasma membrane

becomes increasingly permeable such that dyes like propidium iodide (PI) can readily enter the cell and intercalate into the DNA. Hence cells in later apoptotic stages can be identified by PI staining (Figure 3.19, dot plot: upper right (UR) quadrant). Generally late apoptosis is detected by co-staining the cells with annexinV and PI. Necrotic cells on the other hand do not expose PS to the outer membrane and are hence not detected by annexinV staining. These cells are stained only for PI (Figure 3.19, dot plot: lower right LR quadrant). The live cells with intact membrane and DNA remain unstained and appear in the lower left LL quadrant of the dot plot (Figure 3.19).

Quantification of the live cells from the lower left quadrant of the dot plots revealed that there were just around 41% live cells in the VAMP8^{-/-} thymii compared to 83% live cells in the controls (Figure 3.19B). The remaining cells in the VAMP8^{-/-} thymii were stained either with annexinV or PI or both, indicating a massive cell death in the thymus of the small and sick VAMP8^{-/-} mice. This high cell death was not observed in the thymocytes from VAMP8^{-/-} small but not sick and VAMP8^{-/-} adult mice (Figure 3.19B).

The observed reduction of cellularity and increased cell death could be caused due to an increased susceptibility of the thymocytes to physiological apoptotic stimulus. In order to investigate this possibility, the sensitivity of the thymocytes towards induced apoptosis was studied *in vitro* using several cell death inducing factors.

3.4.2. Dexamethasone induced apoptosis

3.4.2.1. Thymocytes from VAMP8^{-/-} small not sick are sensitive to apoptosis

At first, dexamethasone, a synthetic glucocorticoid hormone, was used as the apoptosis stimulus. Glucocorticoid hormones are known to induce apoptosis in the thymus under physiological conditions and are especially important during the retraction of thymus at adulthood.

Thymocytes from VAMP8^{-/-} small and sick, small not sick and adult mice were treated with 0.1 μ M dexamethasone for 0hr, 3hr and 6 hr in a time course apoptosis assay. Additionally, at each time point there was an untreated control to study spontaneous apoptosis with time.

Two parallel methods were used for the detection of dead cells. In the first method, after each time point the apoptotic and dead cells were stained with annexin V and propidium iodide (PI) and counted in BD FACScan. The live cells were quantified from the lower left quadrant of the dot plot. In the second method, the cells were subjected to sub G1 peak analysis. The cells were fixed in ethanol after each time point and stained with PI. The extent to which PI intercalates in the DNA depends on the DNA content of the cells. Therefore the cells in the normal cell cycle appear as distinct peaks corresponding to the G1, S, or G2 stages. The dead cells on the other hand have small, fragmented DNA that appears as a G_0 peak just before the G1 peak in the area plot.

The thymocytes from the $VAMP8^{-/-}$ small but not sick mice aged day 10-12 were more susceptible to dexamethasone induced cell death compared to the littermate $VAMP8^{+/+}$ controls (Figure 3.20, 3.21).

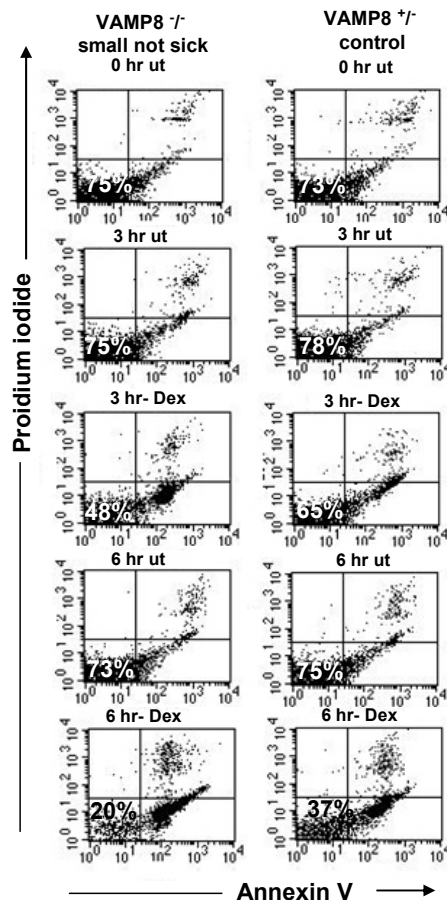


Figure 3.20. Thymocytes from small not sick $VAMP8^{-/-}$ mice show high sensitivity to cell death (dexamethasone treatment): A representative dot plot data for dexamethasone induced apoptosis in $VAMP8^{-/-}$ small not sick mice. For each time point there was one un-induced (ut) sample and one sample treated with $0.1\mu\text{M}$ Dexamethasone (Dex) for 0, 3 and 6 hours. The cells were stained with FITC labeled annexin V and PI. The annexin V labeled apoptotic cells appear in the lower right quadrant, The propidium iodide stained cells appear in the upper left quadrant, the annexin V/PI co stained cells appear in the upper right quadrant while the unstained live cells appear in the lower left quadrant. The live cells were quantified from the lower left quadrant and the induction was measured by subtracting the live cells in the treated sample from the untreated sample at the same time point. It was observed that after 3 and 6 hours of treatment, a larger number of cells underwent apoptosis in the $VAMP8^{-/-}$ small and sick mouse compared to the $VAMP8^{+/+}$ control mouse. The affect being most pronounced after 3 hours of treatment.

There were lower number of live cells after 3 and 6 hours of treatment in thymus from VAMP8^{-/-} small not sick compared to the control mice. The affect was most pronounced after 3 hours of treatment. A dot plot data for dexamethasone induced apoptosis assay is shown in figure 3.20. A lower number of live cells can be seen in the lower left quadrant of the dot plots in the treated samples of a small not sick mouse compared to the controls (Figure 3.20).

Several independent experiments confirmed this result. On an average, the live cells in the VAMP8^{-/-} thymus were reduced by 29% points (from 77% to 48%) compared to 14% points reduction (from 78% live cells to 65%) in the controls after 3 hours of treatment (Figure 3.21). After 6 hours of treatment, the VAMP8^{-/-} mice showed average 27% live cells compared to 40% in the controls.

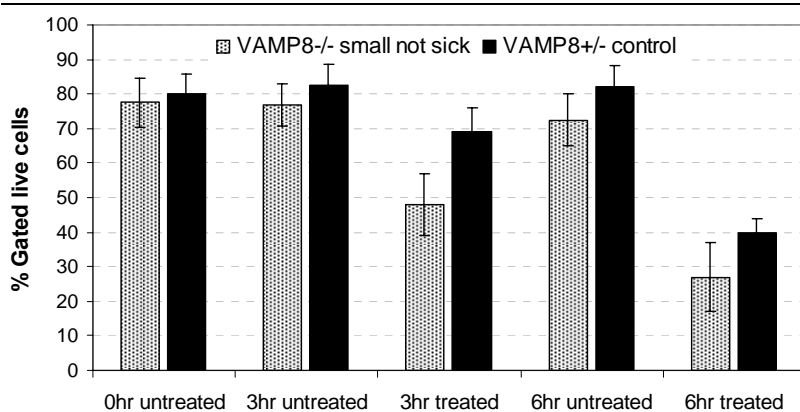


Figure 3.21. Thymocytes from small not sick VAMP8^{-/-} mice show high sensitivity to cell death (dexamethasone treatment): The thymocytes from small not sick VAMP8^{-/-} mice (n=3, 10-12 days old) were treated with 0.1μM dexamethasone for several time points. The samples were fixed stained with annexin V and propidium iodide. The live cells were quantified. The thymus from VAMP8^{-/-} small but not sick mice showed a lower number of live cells after treatment with dexamethasone. After 3 hours of treatment the effect was most pronounced, there was 29% point reduction in live cells in VAMP8^{-/-} thymii compared to around 14% points in the controls.

Treatment	VAMP 8 ^{-/-} small not sick		VAMP 8 ^{+/-} control	
0 hr untreated	78	±5.6	88	±7.2
3hr untreated	77	±6.1	83	±5.9
3hr treated	48	±6.9	69	±8.8
6hr untreated	72	±6.1	82	±7.5
6hr treated	27	±10.0	40	±4.8

The increased susceptibility of thymocytes from VAMP8^{-/-} small and sick mice was confirmed by Sub G1 peak assay. In this method of detection, the most pronounced effect was observed after 6 hours. While apoptosis was induce in 13% cells in the VAMP8^{-/-} thymocytes after 3 hours, the wild type thymus showed 9% induction. After 6 hours of the

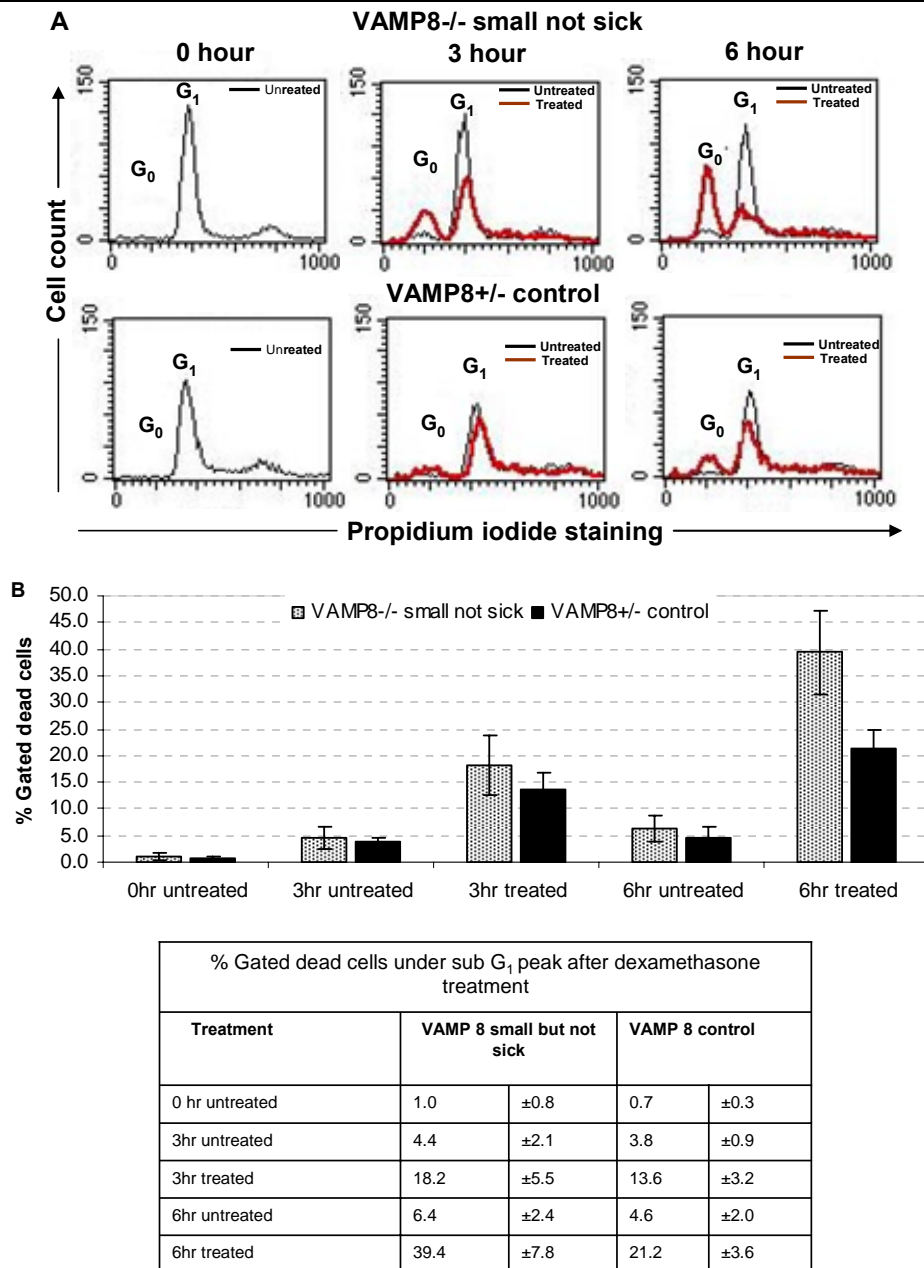


Figure 3.22. Thymocytes from small not sick VAMP8^{-/-} mice show high sensitivity to cell death (dexamethasone treatment): The thymocytes from small not sick VAMP8 mice treated with 0.1 μ M dexamethasone for several time points. The samples were fixed in ethanol and stained with propidium iodide. The dead cells under the G₀ peak were counted. The – line shows untreated control samples while the – line shows the treated samples. The area under the curve represents the cell counts while the intensity of PI staining is depicted on the X axis. The thymus from VAMP8 small but not sick mice had a higher number of dead cells after treatment with dexamethasone for 3 and 6 hours (A). On an average, after 3 hours of treatment, cell death was induced in 13% of thymocytes in thymus from VAMP8^{-/-} mice (n=3, 10-12 days old) compared to 9.8% in the wild type. The effect was more pronounced after 6 hours of treatment, VAMP8^{-/-} thymocytes showed average 33% induction of cell death compared to 16% induction in the control thymii (B).

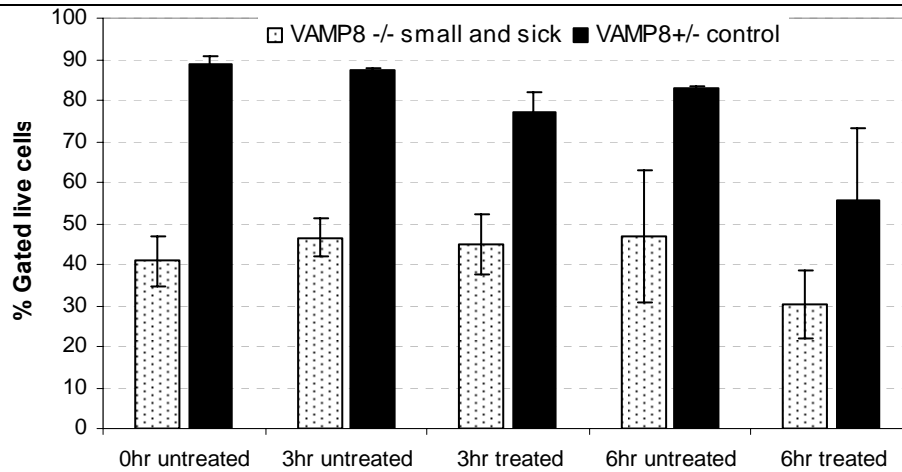
treatment, the induced cell death increased by around 33% points in the thymus from small and sick mice compared to 18% points in the control mice (Figure 3.22).

The two detection methods give slightly varying results because we detect different populations of apoptotic cells with the two methods. Since exposure of phosphatidylserine is one of the earliest hallmarks of apoptosis, annexin V stains the early apoptotic cells. Hence we visualize high numbers of early apoptotic cells within 3 hours after the treatment with annexinV staining method. In the sub G1 peak assay however, the cells are stained with the DNA intercalating dye PI. DNA fragmentation is a feature of late apoptotic stage, hence in this method of detection, late apoptotic cells with highly fragmented DNA are counted. Therefore there were low number of sub G1 cells early on and higher number sub G1 cells after longer periods of induction with Dexamethasone. These experiments clearly show that the thymocytes from *VAMP8*^{-/-} small not sick mice shows increased susceptibility apoptosis upon dexamethasone treatment.

*3.4.2.2. Few live thymocytes in *VAMP8*^{-/-} sick mice: not sensitive to induction*

The next question was whether the thymocytes from the small and sick mice were also susceptible to dexamethasone induced apoptosis. Thymocytes from *VAMP8*^{-/-} small and sick mice aged day 8-13, were treated with 0.1 μ M dexamethasone for several time points and analyzed.

As described before, we observed very few live cells in the thymus of *VAMP8*^{-/-} sick mice at the start of the experiment (i.e. 0hr time point). There were only around 41% live cells compared to 88% in the control mice. After treatment with dexamethasone, the live cells from the control mice showed a reduction both after 3 hours (~ 10% points) and 6 hours (~ 27% points) compared to untreated samples. In small and sick mice however, there was no substantial induction of apoptosis by dexamethasone after 3 hours. There was a reduction in the live cells by 16% points only after 6 hours of treatment (Figure 3.23).



% Gated live cells after dexamethasone treatment; annexin V/PI staining				
Treatment	VAMP 8 small and sick		VAMP 8 control	
0 hr untreated	40.8	±5.9	88.5	±2.3
3hr untreated	46.4	±9.6	87.1	±6.7
3hr treated	44.8	±7.4	77.2	±4.6
6hr untreated	46.9	±16.0	82.8	±0.7
6hr treated	30.4	±8.3	55.6	±17

Figure 3.23. Few live thymocytes in small and sick VAMP8^{-/-} mice: not exceptionally sensitive to (dexamethasone treatment): The thymocytes from VAMP8^{-/-} small and sick (n=4, aged 8-13 days) and littermate control were treated with 0.1 μ M dexamethasone for several time points. The dead cells were stained with annexinV and PI and the percentage of live cells were calculated by subtracting the percentage of dead cells from the percentage of total counted cells. Around 60% of the cells were dead in the thymus of small and sick mice at the beginning of the experiment compared to just about 12% in the control mice. The treatment induced apoptosis in the thymocytes from control mice with time. However, there was no induction of apoptosis in the thymocytes from small and sick mice after 3 hours of treatment and around induction 16 % compared to 27% induction in the control thymocytes after 6 hours.

In the second detection method by sub G1 peak analysis, we had similar observations. There were around 20% dead cells in the thymus from small and sick mice compared to less than 2% in the controls. But we could not induce any substantial apoptosis in the already few live cells in the thymii of small and sick mice. (Figure 3.24).

This is possibly because the most susceptible populations of the thymocytes in the VAMP8^{-/-} small and sick mice were already dead at the time point 0h and the remaining live cells could withstand the dexamethasone treatment.

It is possible that the cells at the VAMP8^{-/-} small not sick stage become increasingly sensitive to cell death and the most sensitive populations of cells die rapidly. This could

also explain why most of the cells are dead by the time the mice reach the small and sick stage and the surviving cells are more resistant to the treatment. Therefore we carried out the experiments with other apoptotic stimuli only on the thymus from VAMP8^{-/-} small not sick mice.

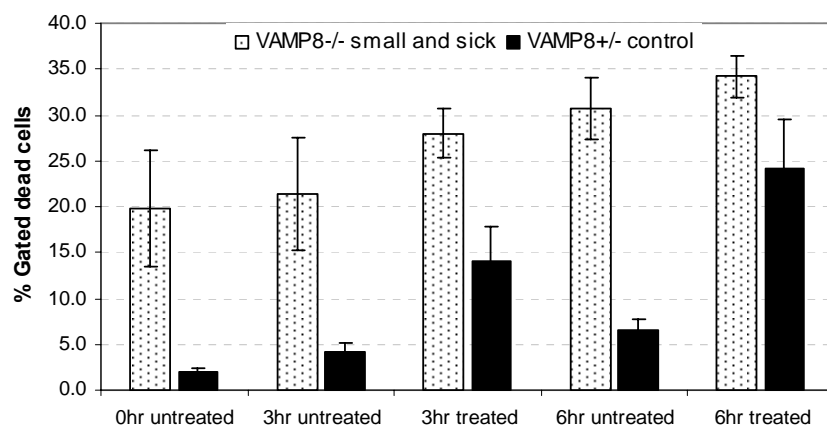


Figure 3.24. Few live Thymocytes in small and sick VAMP8^{-/-} mice: not increasingly sensitive to (dexamethasone treatment): Thymocytes from VAMP8^{-/-} small and sick (n=4, aged 8-13 days) and littermate control were treated with 0.1 μM dexamethasone for several time points. The cells were fixed in ethanol and stained with PI. The dead cells stained in PI were counted in cell sorter and analyzed for a Sub G1 DNA peak. At the start of the experiment, there were around 20% dead cells in the VAMP8^{-/-} mice compared to less than 2% in the control thymii (10 fold higher). The number of dead cells rose steadily with induction in the control

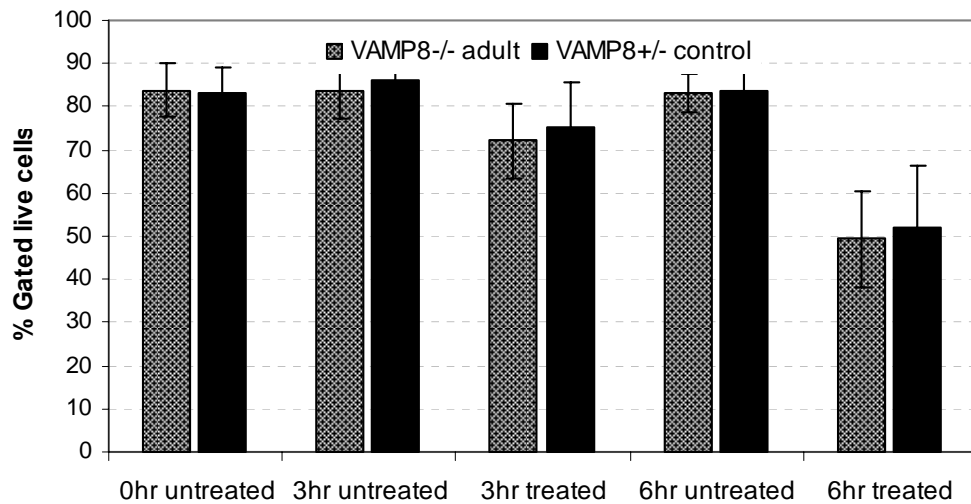
% Gated dead cells after dexamethasone treatment under sub G ₁ peak				
Treatment	VAMP 8 small not sick		VAMP 8 control	
0 hr untreated	19.8	±6.4	1.9	±0.5
3hr untreated	21.4	±6.1	4.2	±0.9
3hr treated	28.0	±2.7	14.1	±3.8
6hr untreated	30.7	±3.4	6.5	±1.3
6hr treated	34.2	±2.3	24.2	±5.4

samples however there was hardly any induction of apoptosis in the thymocytes from the knock out mice.

3.4.2.3. Thymocytes from adult mice: no increased sensitivity to apoptosis

The susceptibility of thymocytes from the adult VAMP8^{-/-} mice towards dexamethasone induced apoptosis was also checked. Single cell suspensions of thymocytes from adult VAMP8 mice age ≥ 1.5 months were treated with 0.1 μM dexamethasone for different time points and analyzed. The number of live cells after each time point of treatment were similar in both the samples indicating a comparable amount of apoptosis in thymocytes of both, VAMP8^{-/-} adult and VAMP8^{+/-} control mice. (Figure 3.25). After 3 hours of induction, live cells were reduced by 11% points compared to the untreated samples in the

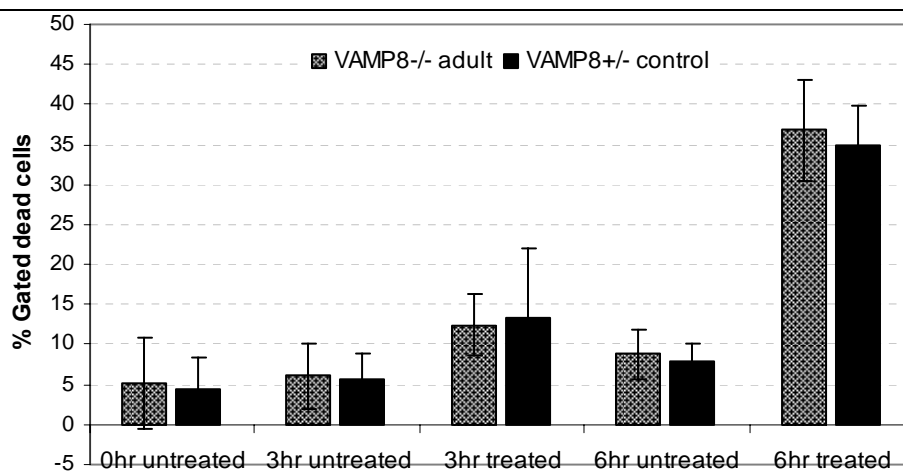
VAMP8^{-/-} adult and control mice. After 6 hours of treatment, live cells were reduced by around 34% points in thymocytes from both the genotypes (Figure 3.25).



% Gated live cells after dexamethasone treatment annexin V/PI staining				
Treatment	VAMP 8 adult		VAMP 8 control	
0 hr untreated	83.9	±6.1	83.3	±5.9
3hr untreated	83.8	±6.8	86.0	±6.5
3hr treated	72.1	±8.8	75.3	±10.2
6hr untreated	83.1	±4.3	83.8	±4.8
6hr treated	49.3	±11.0	51.8	±14.4

Figure 3.25. Thymocytes from adult VAMP8^{-/-} mice do not show high sensitivity to cell death (dexamethasone treatment): Thymocytes from adult VAMP8^{-/-} (n=6, age ≥ 1.5 months) and littermate control mice treated with 0.1μM dexamethasone. The dead cells were stained with annexinV and propidium iodide and the live cells were calculated by subtracting dead cells from the total counted cells. There is no difference in the percentage of live cells after the treatment between the two genotypes.

We could confirm the same finding in the sub G1 assay. The number of dead cells, after treatment at different time points, was comparable between the VAMP8^{-/-} adult and the control mice (Figure 3.26). After 3 hours around 6% cells and after 6 hours, around 28% cells were induced to undergo apoptosis in both, the thymocytes from VAMP8^{-/-} adult and the VAMP8 heterozygous controls.



% Gated dead cells after dexamethasone treatment under sub G ₁ peak				
Treatment	VAMP 8 adult		VAMP 8 control	
0 hr untreated	5.0	±5.6	4.3	±4.0
3hr untreated	6.0	±4.1	5.5	±3.2
3hr treated	12.3	±3.8	13.2	±6.6
6hr untreated	8.7	±3.1	7.9	±2.2
6hr treated	36.7	±6.4	34.8	±5.1

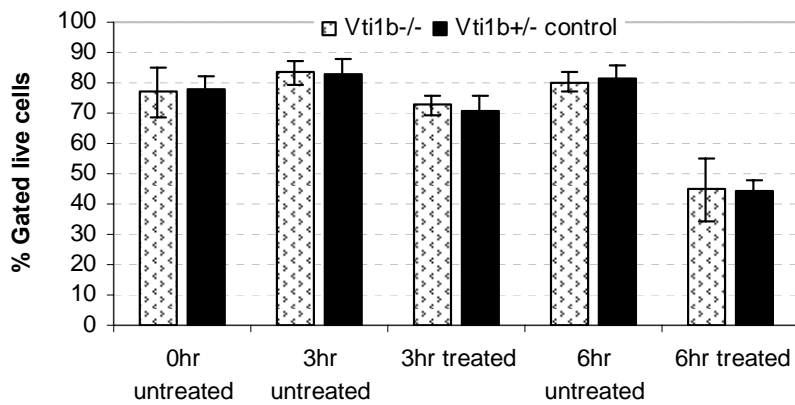
Figure 3.26. Thymocytes from adult VAMP8^{-/-} mice do not show high sensitivity to cell death (dexamethasone treatment): Thymocytes from adult VAMP8^{-/-} (n=6, age ≥ 1.5 months) and littermate control mice treated with 0.1μM dexamethasone. The cells were fixed in ethanol and stained with propidium iodide. There was no difference in the percentage of dead cells in the VAMP8 null adult and the control mice after different time points of treatment.

3.4.2.4. Thymocytes from *Vti1b*^{-/-} mice: no increased sensitivity to apoptosis

The next question was whether the thymocytes from *Vti1b*^{-/-} mice are also more susceptible to dexamethasone induced apoptosis. Thymii from *Vti1b*^{-/-} mice day 10-12 (n=4) were treated with 0.1μM of Dexamethasone and detection was done using annexin V and PI staining and by Sub G1 peak assay.

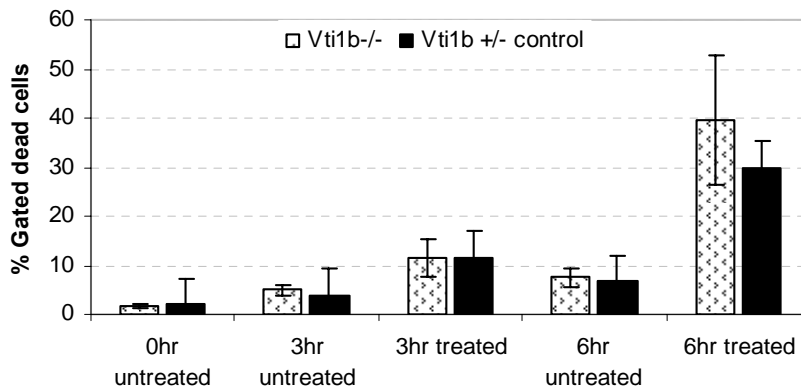
There was no difference in the number of live cells in the *Vti1b*^{+/+} control and the *Vti1b*^{-/-} mice after several time points. Apoptosis was induced in around 12% cells after 3 hours and 36% after 6 hours in both, the *Vti1b*^{+/+} control and *Vti1b*^{-/-} out mice (Figure 3.27).

This was confirmed in the Sub G1 peak assay. The number of dead cells after several intervals of dexamethasone treatment was similar in the *Vti1b*^{-/-} mice and the *Vti1b*^{+/-} controls (Figure 3.28).



Treatment	Vti1b knock out		Vti1b control	
0 hr untreated	76.8	±8.0	77.7	±4.5
3hr untreated	83.5	±3.9	83.21	±4.8
3hr treated	72.58	±3.1	70.43	±5.5
6hr untreated	80.33	±3.0	81.32	±4.3
6hr treated	44.85	±10.3	44.13	±3.8

Figure 3.27. Thymocytes from Vti1b^{-/-} mice do not show high sensitivity to cell death (dexamethasone treatment) Thymocytes from Vti1b^{-/-} 10-12 days mice (n=4) and littermate controls were subjected to 0.1μM dexamethasone treatment for several intervals of time. The cells were stained with annexin V and propidium iodide and counted in cytometer. The live cells were calculated by subtracting the dead cells from the total counted cells. There was no difference in the number of live cells between Vti1b^{-/-} and Vti1b^{+/+} controls after treatment at 3 hours and 6 hours.



Treatment	Vti1b knock out		Vti1b control	
0 hr untreated	1.6	±0.4	1.9	±1.2
3hr untreated	4.9	±0.9	3.8	±0.5
3hr treated	11.4	±3.9	11.6	±1.1
6hr untreated	7.4	±1.9	6.7	±2.5
6hr treated	39.6	±13.2	29.8	±5.3

Figure 3.28. Thymocytes from Vti1b^{-/-} mice do not show high sensitivity to cell death (dexamethasone treatment) Thymocytes from Vti1b^{-/-} 10-12 days mice (n=4) and littermate controls were subjected to 0.1μM dexamethasone treatment for several intervals of time. The cells were fixed in ethanol and propidium iodide. There was no difference in the number of cells undergoing induced apoptosis between the Vti1b knock out mice and the controls, after treatment at 3 hours and 6 hours

3.4.3. FAS induced apoptosis

Under physiological conditions, several cells in the thymus undergo apoptotic death via FAS mediated pathway. In order to see if the thymocytes from the VAMP8^{-/-} small not sick stage were also more susceptible towards FAS induced cell death, thymocytes were treated with 1.0µg of anti-FAS antibody. The exogenously applied antibody cross links the FAS receptors on the surface of the cells and induces the death cascade. Detection of dead cells was done by annexinV and propidium iodide co-staining. Live cells were quantified from the lower left quadrant of the dot plot and the percentage of induction was calculated by subtracting the percentage of live cells in the treated samples from that of the untreated samples at each time point.

Thymocytes from VAMP8^{-/-} small not sick mice were more susceptible to FAS induced cell death. After 3 hours of treatment there was 11.4% induction in VAMP8^{-/-} thymocytes compared to 3.8% in the control (i.e. 7.6% points higher induction). After 6 hours of treatment, the effect was even more pronounced. The percentage of apoptosis induction in the controls was 5.7% compared to 16.7% in the VAMP8^{-/-} mice, a 3 fold higher induction in the small not sick VAMP8^{-/-} mice (Figure 3.29). This confirmed our previous findings with dexamethasone treatment.

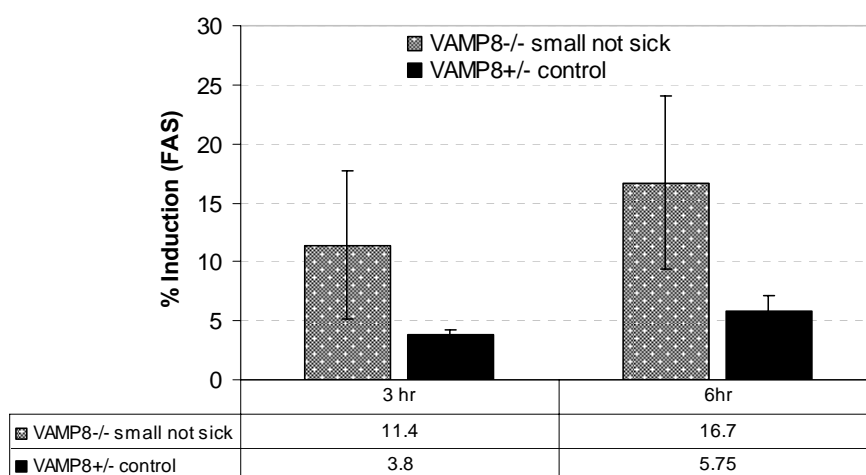


Figure 3.29. Thymocytes from small not sick VAMP8^{-/-} mice show high sensitivity to cell death (anti-FAS antibody treatment): Thymocytes from VAMP8^{-/-} small but not sick (n=4, 8-10days) and littermate control mice treated with anti-FAS antibody for several time points. The thymocytes from the VAMP8^{-/-} small

not sick mice show a high sensitivity to 1.0µg of anti FAS antibody treatment after 3 and 6 hours of treatment. After 3 hours there was 11% induction in the small not sick mice compared to 3.8% in the control mice i.e. 7.6% more induction. After 6 hours of treatment there was a 10% more induction in the small not sick mice compared to control mice.

3.4.2. Apoptosis by crosslinking with anti CD3 and anti CD28 antibodies

Further the thymocytes were checked for their sensitivity to apoptosis by crosslinking with CD3 and CD28 antibodies. This treatment mimicks the physiological condition where a very strong cross-linking of TCR-CD3 leads to enhanced signaling, which in turn commits the T lymphocytes to cell death. Thymocytes were incubated in ELISA plated pre-coated with anti-CD3 or anti-CD3+CD28 antibodies. Dead cells were detected by staining with annexinV and propidium iodide. Live cells were quantified from the lower left quadrant of the dot plot. The percentage of induction of apoptosis was calculated by subtracting the percentage of live cells in the treated samples from the untreated samples at each time point.

We also tried to induce apoptosis by treating the cells with antibodies solution. However, there was no induction of apoptosis after treatment for 3-6 hours by this method. This could possibly be because there is not enough physical interaction between the thymocytes and the antibodies when they are left free in the solution. In addition, in some previous studies it was seen that the use of anti-CD28 together with anti-CD3 suppresses the induction effect. In order to check this possibility, initial experiments were done where anti CD3 antibody alone as well as anti- CD3 and CD28 together were used to induce apoptosis in parallel samples of thymocytes of VAMP8^{-/-} small not sick and VAMP8^{+/-} controls. It was seen that the induction with anti-CD3 alone was much less compared to co-stimulation with anti CD3+CD28 antibodies. Also there was a large variation in the data obtained from several different experiments. Hence it was confirmed that CD28 does not suppress in-vitro induction of apoptosis, rather it strengthens the stimulus. Therefore, the next experiments were done with anti-CD3 and CD28 co-stimulation.

The thymocytes from VAMP8^{-/-} small not sick mice were more sensitive to anti CD3-CD28 treatment. After 6 hours, there was 18% induction of apoptosis in thymocytes from VAMP8^{-/-} small not sick compared to 10% in the controls. While after 24 hours, the

thymocytes from VAMP8^{-/-} small not sick mice had more than 44% induction compared to 22% in the controls (Figure 3.30). Thus we confirm that the thymocytes from the small but not sick mice are more susceptible to stimulus induced apoptosis.

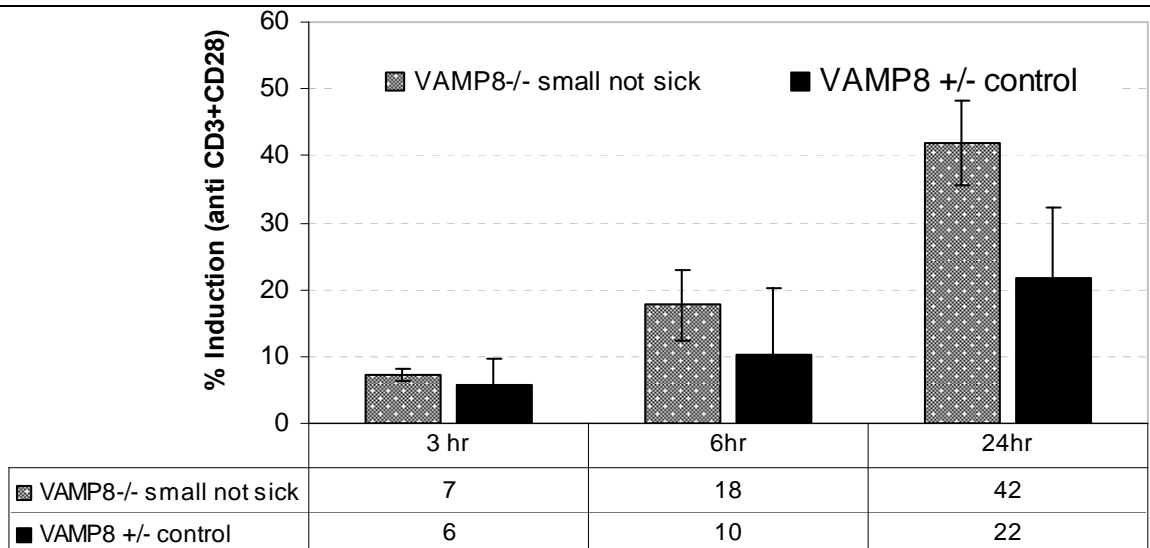


Figure 3.30. Thymocytes from small not sick VAMP8^{-/-} mice show high sensitivity to cell death (anti-CD3+CD28 antibody treatment): Freshly excised thymocytes from small not sick VAMP8^{-/-} mice (n=4, age 8-10 days) were co-stimulated with anti CD3 and CD28 antibodies for 3, 6 and 24 hours. Thymocytes from small not sick VAMP8^{-/-} mice showed a higher susceptibility to apoptosis after 24 hours of treatment compared to controls. The control mice showed a 20% induction after 24 hours in comparison to 44% in the VAMP8^{-/-} mice i.e. a 24% higher induction compared to the control mice.

A delayed response to CD3-CD28 treatment is possibly because CD3 crosslinking induces a different apoptotic pathway than FAS or dexamethasone. However, irrespective of the stimulus used, the thymocytes from VAMP8^{-/-} small not sick mice are always more sensitive to cell death.

3.5. Thymic stroma is affected due to the lack of VAMP8

A constant bidirectional crosstalk between the thymic stroma and the developing T lymphocytes is critical for the survival of both. Reduced thymus cellularity in the VAMP8^{-/-} small and sick mice could be due to a defect of the thymocyte precursors to proliferate or in the thymic stromal cells that fail to signal the developing thymocytes. In order to understand whether the defect lies in the thymic stroma or in the thymocytes, we

transplanted the bone marrow derived stem cell of VAMP8^{-/-} small and sick and VAMP8^{+/-} control mice into RAG2^{-/-} γ c^{-/-} recipient mice. The hematopoietic stem cells have a potential to differentiate into T- as well as B-lymphocytes when subjected to the right environment and stimulus.

The RAG2^{-/-} γ c^{-/-} mice in turn, have a fully functional thymic stroma capable of providing the right microenvironment for the development of the T-lymphocytes. However, these mice do not have any functional T and B lymphocytes because Rag2 (recombinase activating enzyme 2) encodes the DNA recombinase enzyme required for VDJ recombination of the B-cell receptor and T-cell receptor gene loci and thereby the production of BCR and TCR proteins. Additionally, the common gamma chain (γ c) is a subunit of the cytokine receptors for IL-2, -4, -7, -9, and -15 on the lymphocytes. The γ c can combine with other ligand-specific receptors to direct lymphocytes to respond to different cytokines. Therefore, lymphocyte development is greatly compromised in the γ c^{-/-} mice. These mice lack natural killer (NK) cells and produce very few T and B lymphocytes. The double knock out mice for RAG2 and γ c therefore completely lack T and B lymphocytes and NK cells. These mice were obtained from Professor Dr. Rodewald, from the Institute of Immunology, University of Ulm and kept in the C57BL/6J x C57BL/10^{SbSnAi} background.

In three independent experiments, bone marrow derived from 10-12 day old small and sick VAMP8^{-/-} mice and VAMP8^{+/-} littermates were transplanted into irradiated RAG2^{-/-} γ c^{-/-} mice. After 4 weeks, 7 weeks and 9 weeks of transplantation, blood was collected from the recipient RAG2^{-/-} γ c^{-/-} mice and lymphocytes were stained with antibodies against CD4, CD8, CD3 to visualize T-lymphocytes, B220 and CD19 for the B-lymphocytes and NK1.1 for NK cells. Parallel samples were stained with isotype controls.

After 4 weeks of transplantation, there were B220 positive (B220⁺CD19⁺) B-lymphocytes in all the RAG2^{-/-} γ c^{-/-} recipients (Figure 3.31). However, there were no T lymphocytes in the RAG2^{-/-} γ c^{-/-} recipients of both the test and control bone marrow (Figure 3.31).

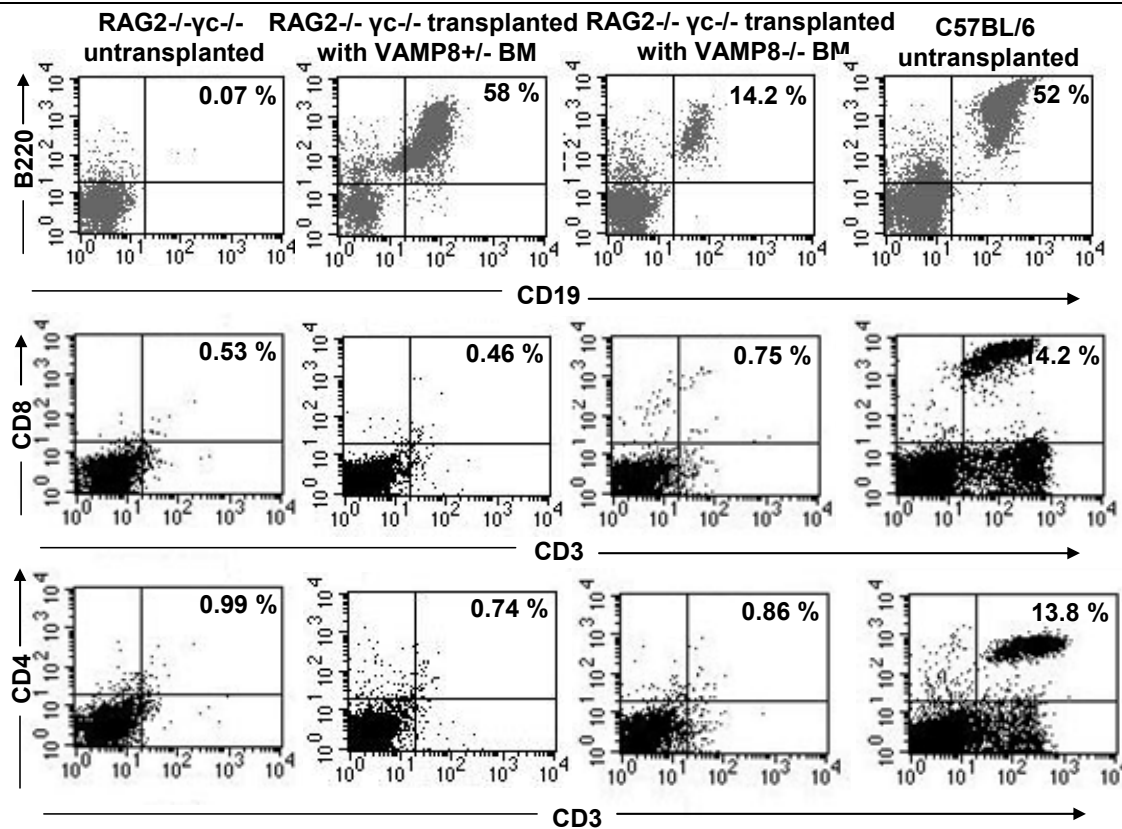


Figure 3.31. Bone marrow cells from VAMP8^{-/-} sick mice develop into normal B-lymphocytes in RAG2^{-/-} γc^{-/-} mice: Dot plots showing the development of B and T lymphocytes in the blood from RAG2^{-/-} γc^{-/-} mice transplanted with bone marrow from VAMP8^{+/+} control and VAMP8^{-/-} small and sick mice after 4 weeks. B lymphocytes developed within 4 weeks in the recipient of both types of bone marrow (Top panel). However, there are no CD4⁺CD3⁺ (bottom panel) or CD8⁺CD3⁺ (middle panel) T lymphocytes in the RAG2^{-/-} γc^{-/-} mice transplanted either with bone marrow from VAMP8^{-/-} small and sick or VAMP8^{+/+} control mice. RAG2^{-/-} γc^{-/-} untransplanted control mice show no B- and T-lymphocytes. *Transplantation was done at the central animal facility and irradiation of the RAG2^{-/-} γc^{-/-} mice was carried out at Strahlentherapie und Radionkologie by Dr. Mirko Nitsche and analysis was done with Dr. Ralf Dressel at Department for Immunogenetics, Georg August Universität Göttingen.

Analysis of blood of all the RAG2^{-/-} γc^{-/-} mice transplanted with bone marrow from VAMP8^{+/+} control mice, showed CD4⁺CD3⁺ and CD8⁺CD3⁺ T lymphocytes by 6th- 9th week after transplantation.

In first experiment, there were few T lymphocytes in the RAG2^{-/-} γc^{-/-} recipient of VAMP8^{-/-} bone marrow after 6 weeks, however, these mice developed CD4⁺CD3⁺ and CD8⁺CD3⁺ T lymphocytes after 9 weeks of transplantation in comparable numbers to the control mice (Figure 3.32). The RAG2^{-/-} γc^{-/-} recipient of VAMP8^{+/+} bone marrow developed CD4⁺CD3⁺ and CD8⁺CD3⁺ T lymphocytes after 6 weeks. After 8 weeks, the

RAG2^{-/-} γ c^{-/-} mouse transplanted with control bone marrow died with symptoms of Graft-versus-Host Disease where ‘Graft’ was the donated bone marrow and the ‘Host’ was the recipient RAG2^{-/-} γ c^{-/-} mouse. This indicates that this recipient mouse developed a functional immune system that eventually recognized the host as non-self and triggered a severe immune response leading to the death of the recipient.

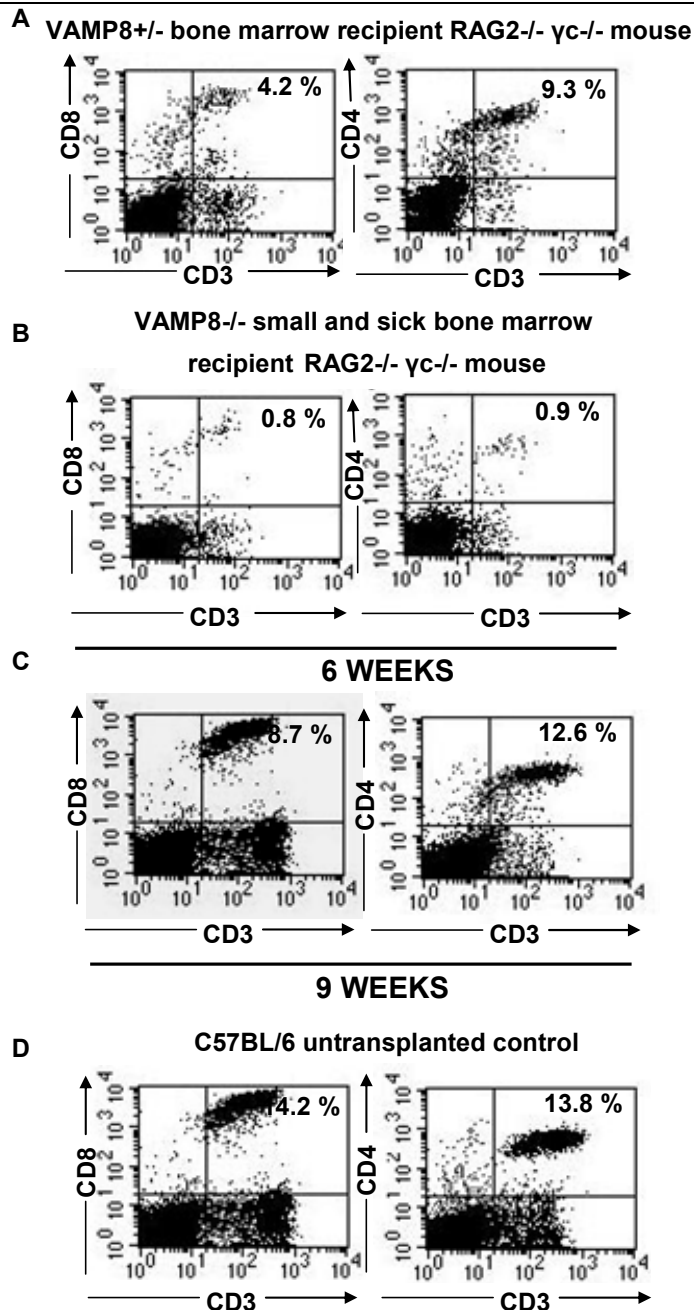


Figure 3.32. Bone marrow cells from VAMP8^{-/-} sick mice develop into normal T-lymphocytes in RAG2^{-/-} γ c^{-/-} mice: Dot plot data showing the development of T-lymphocytes in blood from RAG2^{-/-} γ c^{-/-} recipients of bone marrow from VAMP8^{-/-} small and sick (10 day old) and VAMP8^{+/-} littermate control mice. While CD4⁺CD3⁺ and CD8⁺CD3⁺ T lymphocytes developed in the VAMP8^{+/-} bone marrow recipient RAG2^{-/-} γ c^{-/-} mouse after 6 weeks (A) there were almost no T lymphocytes in the VAMP8^{-/-} bone marrow recipient at this stage (B). However, after 9 weeks, these mice developed both CD4⁺CD3⁺ and CD8⁺CD3⁺ T lymphocytes (C) in numbers comparable to the C57BL/6 control mice (D). *Transplantation was done at the central animal facility and irradiation of the RAG2^{-/-} γ c^{-/-} mice was carried out at Strahlentherapie und Radionkologie by Dr. Mirko Nitsche and analysis was done with Dr. Ralf Dressel at Department for Immunogenetics, Georg August Universität Göttingen.

By contrast the other two experiments, the RAG2^{-/-} γ c^{-/-} recipients of bone marrow from VAMP8^{-/-} small and sick mice developed CD4⁺CD3⁺ and CD8⁺CD3⁺ cells in similar to the RAG2^{-/-} γ c^{-/-} recipients of VAMP8^{+/+} bone marrow 6 weeks after transplantation (Figure 3.33).

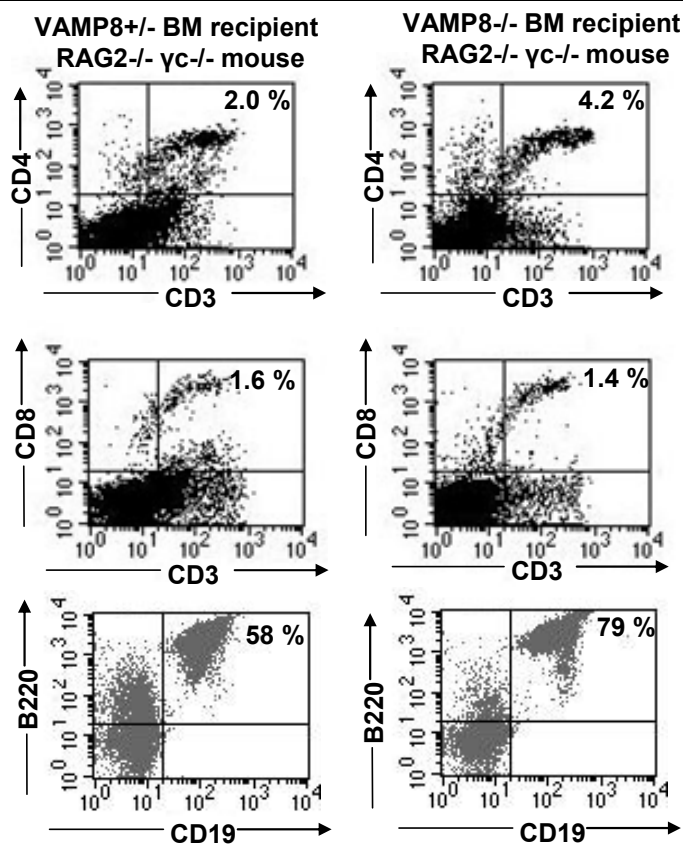


Figure 3.33. Bone marrow cells from VAMP8^{-/-} sick mice develop into normal T-lymphocytes in RAG2^{-/-} γ c^{-/-} mice: Blood analysis of transplanted RAG2^{-/-} γ c^{-/-} mice to look for the development of T- and B- lymphocytes 6 weeks after transplantation. All the RAG2^{-/-} γ c^{-/-} recipient mice transplanted with VAMP8^{+/+} or VAMP8^{-/-} bone marrow developed CD4⁺CD3⁺ and CD8⁺CD3⁺ T lymphocytes and B220 bearing B-lymphocytes in similar numbers. *Transplantation was done at the central animal facility and irradiation of the RAG2^{-/-} γ c^{-/-} mice was carried out at Strahlentherapie und Radionkologie by Dr. Mirko Nitsche and analysis was done with Dr. Ralf Dressel at Department for Immunogenetics, Georg August Universität Göttingen.

These experiments show that the T-lymphocytes progenitors of the VAMP8^{-/-} mice do not have an inherent maturational defect. It is quite likely that the stromal cells of the thymus in VAMP8^{-/-} small and sick mice are abnormal hence they fail to support the development and maturation of the thymocyte precursors.

3.6. Studies on mouse cells derived from VAMP8^{-/-} mice

Since VAMP8 is involved in homotypic late endosomal fusion and in the fusion of secretory granules with the plasma membrane, the loss of VAMP8 could result affect endosomal trafficking. Therefore, it was imperative to study the functionality of the

endosomal system and process such as endocytosis, endosomal transport and lysosomal degradation in cells derived from VAMP8^{-/-} mice.

3.6.1. Lamp staining VAMP8^{-/-} MEFs

Lamp 1 is the lysosome associated membrane protein 1 that is commonly used as a marker to visualize the lysosomes and late endosomes. In order to determine whether the lack of the SNAREs VAMP8 and Vti1b affects the morphology of the endosomal system, lamp1 staining was done on fibroblasts derived from VAMP8^{-/-} Vti1b^{-/-}, VAMP8^{-/-} and VAMP8^{+/+} Vti1b^{+/+} embryos (Figure 3.34). Primary mouse embryonic fibroblasts (MEFs) were isolated from 13.5 day old VAMP8^{-/-} Vti1b^{-/-}, VAMP8^{-/-} embryos and were immortalized by continuous passaging. MEFs isolated from VAMP8^{+/+} Vti1b^{+/+} littermate were used as controls. The immortalized MEFs were seeded on a coverslip overnight and fixed with methanol prior to immunostaining. In all the three cell lines, lamp1 staining appeared in the form of punctuated dots, with higher perinuclear localization in reference to dapi stained nucleus and also spread out in the cell. This shows that there is no defect in the morphology of lysosomes and endosomes in the absence of VAMP8 and Vti1b.

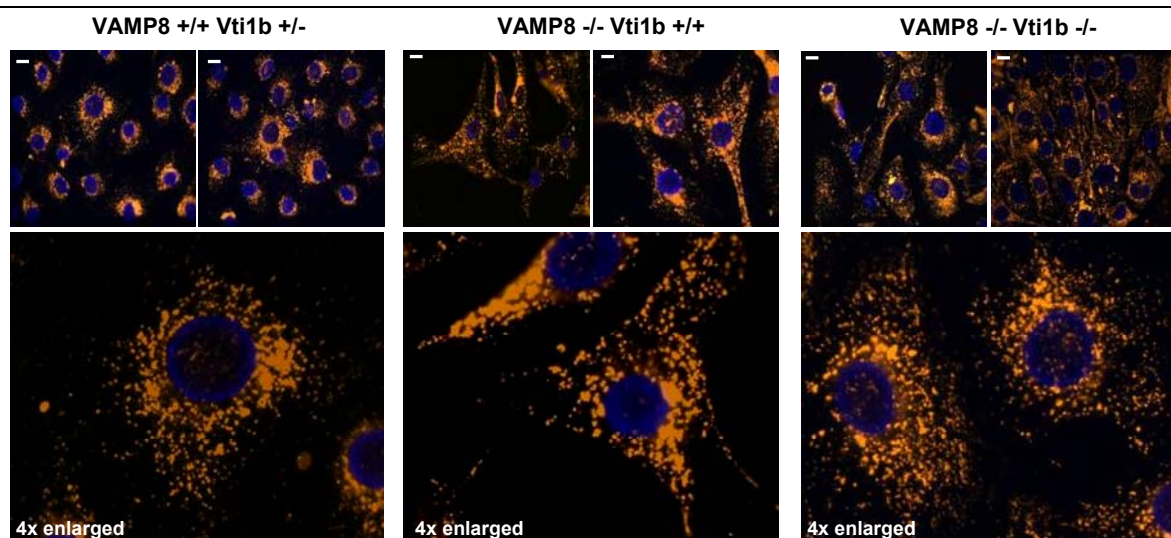


Figure 3.34. The morphology of endosomal system is normal in VAMP8^{-/-} fibroblasts: Lamp1 and Dapi staining of MEFs from VAMP8^{-/-} (middle panel) and VAMP8^{-/-} Vti1b^{-/-} mice (bottom panel) in comparison to VAMP8^{+/+} Vti1b^{+/+} (top panel). In all the three cell types, the lamp1 staining was localized most densely close to the perinuclear region while there was also some punctuated staining spread throughout the cells. Scale bars correspond to 10 μ M.

3.6.2. Uptake and degradation of fluorescently labeled LDL

Next, we wanted to analyze whether the loss of VAMP8 causes a defect in the kinetics of endocytosis, endosomal transport and lysosomal degradation. Fluorescently labeled LDL is commonly used for such studies since its trafficking can be easily followed by fluorescence microscopy. LDL is taken up into the cells by receptor mediated endocytosis. Following this, the receptor is recycled back to the surface while LDL is targeted for degradation in the lysosomes via passage through the early and late endosomes.

Endosomal trafficking was studied in MEFs derived from VAMP8^{-/-} by following the uptake of fluorescently labeled LDL into the cells, its passage through endosomes to the lysosomes and eventual degradation in the lysosomes. The cells were starved in serum free medium for 1 hour and later pulsed with 200 μ l of 10 μ g/ml (2 μ g/cover slip) BODIPY labeled LDL at 4 $^{\circ}$ C for 1 hour to allow receptor binding. Following this, LDL was chased into the cells at 37 $^{\circ}$ C for 0, 15, 30, 60 and 180 minutes. The cells were fixed in *para*-formaldehyde and analyzed by fluorescence microscopy.

Soon after pulse, at the 0hr time point, LDL is bound to its plasma membrane receptors. In the VAMP8^{+/-} MEFs, there were a large number of small dot like structure spread all over the cells. There was a slightly reduced amount of staining at the plasma membranes in the VAMP8^{-/-} MEFs at 0hr. This could indicate lower expression of LDL receptors on the surface of the VAMP8^{-/-} MEFs (Figure 3.35). The punctuated staining at 0hr could be due to clathrin coated pits. After 15 minutes of chase, LDL was expected to reach the endosomes. The BODIPY staining was organized into distinct vesicles spread out in the wild type cells with a slight tendency towards perinuclear localization. In the VAMP8^{-/-} cells, there were fewer fluorescent vesicles compared to the control cells which were spread all over the cells (Figure 3.35).

After 30 minutes of chase LDL was expected to reach the lysosomes. There was a slight difference in the appearance and distribution of the fluorescently labeled vesicles between two cell lines at this time point. The wild type cells showed a strong fluorescent signal in large vesicular structure while in the knock out cells, LDL was still present in small punctuated structures spread out in the cells. (Figure 3.35).

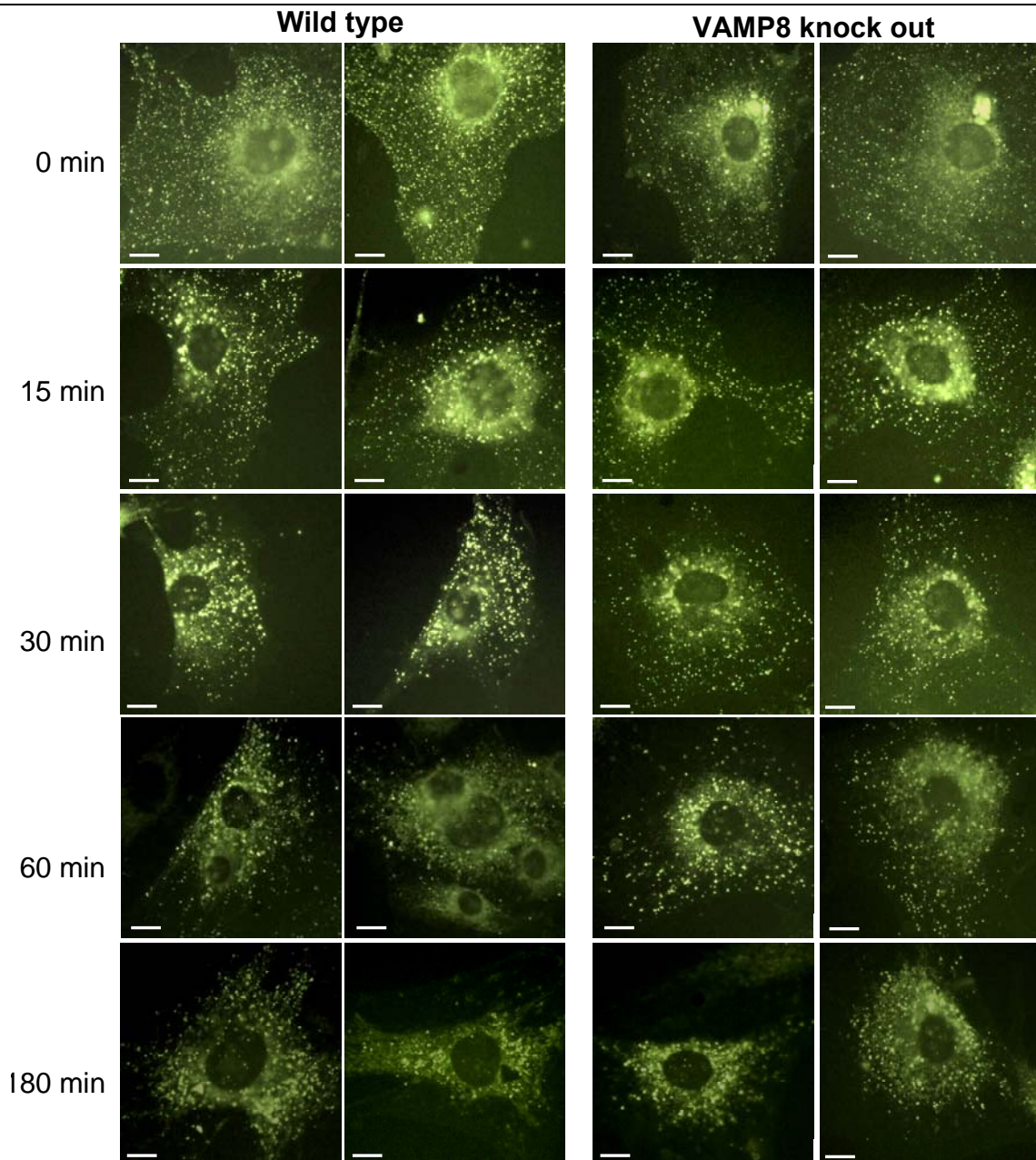


Figure 3.35. Endocytosis, endosomal transport and lysosomal degradation of LDL not affected in VAMP8^{-/-} fibroblasts: MEFs from VAMP8 wild type and VAMP8 knock out mice were pulsed with 200 μ l of 10 μ g/ml BODIPY labeled LDL and chased for different time points. At 0 minute time point, the fluorescent LDL located largely at the periphery of the cells probably bound to the LDL receptors at the cell surface. There was a lower fluorescent staining in the VAMP8 knock out cells at this time point compared to the control cells. After 15 minutes while the LDL seemed taken up into distinct vesicles in the wild type cells, the vesicles were much less distinct and smaller in the knock out cells. After 30 minutes, the vesicles appear largely localized at the perinuclear region of the wild type cells, there is no such localization in the knock out cells. After 1 and 3 hours, the LDL was degraded in the lysosomes in both the cell types. Scale bars correspond to 50 μ M.

After 60 minutes most of the LDL was expected to be degraded in the lysosomes and by 3 hours the whole of the protein should be degraded. We observed that most of the punctuated vesicles disappeared after 1 hour with almost no remaining perinuclear staining in the wild type cells. In the knock out cells too, the fluorescent staining got weaker after 1 hour and was completely lost after 3 hours of chase in both the cell types (Figure 3.35).

Thus it seems that could be a minor defect in the transport of LDL between the endosomes and the lysosomes in the knock out cells that appears most prominently after 30 minutes of chase. However, once inside the lysosomes, the proteins are degraded at similar rate indicating that the lysosomal function are not compromised in the knock out mice.

3.6.3. Bead uptake in VAMP8^{-/-} Vti1b^{-/-} peritoneal macrophages

The next step was to analyze the kinetics of phagocytosis and fusion of phagosomes with lysosomes. Phagocytosis differs from the clathrin mediated endocytosis as it involves uptake of large particles at the cell surface by binding to cell surface receptors and dynamic remodeling of the actin cytoskeleton. It was interesting to know whether the loss of VAMP8 and Vti1b causes a defect in phagocytic pathway. Fluorescently labeled 1 μ M latex beads were used to follow phagocytosis in peritoneal macrophages isolated from VAMP8^{-/-} Vti1b^{-/-} and VAMP8^{+/+}Vti1b^{+/+} control mice. The beads were coated with bovine serum albumin before the experiment in order to increase the uptake. The cells were starved for 1 hour in serum free medium. Following this, they were pulsed with fluorescently labeled beads at a concentration of 50 beads per cell and chased for several time points at 37°C. The cells were fixed with methanol and immunostained with late endosome/lysosomal marker lamp 2. In order to see if the beads were trafficking to the late endosomes and lysosomes, co-localization was done between the beads and lamp2 staining.

The kinetics of bead uptake and co-localization with the lamp2 staining was similar in the macrophages derived from the VAMP8^{-/-} Vti1b^{-/-} and the control wild type mice. After 10 minutes of pulse, the beads appeared attached to the cells, however as expected there was no co-localization with the lamp2 staining (Figure 3.36). After 30 minutes of pulse, the beads started to localize close to the lamp2 staining in both the cells types. After 30 minutes of pulse and 30 minutes of chase, the cells were loaded with large number of beads

(average 7-10) and the beads co-localized with the lamp2 staining (Figure 3.36). After 60 minutes of chase, there were even larger number of beads in the cells and the co-localization between the beads and the lamp2 staining was complete (Figure 3.36). This indicated that there was no major difference in the uptake of beads and their transport to the lamp2 stained vesicles in both the cell types.

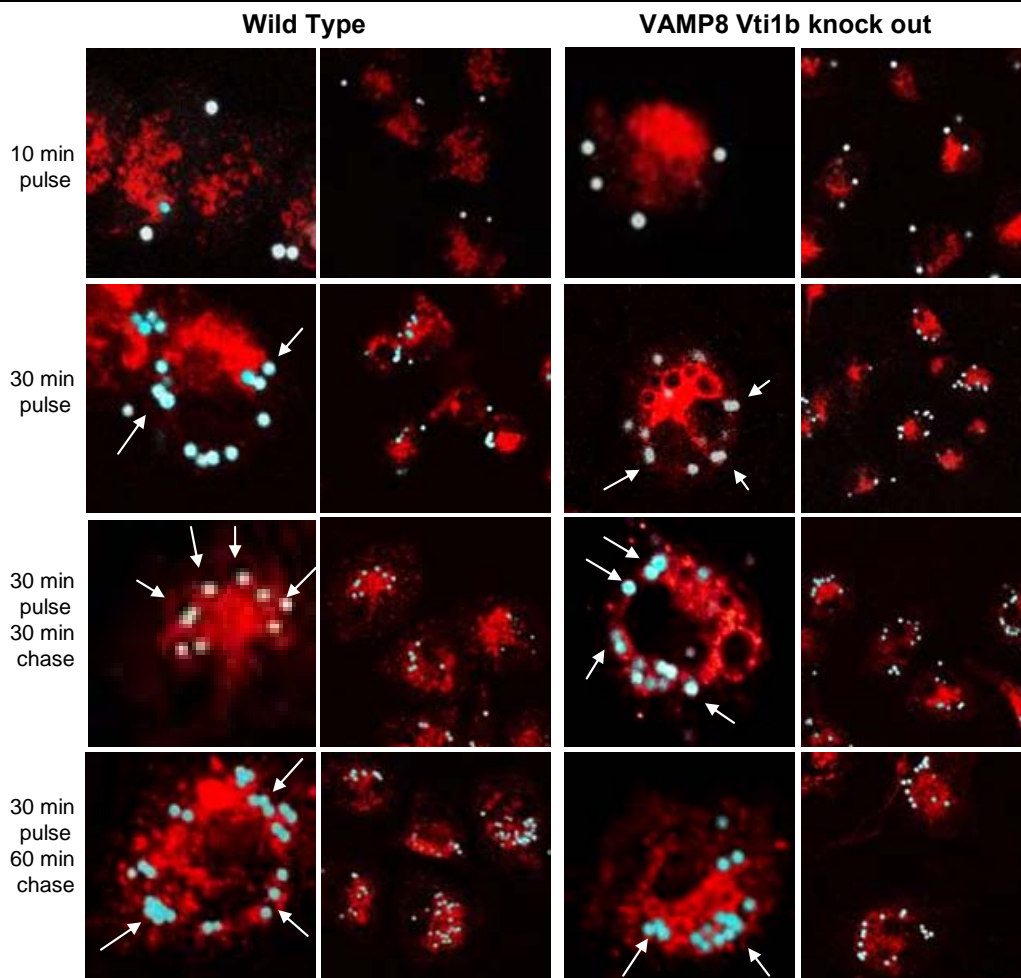


Figure 3.36. Phagocytic uptake and lysosomal delivery is not affected in VAMP8^{-/-} Vti1b^{-/-} macrophages: Phagocytosis of bright blue fluorescent beads (1 μ m diameter) by mouse peritoneal macrophages derived from VAMP8^{-/-} Vti1b^{-/-} mouse (right panel) and the control wild type mouse (left panel). The cells were pulsed with the beads for 10, 20 and 30 minutes and chased for 30 and 60 minutes following 30 minutes pulse. Following this, the cells were fixed with methanol and immunostained with fluorescent antibody against lamp2 and observed under Leica confocal microscope by z-scanning. After 10 and 20 minutes of pulse, there was an increasing uptake of beads into the cells with no colocalization with lamp2 staining. After 30 minutes of pulse the beads start to colocalize with the lamp2 staining. With 30 and 60 minutes of chase times, there was an increasing colocalization of beads with the lamp2 staining both in the macrophages from wild type control and in the VAMP8^{-/-} Vti1b^{-/-}.

3.7. Level of lysosomal enzymes

Lysosomal enzymes are synthesized in the ER in an inactive form and then transported to the lysosomes via endosomes. The proteins get activated in the lysosome largely due to the acidic pH (~4.5). If the homotypic fusion between late endosomes or heterotypic fusion between late endosomes and lysosomes was affected due to the loss of VAMP8, the level of active lysosomal enzymes could be disturbed. Therefore, lysosomal enzymes, β -Hexosaminidase, β -Mannosidase and β -Galactosidase present were tested in the liver of VAMP8^{-/-} mice.

Initial studies on adult VAMP8^{-/-} Vti1b^{-/-} mice showed normal lysosomal enzyme activity in the liver and kidney of these mice (Ref. section 1.4.4). In that study it was confirmed that there is no difference in the activities of β -Hexosaminidase and β -Galactosidase between the VAMP8^{-/-} Vti1b^{-/-} mice, VAMP8^{+/-} Vti1b^{-/-} and age matched wild type controls.

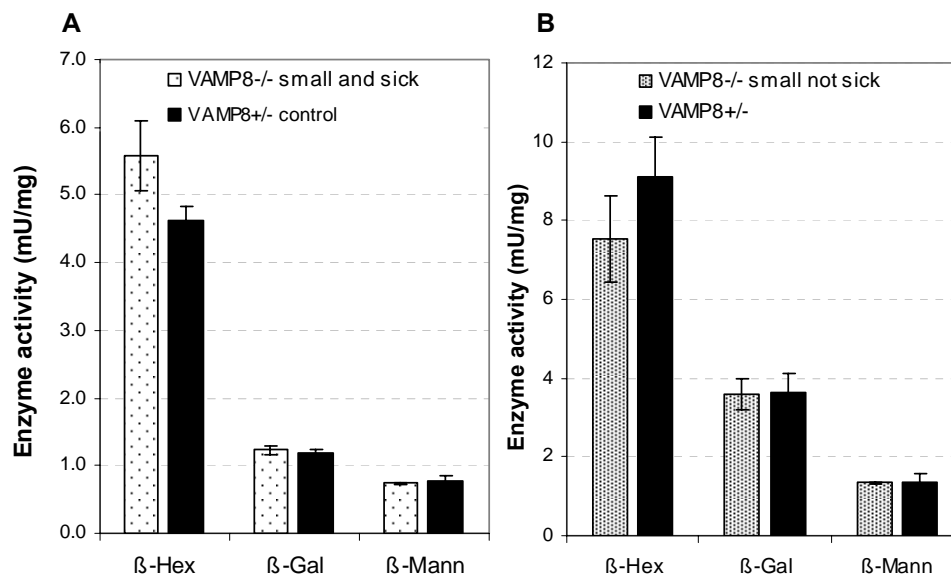


Figure 3.37. Lysosomal enzymes function normally in small VAMP8^{-/-} mice: The activities of three lysosomal enzymes, β -Hexosaminidase (β -Hex), β -Galactosidase (β -Gal) and β -Mannosidase (β -Mann) expressed in mU/mg in 10 day old (n=2) VAMP8^{-/-} small and sick (A) and 8 day old small not sick (n=3) (B). There was no difference in the activities of all the three enzymes between the VAMP8^{-/-} and the VAMP8^{+/-} controls in the liver homogenates.

It is possible that the VAMP8^{-/-} mice at the small and sick and small not sick stage have a defect in the lysosomal transport even though the adult VAMP8^{-/-} mice showed no obvious phenotype and the adult VAMP8^{-/-} Vti1b^{-/-} mice had no defect in lysosome enzyme

activity (Ref. section 1.4.4). Therefore, activity of lysosomal enzymes β hexosaminidase, β galactosidase and β mannosidase was analyzed in liver homogenates from small not sick VAMP8^{-/-} and small and sick VAMP8^{-/-} and compared to age matched VAMP8^{+/-} controls. The activities were calculated in mU/mg. There was no major difference in the activity of any of the tested enzymes in the liver of test and control samples (Figure 3.37), indicating that the activity of the lysosomal enzymes is not compromised due to the lack of VAMP8 and/or Vti1b.

4. Discussion

4.1. Heterogeneity in phenotype manifestation

VAMP8^{-/-} and VAMP8^{-/-} Vti1b^{-/-} mice were born in expected mendelian ratios, suggesting a normal embryonic development. However, 36% VAMP8^{-/-} died within 10-12 days after birth while 66% VAMP8^{-/-} Vti1b^{-/-} and 58% VAMP8^{-/-} Vti1b^{+/-} were dead between 12-29 days after birth. On the other hand, the VAMP8^{+/-} Vti1b^{-/-} mice did not show elevated mortality in the first three weeks after birth. Not all VAMP8^{-/-} mice were affected, rather there was a well marked heterogeneity in the phenotypic manifestation. There were two distinct pools of mice in both VAMP8^{-/-} and the VAMP8^{-/-} Vti1b^{-/-} genotypes. The first pool of mice showed progressive loss of weight at ~ 8-9 days in VAMP8^{-/-}. After two-three days of weight loss, the mice were half the weight of their VAMP8^{+/-} littermates and these mice eventually died. By contrast the second pool of mice did not loose weight and became healthy adults although they were smaller and lighter than their littermates.

Wang and coworkers reported the same findings in their VAMP8^{-/-} mice (Wang et al. 2004). They observed that upto one thirds of VAMP8^{-/-} mice were dead before weaning and these mice were half the weight of their littermates at the time of death. They also observed growth retardation in the surviving mice similar to the findings in this study. In addition, they reported a defect in the pancreas of the surviving VAMP8^{-/-} mice (Wang et al. 2004). These mice extremely enlarged pancreas that had a creamy appearance rather than translucent pancreas as seen in the VAMP8^{+/-} controls. In this study also we observed that the same abnormalities in the pancreas of VAMP8^{-/-} adult as well as small mice.

The mice analyzed by Wang and co-workers in their study were real knock out mice created by replacement of the second exon of the VAMP8 gene with a neo^r cassette, while the VAMP8^{-/-} mice used in this study were created by genetrapping . Since our genetrapped mice behave just as the real knock out mice it shows that the heterogeneity in the phenotype is not due to a possible residual protein levels in the VAMP8^{-/-} genetrapped mice.

Rather, it appears that there is a critical point in the lives of the VAMP8 -/- mice soon after the first week of birth. The mice which successfully overcome this threshold become healthy adults while the ones that fail to overcome it, eventually die.

The observed heterogeneity can at least in part be explained due to the mixed background of the mice. The genetrap was inserted into VAMP8 gene of embryonic stem cells derived from 129S5/Sv^{EvBrd} while the blastocyst was from C57BL/6-*Tyr^{c-Brd/c-Brd}* strain (Zambrowicz et al. 1998). Similarly, the *Vt1b* gene was knocked out in 129S5/ Sv^{Ole} ES cells and injected into C57BL/6-*Tyr^{c-Brd/c-Brd}* blastocyst (Atlashkin et al. 2003). This means that the offspring acquire genetic information from two different parental background strains. The traits are randomly distributed among the different pups of a litter that could explain why some VAMP8 -/- pups could be more resistant to the factors that cause the phenotype than the others in the same litter.

4.2 Thymus specific effect of VAMP8 ablation

The results from this study point primarily towards the importance of VAMP8 for development of T lymphocytes and maintenance of thymic integrity. The lack of VAMP8 causes severe disruption of the thymus morphology and thymocytes maturation.

4.2.1. Effect of VAMP8 ablation on T cell development and thymic stroma

Thymus is a structurally complex organ comprising of epithelial cells derived from ecto- and endoderm as well as cells from hemopoietic bone marrow origin such as dendritic cells and T lymphocytes. The epithelial cells, dendritic cells, fibroblasts and macrophages together form the stroma of the thymus and are organized into well defined structure comprising of histologically distinct cortical and medullary regions. Depending on their location, the thymic epithelial cells are termed medullary thymic epithelial cells (mTECs) or cortical epithelial cells cTECs (Takahama 2006). This compartmentalization provides distinct micro-environments to the T-lymphocytes at different stages of maturation.

The T lymphocytes on the other hand migrate from the bone marrow into the thymus. The maturation stages of T lymphocytes are highly sequential and are characterized by the expression and/or down regulation of several surface markers. A simplified view of T cells

development is as follows: CD44⁺CD25⁻ (DN1), CD44⁺CD25⁺ (DN2), CD44⁻CD25⁺ (DN3), CD44⁻CD25⁻ (DN4), CD4⁺CD8⁺ (DP), CD3⁺CD8⁺ (SP) or CD3⁺CD4⁺ (SP). The bone marrow derived CD3⁻CD4⁻CD8⁻ triple negative cells arrive at the sub-capsular zone. The DN1-DN4 subsets mature in the cortex while the DP cells migrate into the thymic medulla and mature into SP cells there. The intrathymic development of T lymphocytes is a series of lessons each provided by a distinct region of microenvironment and are under several stringent checkpoints (Ritter and Boyd 1993; Takahama 2006). The developing T-cells are given signals for proliferation, receptor gene rearrangement, positive selection for MHC restriction, negative selection for deletion of self reactive cells and molecular and functional maturation by the stromal cells.

Table XIII. Chemokines implicated in guiding thymocytes

Receptor	Receptor-expressing cells in the thymus [‡]	Ligand [§]	Ligand-expressing cells in the thymus [‡]	Role in the thymus as identified in gene-knockout mice
CCR4	CD62L-CD69 ⁺ SP thymocytes (R, F) ⁵³ CD3 ⁺ CD4 ⁺ CD8 ^{low} thymocytes (F) ⁵² Medullary thymocytes (R) ^{53*} CD4 ⁺ CD8 ^{low} and DP thymocytes (F) ^{93*}	CCL17 (TARC) CCL22 (MDC)	Dendritic cells (R) ^{90,91} Mostly in the medulla (R) ⁹¹ Outer walls of Hassall's corpuscles (H) ^{92,93*} A fraction of mTECs (H) ^{92*}	Not determined, although possibly associated with negative selection
CCR7	SP thymocytes (R, F) ^{52,53,92} (P) ^{41,54} TCR-stimulated DP thymocytes (P) ⁵⁴ DN1 and DN2 thymocytes (P) ⁴¹ SP and a fraction of DP thymocytes (F) ^{93,108*}	CCL19 (ELC, MIP3β) CCL21 (SLC, 6CKine)	A fraction of mTECs (H) ⁵⁴ Endothelial venules in the medulla (H) ⁹⁵ Medulla, CMJ, blood vessels (H) ⁴¹ mTECs (high levels), cTECs (low levels), dendritic cells (R) ⁹⁸ mTECs (H) ^{93*} Most mTECs (H) ⁵⁴ Medulla, CMJ, cortical dendritic cells and macrophages (H) ⁴¹ mTECs (high levels), cTECs (low levels) ⁹⁸	Attraction of positively selected thymocytes to the medulla ⁵⁴ Guidance of postnatal thymus exit ⁹⁸ Outward relocation of DN thymocytes towards the outer cortex ⁴¹ Attraction of fetal progenitor cells to pre-vascular fetal thymus ²⁰
CCR9	DP thymocytes and CD62L-CD69 ⁺ SP thymocytes (F) ^{53,109-111} DN3-DN4, DP and a fraction of SP thymocytes (P) ⁴² DP thymocytes and γδ T cells (P) ¹¹² DP thymocytes (high levels), SP thymocytes (low levels) (R) ¹¹⁰ DP and SP thymocytes (F) ^{113*}	CCL25 (TECK)	cTECs and mTECs (H) ⁴¹ cTECs and a fraction of mTECs (H) ¹⁰⁹ mTECs (high levels), cTECs (low levels) (R) ¹⁰⁹	Outward relocation of DN2 or DN3 thymocytes to the subcapsular region ⁴² Fetal thymus accumulation ²¹
CXCR4	DN1-DN4 thymocytes (R, F) ^{22,40,52} DN, DP and SP thymocytes (R, F) ^{22,52} Dendritic cells (H) ^{114*} DP and SP thymocytes (P, F) ^{108*}	CXCL12 (SDF1, SDF1α)	Medulla, CMJ (H) ⁴¹ A subset of cTECs, not in the medulla (R) ⁴⁰ Hassall's corpuscles, epithelial cells (H) ^{114*}	Outward relocation of DN thymocytes towards the outer cortex ⁴⁰ Development of DN thymocytes ²²

*These data were obtained from human tissues and cells; all other data are derived from mouse studies. †The method of detection is indicated in parentheses by: R, RNA analysis including *in situ* hybridization; F, functional analysis of chemotaxis; P, protein detection by flow cytometry; H, histological analysis of sections using antibodies. ‡The popular synonym(s) for the ligand are shown in parentheses. CCL, CC-chemokine ligand; CCR, CC-chemokine receptor; CMJ, cortico-medullary junction; cTECs, cortical thymic epithelial cells; CXCL, CXC-chemokine ligand; CXCR, CXC-chemokine receptor; DN, double negative; DP, double positive; ELC, Epstein-Barr virus-induced molecule 1 ligand chemokine; MDC, macrophage-derived chemokine; MIP3β, macrophage inflammatory protein 3β; mTECs, medullary thymic epithelial cells; SDF, stromal-cell-derived factor; SLC, secondary lymphoid-tissue chemokine; SP, single positive; TARC, thymus and activation-regulated chemokine; TCR, T-cell receptor; TECK, thymus-expressed chemokine.

Table adopted from Takahama et al. 2006, Nature Reviews Immunology, Volume 6, pg 127-135, February 2006.

However, signaling in the thymus is not monologous. Studies have established that there is a constant dialogue between the maturing T lymphocytes and stromal cells either by cell-cell interaction or by soluble molecules (Ritter and Boyd 1993). Interaction between chemokines secreted by stromal cells in their specific micro environments with their receptors on the developing T cells is pivotal for guiding the thymocytes (Shores et al. 1991; Takahama 2006). The thymic epithelial cells and thymocytes secrete cytokines such as IL-1, IL-4, IL-6, IL7 and tumor necrosis factor α (TNF α) and express the complimentary receptors IL-1R, IL-4R, IL-6R, IL7R and TNFR (Ritter and Boyd 1993). Chemokine receptors CXCR4, CCR4, CCR7 and CCR9 are involved movement of immature thymocytes (Ref. Table XIII). In addition, adhesion molecules such as CD2/CD58, CD54/CD11a, and CD18 also mediate the lympho-stromal interaction (Ritter and Boyd 1993).

4.2.1.1. Defect in thymic stroma

The thymii from VAMP8^{-/-} sick mice had all the subpopulations of developing T lymphocytes, indicating that thymocyte differentiation is not completely blocked in the absence of VAMP8. This view was also supported by the data from bone marrow transplantation experiments. The bone marrow derived hemopoietic precursors from VAMP8^{-/-} small and sick mice were transplanted into RAG2^{-/-} γ c^{-/-} recipient mice. The RAG2^{-/-} γ c^{-/-} mice inturn, have a fully functional thymic stroma capable of providing the right microenvironment for the development of the T-lymphocytes. However, these mice do not have any functional T and B lymphocytes because Rag2 (recombinase activating enzyme 2) encodes the DNA recombinase enzyme required for V(D)J recombination of the B-cell receptor and T-cell receptor gene loci and thereby the production of BCR and TCR proteins. The common gamma chain (γ c) is a subunit of the cytokine receptors for IL-2, -4, -7, -9, and -15 on the lymphocytes. The γ c can combine with other ligand-specific receptors to direct lymphocytes to respond to different cytokines. Therefore, lymphocyte development is greatly compromised in the γ c^{-/-} mice. These mice lack natural killer (NK) cells and produce very few T and B lymphocytes. The double knock out mice for RAG2 and γ c therefore completely lack T and B lymphocytes and NK cells.

The idea was to transplant the stem cells from the VAMP8^{-/-} sick mice into RAG2^{-/-} γ c^{-/-} mice and analyze whether or not the stem cells from the sick mice can develop in the right environment of RAG2^{-/-} γ c^{-/-} mice. If the bone marrow cells from VAMP8^{-/-} sick fail to develop into T lymphocytes in the RAG2^{-/-} γ c^{-/-} mice, it would indicate towards an inherent maturational defect of the T lymphocyte precursors. On the other hand, if the RAG2^{-/-} γ c^{-/-} recipients are populated from the donor derived T lymphocytes, it would indicate that the thymic phenotype in the VAMP8^{-/-} small and sick mice could be due to a defective thymic stroma. Through three independent experiments it was established that bone marrow from VAMP8^{-/-} small and sick mice successfully gave rise to CD4⁺CD3⁺ and CD8⁺CD3⁺ T lymphocytes in the RAG2^{-/-} γ c^{-/-} mice in similar numbers as the control C57BL/6 mice. This shows that lack of VAMP8 does not cause an inherent defect in the T lymphocytes. Rather it seems that the thymic stromal cells are abnormal and probably fail to support the development of thymus and T lymphocytes.

4.2.1.2. Defect in DN subsets

First striking observation was a massive disturbance in DN1-4 subsets in the thymus from VAMP8^{-/-} small and sick mice. There was an accumulation in DN1 and DN4 thymocytes and a reduction in the succeeding DN2 and DP subsets respectively. As discussed above, signals from cortical stromal cells are critical for the maturation of DN thymocytes.

The survival of DN1 and DN2 thymocytes is mediated by initially by stem cell factor (SCF) and interleukin 7 (IL-7), both of which are secreted by the thymic stromal cells while the DN thymocytes express c-Kit (receptor for SCF) and IL7-R. Later these cells express preT α protein which is critical to the survival of these cells. In DN3 stage, the cells enter G1/G0 phase and start to rearrange the TCR β locus and the β chain is expressed together with preT α protein (Moroy and Karsunky 2000). This is a critical event for the DN cells since the first major checkpoint arises at the transition from DN to DP. It is largely influenced by the preTCR α : β signaling and cTECs (Lacorazza et al. 2001; Minter and Osborne. 2003). The cells that fail to rearrange a functional α β chain are cleared from the T-cell repertoire (Owen and Venkitaraman 1996; von Boehmer 1992). Since the lymphostromal interaction is so critical to DN differentiation, a failure in thymic stromal cells to signal the thymocytes could explain the maturational disturbance of DN thymocytes. Thus,

a stromal defect in VAMP8^{-/-} small and sick mice could cause a transitional block from DN1 to DN2 and from DN4-DP.

4.2.1.3. Defect in CD4/CD8 subsets

Further there was an accumulation of the CD4⁺ and CD8⁺ (SP) cells in the thymii from VAMP8^{-/-} small and sick mice. The DP cells rearrange the α chain locus and express it together with the β chain to form a TCR $\alpha\beta$. The second important checkpoint occurs in transition from CD4⁺CD8⁺ (DP) to SP and is controlled by signals via the $\alpha\beta$ TCR-CD3 complex. This selection of the T lymphocytes is under a strict vigilance of the medullary stromal cells, especially the antigen presenting cells (APC): the dendritic cells and macrophages. The APCs process the self peptides and together with MHC molecules, present these peptides to the developing T lymphocytes. Only the T lymphocytes that are able to recognize MHC/peptide complexes via their TCR $\alpha\beta$ with medium avidity are selected positively in a process termed MHC restriction. While the cells that show a hypo- or hyper- responsiveness to MHC-self peptide complex are committed to cell death (positive or negative selection) (Owen and Venkitaraman 1996; von Boehmer 1992). A defect in either positive or negative selection of DP cells would possibly result in a reduction of SP cells. However, since we do not see a reduction in CD4⁺ and CD8⁺ SP cells, these processes are less likely to be affected in the VAMP8^{-/-} small and sick mice.

The accumulation of CD4⁺ and CD8⁺ SP cells could possibly result from the observed morphological defect of the thymus in VAMP8^{-/-} small and sick. The thymii of these mice had a substantial cortical region as seen by histological staining however; the medullary region was reduced to mere remnants. The SP cells stay in the medulla for around 12 days and undergo maturational process characterized by the expression of CD62L and CD69. The CD62L^{low}CD69^{high} SP cells are semi mature and susceptible to several apoptotic signals such as Dexamethasone (Takahama 2006). These cells mature into functional and Dexamethasone resistant CD62L^{high}CD69^{low} SP cells and finally exit into the systemic circulation (Takahama 2006). It is possible that the loss of medullary region in the thymii from VAMP8^{-/-} mice leads to migrational blockage of SP cells from the thymus. In order to test this hypothesis, attempts were made to analyze the CD4⁺ and CD8⁺ mature peripheral

T lymphocytes in the VAMP8^{-/-} small and sick mice. However, these mice had very small spleen and did not have enough blood to get adequate T lymphocytes for this analysis.

Our arguments are also supported by several other knock out mouse models such as Rho^{-/-} (Henning et al. 1997), STAT3^{-/-} (Sano et al. 2001; Shen et al. 2004), Eph4A^{-/-} (Muñoz et al. 2006) (Ref. section 4.2.3). These mice show a disrupted compartmentalization of the thymus into cortex and medulla. This was accompanied by a T lymphocyte maturation defect and in some models it could be explained in part due to a block at certain transition stages and loss of signaling between the stromal cells and thymocytes.

4.2.1.4. Loss of cortico-medullary morphology

It is a well known that the medullary stroma can not survive without the medullary thymocytes. Treatment with cyclosporine A blocks the interface between DP to SP cells that results in massively reduced medulla. However, cortex comprises of normal immature thymocytes and has a normal structure even after treatment (Sprent et al. 1988). Similar findings were made in TCR α knock out mice. These mice have a developmental block at DP stage as consequence medullary stromal cells are reduced to remnants while cortical epithelial cells are normal (Philpott et al. 1992).

The VAMP8^{-/-} small and sick mice had a massively disturbance in DN1-4 subsets and a marked reduction DP cells. This reduction in DP populations could possibly result in reduced medullary region and loss of cortico-medullary boundary similar to the CSA treatment and TCR α knock out mice. On the other hand, this defect could also result from an inherent defect in the thymic medullary stromal cells due to the loss of VAMP8.

An inherent defect in thymic stroma adequately explains the findings in this study. However, one point to be kept in mind is that the health status of the VAMP8^{-/-} mice analyzed in this study was not normal. Therefore, it is possible the loss of VAMP8 does not directly affect the stroma rather there could be other health factors that indirectly affect the thymic stromal cells and render them incapable of supporting thymocytes development.

4.2.2. Cell death in VAMP8^{-/-} thymus and thymus cellularity

The thymus from the small and sick VAMP8^{-/-} and VAMP^{-/-} Vti1b^{-/-} mice showed an increased cell death. The inability of stromal cells to signal to the developing T

lymphocytes could also explain this increased apoptosis. The developing thymocytes that fail to pass through the transitional boundaries are committed cell death. This includes the DN cells that fail to express a TCR β chain, the DP cells that fail to rearrange and express a functional TCR $\alpha\beta$ receptor, the DP cells that either do not recognize the self MHC or recognize it with a very high affinity. As has been discussed above, for all these processes, the T lymphocytes get signals from the stromal cells. Only about 5% of the thymocytes are allowed to exit into the periphery. Either a lack of stimulus or too strong signaling by the stromal cells to the thymocytes in VAMP8^{-/-} small and sick mice could lead to an increased thymocyte death. The massive reduction in the CD4⁺CD8⁺ DP cells could also be in part explained due to an increased apoptosis of this subset. At the DP stage, the cells rearrange the α chain of the TCR $\alpha\beta$. Thymocytes that lack a productively rearranged TCR $\alpha\beta$ are deleted from the T cell repertoire (Owen and Venkitaraman 1996; von Boehmer 1992). Hence this population is especially sensitive to apoptotic stimulus. In addition, the stromal cells that either fail to signal or could themselves be subjected to apoptosis.

In vitro apoptosis induction assays show that thymocytes from the VAMP8^{-/-} small not sick mice are highly susceptible to cell death. Although the apoptotic stimuli arise from several sources, the signaling cascades converge at the level of caspase activation. Glucocorticoid hormones play a major role in negative selection. The thymic epithelial cells serve as the intrathymic source of glucocorticoids (GC) (Ashwell et al. 1996; Pazirandeh et al. 1999). The level of GC remains constant in the thymus at steady state, the levels of GC receptors (GR) varies during thymocyte development (Brewer et al. 2002). Although the mechanism of GC mediated cell death is not clearly defined, according to a current view dexamethasone exerts its apoptotic effect primarily via diacyl glycerol (DAG) generation (Cifone et al. 1999). In this study, Dexamethasone, a synthetic GC was used to induce and study apoptosis.

As a second stimulus, probably more relevant to thymocytes development, is the use of anti CD3 antibody. Crosslinking with anti CD3 antibody leads to clustering of CD3 molecules and mimicks the physiological condition where a very strong engagement of TCR: CD3 complex leads to negative selection of the T-lymphocytes. *In vitro* activation of T lymphocytes also requires a co-stimulation with anti CD28 antibody. Therefore, in this

study anti- CD3 and -CD28 antibodies were used, which resulted in a stronger effect than anti CD3 treatment alone. As third stimuli, anti FAS antibody was used. Treatment with anti-FAS antibody also triggers a constitutively active signaling that leads to apoptosis via caspase cascade. Interaction between FAS and FAS ligand is critical for negative selection in the thymus (Minter and Osborne 2003). In this study, irrespective of the stimulus used, the thymocytes of VAMP8^{-/-} small not sick mice showed an increased sensitivity towards apoptosis. At physiological level this could mean that during the onset of the phenotype i.e. in the small not sick stage, the thymocytes become increasingly sensitized towards physiological apoptotic stimuli. This could result in the death of the most sensitive thymocytes populations in the VAMP8^{-/-} small and sick mice. This could also explain the massive cell death and reduction in thymus cellularity seen in the VAMP8^{-/-} small and sick mice.

On the other hand, the sensitivity of the thymocytes to apoptotic stimuli could be a leading cause for reduced thymus cellularity and disruption of morphology in the VAMP8^{-/-} sick mice. These affects could have probably been surpassed in the transplantation experiment since the transplanted RAG^{-/-} γ c^{-/-} mice had normal levels of factors such as glucocorticoid hormones and cytokines which could be deregulated in the VAMP8^{-/-} sick mice.

4.2.3. Thymic morphology and T cell defect: Similarities to other knock out models

How VAMP8 possibly regulates the thymus development and the mechanism by which the loss of VAMP8 causes a defect in the thymus can possibly be understood by co-relating the findings of this study with other similar studies on knock out mice. There are several knock out mouse models that share similar phenotypic manifestation with the VAMP8^{-/-} mice.

One of the most interesting studies involves c-Cbl mice. c-Cbl is a E3 ubiquitin ligase that recruits ubiquitin conjugating enzyme and is the main negative regulator of the level of TCR and its downstream signaling. After $\alpha\beta$ TCR engagement, the ζ chain of CD3 gets monoubiquitinated by c-Cbl at its dileucine based motif. The ubiquitinylation acts as a signal for endocytosis of the TCR-CD3, their sorting into multivesicular bodies and eventual degradation in the lysosomes (Naramura et al. 2002; Panigada et al. 2002). Hence c-Cbl down regulates the signaling by T lymphocytes by subjecting the TCR to

internalization and degradation in the lysosomes. In line with this, a mouse mutant with loss of function mutation in the RING finger domain of c-Cbl gene showed enhanced levels of TCR and CD3 on the surface of the DP thymocytes (Thien et al. 2005a). The thymocytes from these mice showed excessive signaling by the TCR-CD3 complex since the activated TCR is not endocytosed and degraded. In addition, the mice showed progressive loss of the thymus towards adulthood. The thymocyte cell count was reduced by 25% in 15 day old mice, by 85% in 29 days old and by upto 99% in 40 days old c-Cbl mutant mice. (Thien et al. 2005a). The phenotypic manifestation seen in this loss of function c-Cbl mutant is very close to what was seen in the VAMP8^{-/-} mice. The VAMP8^{-/-} mice had a progressive reduction in thymic cellularity. The VAMP8^{-/-} small not sick mice showed 2 fold reduction in thymus cellularity at 9-10 days of age while the the VAMP8^{-/-} small and sick mice (10-12 days of age) showed a 10 fold decrease. There was a massive decrease in absolute cell counts in the VAMP8^{-/-} small and sick mice. Much like the VAMP8^{-/-} small not sick mice, the thymocytes from c-Cbl mutant showed increased sensitivity to anti-CD3 induced cell death (Thien et al. 2005a). However unlike the VAMP8^{-/-} mice, the c-Cbl mutant mice did not show a major defect in thymocytes development and in progression of thymocytes through DN-DP and DP-SP stages. Although the authors did observe a slight increase in DN cells and a corresponding decrease in DP cells in the mice with maximum thymic loss (Thien et al. 2005a). Also unlike the c-Cbl mice, in this study the level TCR was found to be normal on the cell surface of T lymphocytes. Despite the few differences between phenotypic manifestation in the c-Cbl mutant and VAMP8^{-/-} mice, it is interesting that some of the affects are similar in both the mice. It is known that VAMP8 is involved in the homotypic fusion of late endosomes. It is possible that the absence VAMP8 results in a blockage at the late endosomal fusion, hence the activated TCR is not trafficked to the lysosomes resulting in excessive signaling. Therefore, the deficiency of VAMP8 could lead to phenotypic manifestations by a mechanism similar to the c-Cbl mutant.

Lymphostromal interaction is critical to the development of thymocytes and the stroma and hence the function of thymus. There are some knock out mouse models have an abnormal lymphostromal interaction and signaling and exhibit a phenotype similar to the VAMP8^{-/-}

mice. One such study that could give an insight into the possible role of VAMP8 in thymus development is the one involving EphA4^{-/-} mice. Ephrin receptors (Ephs) are receptor tyrosine kinases that interact with their ligands Ephrins (class A and/or B) and mediate cell-cell contact, bidirectional signaling, cell movement and guidance in several developmental processes including morphogenesis, establishment of tissue domains and neuronal networking (Palmer and Klein 2003). EphA4 is a receptor for ephrins A and B and activates the Jak/STAT pathway in the thymus. It was shown to be critical for generation of epithelial network and for the T cell development (Munoz et al. 2006). The thymus from EphA4^{-/-} mice was smaller than the littermates and the mice showed a progressive increase in thymus abnormality. The thymus was very small with total cell count reduced to 40% of the EphA4^{+/+} by day 10 and to 15% by 3 weeks of age. The absolute cell number of all lymphoid cells was reduced. Interestingly, the transition from DN-DP and DP-SP was compromised in these mice and several developing subsets of thymocytes were disturbed. There was an increased cell death in the thymus of these mice. Additionally, the thymus morphology was disrupted in the EphA4^{-/-} mice. There was a major disturbance in the cortex, with heavily reduced cortical epithelial cells and a very sharp cortico-medullary boundary (Munoz et al. 2006). The VAMP8^{-/-} mice also had a massively reduced thymus with increased cell death and disturbed thymocytes populations. The morphology of the thymus was also disrupted in the VAMP8^{-/-} small and sick mice, however the defect was different from what as seen in the EphA4^{-/-} mice. These VAMP8^{-/-} mice had normal cortex while the medulla was reduced to remnants and the cortico-medullary boundary was not clearly defined. Although there are some differences, it is interesting that most of the phenotypic manifestations of the loss of VAMP8 and EphA4 are similar. The similarity could indicate towards the involvement of VAMP8 in promoting cell-cell interaction either directly or indirectly. Besides, it is known that the Eph receptors are trafficked within the cell and the signaling via the Eph is terminated by subjecting the Eph receptors to endocytosis, traffic via late endosomal compartments finally to lysosomal degradation (Palmer and Klein 2003). It is also possible that the loss of VAMP8 results in a loss of recycling of the Eph receptors or similar receptors due to blockage at the late endosomal step thereby causing a defect in the thymus similar to EphA4^{-/-} mice.

Another example that shows the importance of lympho-stromal interaction is the SCID mice. These mice lack functional T- cell receptors molecule that results in the absence of medullary lymphocytes in these mice. This in turn, causes the medullary epithelium to reduce to rudiments in the SCID mice (Bosma et al. 1983; Shores et al. 1990). Hence, from the findings in SCID and $TCR\alpha^{-/-}$ mice it is known that medullary stromal cells are highly dependent on the medullary T-cell population for their existence. In a similar way, the massive disturbance in DN1-4 subsets and an excessive loss of DP cells in the $VAMP8^{-/-}$ small and sick mice could also result in the observed disruption of the thymic medulla and cortico-medullary boundary.

There are some studies involving defective signaling cascades in the thymus that also show similarities to the $VAMP8^{-/-}$ mice. One such study involves STAT3. STATs are activators of transcription that work downstream of the Janus kinases (JAKs). The activation of JAKs and consequently STATs occurs when cytokines bind to their receptors on the surface of the responsive cells. STATs have anti-apoptotic activity by modulating Bcl-2 family of proteins. STAT3 is a member of the STAT family that is involved in signaling by IL-6 type cytokines, epidermal growth factor (EGF), Platelet derived growth factor (PDGF), Hepatocyte growth factor (HGF) etc. The specific ablation of STAT3 in the thymic epithelial cells using a K5 tissue specific promoter to express the cre-recombinase resulted in a phenotype of the thymus similar to $VAMP8^{-/-}$ mice. The neonatal mice had a normal thymus. The thymocytes cell count reduced starting at 6 weeks of age and the affect was most severe after adolescence i.e. 10-12 weeks of age. After 9 weeks $STAT3^{-/-}$ thymii had no cortico-medullary distinction similar to what was seen in the $VAMP8^{-/-}$ mice at 9-12 days of age. The mice had excessive cell death in the thymus and the thymocytes were highly sensitive to apoptotic stimuli such as Dexamethasone *in vivo* but this effect was not seen *in vitro*. The T cell progenitors were found to be normal in these mice however their thymic epithelial cells (TECs) were abnormal. The phenotype in these mice was atleast in part explained due to the inability of the thymic epithelial cells to signal to the developing thymocytes due to the loss of the signaling molecule STAT3 (Sano et al. 2001; Shen et al. 2004). The similarity in phenotype between $STAT3^{-/-}$ and $VAMP8^{-/-}$ mice could point towards a possible role of VAMP8 in regulating the activity and availability of certain

signaling molecules or their receptors on the developing thymocytes and/or the stromal cells.

In order to limit the signaling by cytokines, the activity of JAKs and STATs is downregulated by certain inhibitory proteins. One such protein is STAT induced STAT inhibitor-1 (SSI-1 also called SOCS-1). The SSI-1^{-/-} mice fail to downregulate the cytokine signaling and interestingly, show phenotypic similarities to the VAMP8^{-/-} mice (Kishimoto et al. 1998). *In-vitro*, the thymocytes show excessive proliferation in response to cytokines. The SSI-1^{-/-} mice were healthy at birth but mice showed upto 40% weight loss at postnatal day 9 and were dead within 3 weeks of age. At around 10 days of age, the mice had massive reduction in lymphocytes in the thymus and the spleen and upto 75-80% thymocytes were lost in the thymus of these mice. However, unlike the VAMP8^{-/-} sick mice, despite the loss of massive reduction in thymocyte count, there was no disturbance in the CD4/CD8 subsets in the SSI-1^{-/-} mice compare to SSI-1^{+/+} mice. Most interestingly, the SSI-1^{-/-} mice had no clear cortico-medullary boundary at around 10 days of age just as in the VAMP8^{-/-} mice. Similar to the VAMP8^{-/-} small and sick mice, the SSI-1^{-/-} mice had a high number of dead cells in the thymus which was explained due to an increased expression of the pro-apoptotic factor Bax (Kishimoto et al. 1998). These similarities between VAMP8^{-/-} and SSI-1 mice point towards the involvement of VAMP8 in down regulation of certain signaling molecules or events in the thymus. Hence the loss of VAMP8 could lead to excessive the signaling and leading to the phenotypic manifestation just as seen in SSI-1^{-/-} mice.

Another model that bears phenotypic similarity to VAMP8^{-/-} mice is the TCR α ^{-/-} mice. The expression of the α chain of the TCR starts at the CD4⁺CD8⁺ (DP) stage and is important for the transition of DP cells to SP T-lymphocytes and in turn the migration of the T lymphocytes from the cortex to the medulla. The TCR α ^{-/-} mice had normal numbers of all thymocytes before the DP stage. However there was a developmental block in the CD4⁺CD8⁺ stage. As a result, these mice had a normal thymic cortex while the medulla was reduced to rudiments (Philpott et al. 1992); (Ritter and Boyd 1993). Similar thymic morphology disruption was also observed in mice treated *in vivo* with anti CD3 antibodies (Kyewski et al. 1989) and immunosuppressant Cyclosporine A.

TSG is an antagonist of Bone morphogenetic protein 4 (BMP4) which is a member of transforming growth factor β super family. TSG is supposed to be a positive regulator of thymocytes development. Knock out mice for TSG showed impairment of thymus among other organs (Nosaka et al. 2003). 12% of the TSG^{-/-} mice died at birth while the rest were 10-20% smaller than their littermates. More than half the TSG^{-/-} mice showed progressive growth retardation became severely sick and some died. The mice had poorly developed thymii with several mice between 10-40 days of age showing, upto two fold reduction in thymocytes number. It was interesting that these mice also exhibit heterogeneity in the phenotype similar to the VAMP8^{-/-} mice. This heterogeneity was in part explained due to unbalanced distribution of soluble factors such as BMPs and Chordin in the absence of TSG (Nosaka et al. 2003). In addition, there was an increase in SP cells and a decrease in the DP cells in around 3 weeks old TSG^{-/-} mice similar to what was seen in the VAMP8^{-/-} small and sick mice although the phenotype appeared much early (day 10-12) on the VAMP8^{-/-} mice. The lymphoid deficiency in these mice was not due to an intrinsic defect in the T or B cells rather due to the microenvironment such as stroma or cytokine production (Nosaka et al. 2003). It is known that a constant BMP signaling is required for normal development of the stroma but the kinetics of thymocytes development is not affected in the absence of BMPs (Bleul et al. 2005). Hence the similarity of phenotype in VAMP8^{-/-} mice with BMP4^{-/-} mice strongly indicates that VAMP8 is involved in the regulation of signaling molecules in the thymus possibly in the trafficking these molecules. Mice lacking the activity of Rho GTPases in the thymus due to expression of *Clostridium botulinum* C3 transferase, also show a striking similarity in the phenotype to the VAMP8^{-/-} sick mice. The mice show a progressively degenerating health status, reduced thymic cellularity and increased cell death at 5-8 weeks of age (Henning et al. 1997). Additionally, there was a major alteration in the DN1-4 thymocyte subsets in the thymus of these mice. Interestingly, the thymus had no clear compartmentalization into cortex and medulla, very similar to what was observed in the VAMP8^{-/-} mice. Rho proteins act on the actin cytoskeleton and mediate actin modulation. In addition members of the Rho family are also localize to the vesicular membranes and have been implicated in guiding vesicle movement during exo- and endocytic pathways (Ridley 2001). The phenotype in the Rho^{-/-} was at least

in part explained due to a cell cycle block during progression of DN thymocytes from G₁ phase in these mice (Henning et al. 1997). Thus Rho is thought to be important for the signaling events that take the T lymphocytes through the G₁ phase and give them the survival stimulus. Since the phenotypic manifestations of the VAMP8 deficiency completely coincides with the phenotypic manifestations of Rho deficiency, it could be that VAMP8 is involved in trafficking of certain factors that provide survival signals to the T lymphocytes by the stromal cells of the thymus.

The above mentioned knock out studies involve molecules that are implicated either in regulation of intracellular traffic in the thymus, lympho-stromal interactions or signaling during thymocyte differentiation. From the observed phenotypic similarities between the VAMP8^{-/-} mice and these knock out studies, it seems that VAMP8 could be directly or indirectly be involved in the regulation of thymo-stromal interactions or the traffic of certain signaling molecules in the thymus. Hence the disruption of VAMP8 leads to abnormal differentiation of T lymphocytes and abnormal thymus development in the VAMP8^{-/-} mice. However the study could not point out which mechanism in the thymus is disrupted due to the loss of VAMP8 that results in the observed phenotype.

4.2.4 Is thymus defect the cause of death of the mice?

The thymus defect as being the singular cause of death is less likely in the VAMP8^{-/-} mice. There are several mouse models that lack thymus such as nude mice or have an immuno-compromised situation such as in the SCID mice that can survive under pathogen free conditions. This is an indicator that the loss of thymus or immuno-compromised state is not lethal.

VAMP8 was initially identified as a late endosomal v-SNARE that forms complex with Syntaxin 7, Syntaxin8 and Vti1b and mediates homotypic late endosomal fusion (Antonin et al. 2000a). Additionally, VAMP8^{-/-} has also been shown to form a complex with SNAP 23 and Syntaxin 4 and mediates regulated exocytosis of zymogen granules from the pancreatic acinar cells (Wang et al. 2004). VAMP8 has recently been shown to be the primary v-SNARE responsible for regulated exocytosis of alpha and dense core granules and secretory lysosomes from the platelets (Ren et al. 2006, Polgar et al. 2002). VAMP8 is

also implicated in exocytosis of secretory granules from mast cells together with Syntaxin 4 (Paumet et al. 2000a). It was shown that VAMP8 is important for the terminal step of cytokinesis in mammalian cells (Low et al. 2003). Hence, VAMP8 has gained increasing attention in recent years especially as a mediator of regulated exocytosis in several cell types. Therefore, loss of VAMP8 could result simultaneously in the failure of several critical cellular processes in different tissues. In addition, although the data from this work and also from previous study (Wang et al. 2004) suggests that VAMP8 is not essential for homotypic late endosomal fusion, however the role of VAMP8 in endosomal fusion events can not be completely ruled out. Considering the role of VAMP8 in endosomal and secretory pathways, its possible quite likely that early mortality in VAMP8^{-/-} mice is not caused by the loss of thymus, rather by a wide spread defect in several trafficking and exocytic events in the mice.

4.3 Endosomal trafficking in VAMP8^{-/-} mice

Work from two independent groups showed the involvement of VAMP8 in late endosomal homotypic fusion (Antonin et al. 2000a) and in regulated exocytosis of secretory granules of the exocrine pancreas (Wang et al. 2004). VAMP8 forms a complex with Syntaxin7, Syntaxin8 and Vti1b during late endosomal trafficking (Antonin et al. 2000a) while it is associated with SNAP23 and Syntaxin4 during exocytotic events (Wang et al. 2004).

In vitro studies from Wang and co workers showed that the ablation of VAMP8 does not cause any defect in the late endosomal membrane fusion. Receptor mediated endocytosis and lysosomal degradation of LDL, trafficking of transferrin and asialofetuin was found to be normal in the fibroblasts derived from VAMP8^{-/-} mice. On the other hand, they found a major defect in the secretagogue mediated exocytosis of zymogen granules (storage lysosomes) of pancreatic acinar cells in the absence VAMP8 (Wang et al. 2004).

In this work, the role of VAMP8 in late endosomal trafficking was studied by several *in vitro* assays in cells derived from VAMP8^{-/-} and VAMP8^{-/-} Vti1b^{-/-} mice. Phagocytic uptake of latex beads by macrophages and its traffic to lamp1 stained lysosomal/late endosomal compartments was not affected in the VAMP8^{-/-} Vti1b^{-/-} macrophages. There was no major defect in receptor mediated uptake of LDL in the fibroblasts of the VAMP8^{-/-}

mice. In addition, the activity of lysosomal enzymes was studied by enzyme-substrate reaction assays with liver as the source of lysosomal enzymes. There was no defect in the activity of β -Hexosaminidase, β -Galactosidase and β -Mannosidase in the liver of small and sick as well as small not sick VAMP8^{-/-} mice and adult VAMP8^{-/-} Vti1b^{-/-} mice. This data is in line with the previous findings (Wang et al. 2004). Apparently, the absence of VAMP8 does not cause any major defect in the late endosomal trafficking in different cell types and tissues. It is possible that VAMP8 and some other v SNAREs have redundant function and can replace each other in the endosomal trafficking.

Recently it was shown that although VAMP8 is the primary SNARE in platelet exocytosis, some tetanus sensitive VAMPs (VAMP3/VAMP2) could promote fusion in its absence (Ren et al. 2006). This indicates towards a redundancy in the usage of VAMPs in a system. However, there are certain points to be considered in these experiments. Firstly, the fibroblasts were isolated from the embryos. At the embryonic stage, all the pups are phenotypically normal while the defect appears only after first postnatal day week. Therefore it could be that the studies on the embryonic fibroblasts do not reflect the real situation as it happens in the VAMP8^{-/-} deficient small and sick mice. Similarly, the phagocytic assays were done on peritoneal macrophages derived from mice older than 3-4 weeks. This means the macrophages investigated were from phenotypically normal mice. It would be interesting to study the cells derived from the sick stage of mice and see if the endosomal trafficking is normal or disturbed in these mice or not.

4.4 What could functionally replace VAMP8?

A SNARE complex always consists of four SNARE motifs (Qa,Qb,Qc,R). In principal it is possible for one SNARE to functionally replace another of the same type in a complex. Recombinant purified SNAREs have been shown form complexes in several combinations although the stability of the complexes varies greatly (Jahn and Sudhof 1999). Additionally, some SNAREs have been shown to be involved in more than one SNARE complex. Since there was no major defect in the late endosomal trafficking in the absence of VAMP8 (R), it was though that some other endosomal SNAREs could functionally replace VAMP8 in the late endosomal complex.

Out of other members of the v SNARE family, VAMP1 and VAMP2 are preferentially distributed in neuronal and exo- and endocrine cells (Jahn and Sudhof 1999). VAMP4 is localized to the trans-golgi network (Steggmaier et al. 1999b; Zeng et al. 2003) while VAMP5 is present largely in the plasma membrane of the skeletal muscles (Zeng et al. 1998b; Zeng et al. 2003).

VAMP7 is distributed at later compartments of the endocytic pathway similar to VAMP8 (Advani et al. 1999). VAMP7 mediates the fusion between late endosomes and lysosomes in a complex with Syntaxin 7 (Qa), Syntaxin 8 (Qc) and Vti1b (Qb) (Pryor et al. 2004). Since VAMP7 and VAMP8 shares the same SNARE partners (Syntaxin 7 (Qa), Syntaxin 8 (Qc) and Vti1b (Qb) it is quite likely the VAMP7 could compensate for the homotypic late endosomal fusion complex in the absence of VAMP8. In this study, attempts were made to raise antibodies against VAMP7 so as to enable detection of VAMP7 in thymus from VAMP8^{-/-} mice. However despite several efforts, we could not obtain an anti VAMP7 antibody that could detect the protein in tissue homogenates.

Wang and coworkers (Wang et al. 2004) suggest that VAMP3 could have a redundant function with VAMP8 as these two v-SNAREs share similar properties. VAMP3 has a ubiquitous expression and preferential localization to endosomal compartments (Galli et al. 1994; McMahon et al. 1993b). However, VAMP3 knock out mice showed no abnormality in the endosomal trafficking (Yang et al. 2001). In line with this hypothesis, it was shown that one of the toxin sensitive VAMPs (VAMP3/2) could compensate for VAMP8, though less efficiently; in platelet granule release (Ren et al. 2006). In addition, VAMP3 and VAMP8 double knock out mice are embryonic lethal which shows that these two R SNAREs can possibly compensate for each other functionally (mentioned in Ren et al. 2006).

It is known that VAMP4, syntaxin 6, syntaxin 16 and Vti1a form a complex during early endosomal fusion. To test the possibility whether this complex can compensate for the loss of VAMP8 and Vti1b in the thymus, western blot detection was done for syntaxin 16, Vti1a and VAMP4. There was no considerable increase in the expression of any of these SNAREs, indicating that the early endosomal SNARE complex does not compensate for the loss of the late endosomal complex. However, it is possible that Vti1a could replace Vti1b in its constitutive expression level. The functional redundancy of Vti1b by Vti1a is

demonstrated by the fact that *Vti1a*^{-/-} *Vti1b*^{-/-} mice are postnatal lethal (Unpublished work from our lab).

In addition the expression level of SNAP29 was tested. SNAP29 has two SNARE motifs that contribute two Glutamines (Qb and Qc) to the core complex. It lacks a poly-cystein rich domain hence it can not anchor to the membranes via palmitoylation of cystein residues. Therefore, SNAP29 could possibly interact with several other SNAREs. *Vti1b* is also a Qb SNARE, although SNAP29 bears only 24% amino acid identity with *Vti1b*, it was interesting to study whether or not SNAP29 has an increased expression in *VAMP8*^{-/-} *Vti1b*^{-/-} tissues. However, there was no substantial increase in SNAP29 expression in thymus from *VAMP8*^{-/-} mice.

Atlashkin and co-workers reported that syntaxin8 is increasingly destabilized and degraded in absence of *Vti1b* (Atlashkin et al. 2003). In this study too, the level of syntaxin 8 was found reduced in the thymus of *VAMP8*^{-/-} *Vti1b*^{-/-} mice. In order to check if the loss of *VAMP8* also causes destabilization of other complex members, levels of syntaxin7, *Vti1b*, syntaxin8 were checked by western blot. However, there was no substantial decrease in any of these SNAREs in the thymus of *VAMP8*^{-/-} mice indicating that the loss of *VAMP8* does not affect the other SNARE partners of the late endosomal complex.

5. Summary

VAMP8 also called endobrevin is an R SNARE protein involved in two distinct steps in the endosomal / lysosomal trafficking. VAMP8 forms a complex with syntaxin8, syntaxin7 and Vti1b that is involved in homotypic late endosomal fusion. In addition, VAMP8 together with SNAP23 and syntaxin4 regulates exocytosis of secretory granules in the acinar cells of the exocrine pancreas. VAMP8 was also shown to function in regulated exocytosis of secretory granules from mast cells and platelets.

The aim of this study was to analyze the physiological role of VAMP8 in VAMP8 knock out mouse model. In addition, double knock out mice deficient in VAMP8 and Vti1b, a Qb SNARE partner of VAMP8 in late endosomal fusion complex, were also analysed to study the effect of deleting two SNAREs of the same complex.

Both the VAMP8^{-/-} and VAMP8^{-/-} Vti1b^{-/-} mice were born in expected mendelian ratios indicating a normal prenatal development. The mice showed phenotypic manifestation early in postnatal life however there was heterogeneity in the phenotype. Large percentage of VAMP8^{-/-} Vti1b^{-/-} and VAMP8^{-/-} mice showed progressively degenerating health and died within the first one month of post natal life. The remaining VAMP8^{-/-} and VAMP8^{-/-} Vti1b^{-/-} survivors became fertile adults although they were a little lighter than their heterozygous littermates.

At the onset of the phenotype, the mice started to loose weight (defined in this work as small not sick stage). After 2-3 days of consecutive weight loss, the mice became increasingly sick (defined as small and sick stage) and eventually died. At the time of death, these mice were half the weight of their littermates and had an unstable gait.

Thymus from VAMP8^{-/-} and VAMP8^{-/-} Vti1b^{-/-} small and sick mice showed gross abnormality. While normal wild type thymus had a well defined boundary between the cortex and medulla, the thymii from the VAMP8^{-/-} and VAMP8^{-/-} Vti1b^{-/-} small and sick mice had no clear compartmentalization, with medullary cells scattered within the cortical region. Additionally, there was a progressive reduction in the thymus cellularity with the reduction being most prominent at the small and sick stage.

Since the disruption of thymic morphology could result in aberrant T-lymphocyte maturation, different developmental stages of thymocytes were analyzed. In both, VAMP8^{-/-} and VAMP8^{-/-} Vti1b^{-/-} small and sick mice, distribution of thymocyte progenitors DN1-DN4 was disturbed. There was an increase in the percentage of DN1 (CD44⁺CD25⁻) and DN4 (CD44⁻CD25⁻) subsets while DN2 (CD44⁺CD25⁺) and DN3 (CD44⁻CD25⁺) cells were reduced. Further, there was an increase in the percentage of CD4⁺, CD8⁺ and CD4-CD8⁻ cells while the CD4⁺CD8⁺ were reduced. In addition, the thymus showed an elevated number of dead cells. All these observations were observed only in the small and sick VAMP8^{-/-} and VAMP8^{-/-} Vti1b^{-/-} mice and not in the small not sick and the adult mice.

Reduction in thymus cellularity of VAMP8^{-/-} mice could be due to excessive cell death of the thymocytes. *In vitro* apoptosis stimulation assays showed that the thymocytes from small not sick stage were highly susceptible to death upon induction with dexamethasone, anti FAS (CD95) antibody treatment and CD3-CD28 crosslinking. While there was a very high number of dead cells (~60%) in the thymus of the small and sick mice and these surviving cells were more resistant to dexamethasone treatment. Hence, it seems that the thymus from the small not sick mice becomes increasingly sensitive to physiological apoptotic stimulus. Eventually, most of the thymocytes die by the time the mice reach the small and sick stage.

In order to understand whether the thymus phenotype resulted due to an inherent defect in T-lymphocyte precursors or due to a defective thymic stroma, transplantation experiments were done. Bone marrow derived lymphoid progenitors from VAMP8^{-/-} small and sick and VAMP8^{+/+} controls were transplanted into recipient RAG2^{-/-} γ c^{-/-} mice. Bone marrow cells from both, the VAMP8^{+/+} and VAMP8^{-/-} mice could repopulate the immune system of the RAG2^{-/-} γ c^{-/-} recipient mice with both B and T lymphocytes after 4 and 6-9 weeks of transplantation respectively. This indicates that the T lymphocyte progenitors of VAMP8^{-/-} small and sick mice do not have an inherent maturational defect. The thymic stromal cells in these mice are probably abnormal and therefore can not support proper maturation and development of T lymphocytes in these mice.

In addition, endosomal trafficking was studied in the cells derived from VAMP8^{-/-} mice. Lamp1 staining was done to visualize the morphology of lysosomes / late endosomes in the

VAMP8^{-/-} and VAMP8^{-/-} Vti1b^{-/-} fibroblasts. In addition, phagocytosis and the traffic of phagosome to lysosomes was studied in peritoneal macrophages from VAMP8^{-/-} Vti1b^{-/-} mice using fluorescent beads in pulse chase experiments. The receptor mediated endocytosis and lysosomal degradation of fluorescently labeled LDL was studied in the embryonic fibroblasts of the VAMP8^{-/-} and VAMP8^{-/-} Vti1b^{-/-} mice. These experiments showed no defect in the endosomal vesicular trafficking. A defect in late endosomal-lysosomal trafficking could result in reduced amount of active lysosomal enzymes. To check this, activity of several lysosomal enzymes was studied in the liver of VAMP8^{-/-} and VAMP8^{-/-} Vti1b^{-/-} mice. VAMP8^{-/-} small not sick as well as small and sick mice had normal enzyme activity in the liver homogenates. Hence this data indicates that the late endosomal fusion event is not compromised in the absence of VAMP8 and Vti1b. Additionally, VAMP8 seems non essential or can be compensated during homotypic late endosomal fusion events. However, western blot analysis of liver, kidney and thymus from the VAMP8^{-/-} and VAMP8^{-/-} Vti1b^{-/-} mice did not reveal any major difference in the expression of other SNARE proteins that could possibly exert a compensatory role in the absence of VAMP8.

Hence this study shows that VAMP8 is important for the development of thymus and possibly the function of the thymic stromal cells. A lack of VAMP8 probably results in a defective stroma that in turn leads to developmental and maturational defect in T lymphocytes. A lack of functional stroma could also explain the excessive cell death seen in the thymus from VAMP8^{-/-} mice. From our data it seems that the absence of VAMP8 does not hinder the late endosomal fusion events possibly due to a compensatory mechanism. However the mechanism by which VAMP8 exerts a regulatory role in thymus is still unclear.

6. Conclusion and Outlook

The current work shows that VAMP8 or endobrevin, plays a role in thymus development and T lymphocyte differentiation in mice. VAMP8 probably regulates the function of thymic stromal cells that in turn support the thymic morphology as well as guide the thymocytes in their course of development through the thymus. Thus the loss of VAMP8 results in disruption of thymus morphology and maturational defect in thymocytes. This in turn possibly commits increasing number of thymocytes to cell death. The study also shows that VAMP8 is not essential for late-endosomal fusion events.

However there are several questions that still remain unanswered. From the bone marrow transplantation experiments it is certain that the T lymphocyte progenitors of the VAMP8^{-/-} small and sick mice do not have an inherent defect of differentiation and maturation. However, since these mice have an abnormal health status, it can not be ascertained that the defect indeed lies in the stromal cells. This problem could possibly be solved by thymus graft experiments, where the thymus from VAMP8^{-/-} small and sick mice could be grafted under the renal capsule of the SCID mice. The SCID mice can then be supplied with normal bone marrow from wild type mouse. The failure of the VAMP8^{-/-} grafted thymus to get repopulated by thymocytes derived from wild type bone marrow could definitively suggest an inherent defect in stromal cells of thymus from VAMP8^{-/-} sick mice.

Further, it would be important to pinpoint whether the defect lies in the cortical or in the medullary stromal cells. It could be possible to answer these questions by using thymic cultures, either as complex organ cultures or as selective cultures of specific stromal cells from VAMP8^{-/-} small and sick mice. The development, proliferation and survival of thymic stromal cells under the effect of stimulatory chemokines could be studied in vitro. Analysis of vesicular trafficking, cytokines, growth factors release and expression of adhesion molecules in the cultured thymic cells could give an indication towards to underlying reason for the thymus phenotype.

VAMP8 is involved in regulated exocytosis of secretory vesicles from several cell types. Cytotoxic T lymphocytes (CTLs) are known to store the lytic proteins in specialized granules that are released upon stimulation. CTLs from VAMP8^{-/-} small and adult mice

could therefore serve as a model to study the role of VAMP8 in regulated exocytosis in T lymphocytes and could give an insight into the affect of VAMP8 ablation on mature T lymphocytes.

Dendritic cells are antigen presenting cells that process and present the antigen to cell surface and stimulate the T lymphocytes. It could be helpful to study whether or not the dendritic cells from VAMP8^{-/-} sick mice are capable of processing the antigenic peptides and stimulating the T lymphocytes. It would also be interesting to check whether the T lymphocytes from the VAMP8^{-/-} sick mice respond to stimulatory signals from wild type dendritic cells. This could give a clue whether the defect lies in dendritic cells derived from VAMP8^{-/-} mice.

Lastly, in order to understand the compensatory mechanism of VAMP8, it would be interesting to carry out a study of systems which lack two or more R SNAREs simultaneously. This could either be done in by creating double knock out mice or by silencing of specific v-SNAREs in specific cell type. Studying the affect of ablating VAMP8 together with VAMP7 and VAMP3/2 would be specifically interesting. Such analysis could shed some more light into the functional redundancy of the R-SNAREs.

7. Bibliography

Advani R.J., Bae H.R., Bock J.B., Chao D.S., Doung Y.C., Prekeris R., Yoo J.S., and Scheller R.H. (1998). Seven novel mammalian SNARE proteins localize to distinct membrane compartments. *Journal of Biological Chemistry* **273**:10317-10324.

Advani R.J., Yang B., Prekeris R., Lee K.C., Klumperman J., and Scheller R.H. (1999). VAMP-7 mediates vesicular transport from endosomes to lysosomes. *Journal of Cell Biology* **146**:765-775.

Aguilar R.C., Boehm M., Gorshkova I., Crouch R.J., Tomita K., Saito T., Ohno H., and Bonifacino J.S. (2001). Signal-binding specificity of the mu 4 subunit of the adaptor protein complex AP-4. *Journal of Biological Chemistry* **276**:13145-13152.

Aikawa Y., Lynch K.L., Boswell K.L., and Martin T.F.J. (2006). A second SNARE role for exocytic SNAP25 in endosome fusion. *Molecular Biology of the Cell* **17**:2113-2124.

Anderson G., Moore N.C., Owen J.J.T., and Jenkinson E.J. (1996). Cellular interactions in thymocyte development. *Annual Review of Immunology* **14**:73-99.

Antonin W., Fasshauer D., Becker S., Jahn R., and Schneider T.R. (2002). Crystal structure of the endosomal SNARE complex reveals common structural principles of all SNAREs. *Nature Structural Biology* **9**:107-111.

Antonin W., Holroyd C., Fasshauer D., Pabst S., von Mollard G.F., and Jahn R. (2000b). A SNARE complex mediating fusion of late endosomes defines conserved properties of SNARE structure and function. *EMBO Journal* **19**:6453-6464.

Antonin W., Holroyd C., Tikkanen R., Honing S., and Jahn R. (2000c). The R-SNARE endobrevin/VAMP-8 mediates homotypic fusion of early endosomes and late endosomes. *Molecular Biology of the Cell* **11**:3289-3298.

Antonin W., Riedel D., and von Mollard G.F. (2000d). The SNARE Vti1a-beta is localized to small synaptic vesicles and participates in a novel SNARE complex. *Journal of Neuroscience* **20**:5724-5732.

Ashwell J.D., King L.B., and Vacchio M.S. (1996). Cross-talk between the T cell antigen receptor and the glucocorticoid receptor regulates thymocyte development. *Stem Cells* **14**:490-500.

Atlashkin V., Kreykenbohm V., Eskelinen E.L., Wenzel D., Fayyazi A., and von Mollard G.F. (2003). Deletion of the SNARE vti1b in mice results in the loss of a single SNARE partner, syntaxin 8. *Molecular and Cellular Biology* **23**:5198-5207.

- Baumert M., Maycox P.R., Navone F., Decamilli P., and Jahn R. (1989). Synaptobrevin - an integral membrane protein of 18000 daltons present in small synaptic vesicles of rat brain. *EMBO Journal* **8**:379-384.
- Bennett M.K., Calakos N., Miller K.G., and Scheller R.H. (1992). Syntaxin - a synaptic protein implicated in docking of synaptic vesicles at presynaptic active zones. *Science* **3**:255-259.
- Bennett M.K., Garciaarraras J.E., Elferink L.A., Peterson K., Fleming A.M., Hazuka C.D., and Scheller R.H. (1993). The syntaxin family of vesicular transport receptors. *Cell* **74**:863-873.
- Bilan F., Thoreau V., Nacfer M., Derand R., Norez C., Cantereau A., Garcia M., Becq F., and Kitzis A. (2004). Syntaxin 8 impairs trafficking of cystic fibrosis transmembrane conductance regulator (CFTR) and inhibits its channel activity. *Journal of Cell Science* **117**:1923-1935.
- Blanchard N., Lankar D., Faure F., Regnault A., Dumont C., Raposo G., and Hivroz C. (2002). TCR activation of human T cells induces the production of exosomes bearing the TCR/CD3/zeta complex. *Journal of Immunology* **168**:3235-3241.
- Blasi J., Chapman E.R., Link E., Binz T., Yamasaki S., Decamilli P., Sudhof T.C., Niemann H., and Jahn R. (1993). Botulinum neurotoxin-A selectively cleaves the synaptic protein SNAP-25. *Nature* **365**:160-163.
- Bleul C.C. and Boehm T. (2005). BMP signaling is required for normal thymus development. *Journal of Immunology* **175**:5213-5221.
- Blobel G. (1980). Intracellular protein topogenesis. *European Journal of Cell Biology* **22**:153-153.
- Block M.R., Glick B.S., Wilcox C.A., Wieland F.T., and Rothman J.E. (1988). Purification of an N-Ethylmaleimide-sensitive protein catalyzing vesicular transport. *Proceedings of the National Academy of Sciences of the United States of America* **85**:7852-7856.
- Blott E.J. and Griffiths G.M. (2002). Secretory lysosomes. *Nature Reviews Molecular Cell Biology* **3**:122-131.
- Bordier C. (1981). Phase separation of integral membrane proteins in Triton X-114 solution. *Journal of Biological Chemistry* **256**:1604-1607.
- Bosma G.C., Custer R.P., and Bosma M.J. (1983). A severe combined immunodeficiency mutation in the mouse. *Nature* **301**:527-530.

Bouillet P., Cory S., Zhang L.C., Strasser A., and Adams J.M. (2001). Degenerative disorders caused by Bcl-2 deficiency prevented by loss of its BH3-only antagonist bim. *Developmental Cell* **1**:645-653.

Brandhorst D., Zwillig D., Rizzoli S.O., Lippert U., Lang T., and Jahn R. (2006). Homotypic fusion of early endosomes: SNAREs do not determine fusion specificity. *Proceedings of the National Academy of Sciences of the United States of America* **103**:2701-2706.

Braun V., Fraissier V., Raposo G., Hurbain I., Sibarita J.B., Chavrier P., Galli T., and Niedergang F. (2004). TI-VAMP/VAMP7 is required for optimal phagocytosis of opsonised particles in macrophages. *EMBO Journal* **23**:4166-4176.

Brenner S. (1974). Genetics of *Caenorhabditis elegans*. *Genetics* **77**:71-94.

Brewer J.A., Sleckman B.P., Swat W., and Muglia L.J. (2002). Green fluorescent protein-glucocorticoid receptor knockin mice reveal dynamic receptor modulation during thymocyte development. *Journal of Immunology* **169**:1309-1318.

Bright N.A., Reaves B.J., Mullock B.M., and Luzio J.P. (1997). Dense core lysosomes can fuse with late endosomes and are re-formed from the resultant hybrid organelles. *Journal of Cell Science* **110**:2027-2040.

Brose N., Petrenko A.G., Südhof T.C., and Jahn R. (1992). Synaptotagmin: A calcium sensor on the synaptic vesicle surface. *Science* **256**:1021-1025.

Burkhardt J.K., Hester S., Lapham C.K., and Argon Y. (1990). The lytic granules of natural-killer-cells are dual-function organelles combining secretory and pre-lysosomal compartments. *Journal of Cell Biology* **111**:2327-2340.

Cante-Barrett K., Gallo E.M., Winslow M.M., and Crabtree G.R. (2006). Thymocyte negative selection is mediated by protein kinase C- and Ca^{2+} dependent transcriptional induction of bim of cell death. *Journal of Immunology* **176**:2299-2306.

Chapman E.R., Hanson P.I., An S., and Jahn R. (1995). Ca^{2+} Regulates the Interaction Between Synaptotagmin and Syntaxin-1. *Journal of Biological Chemistry* **270**:23667-23671.

Chen Y.A. and Scheller R.H. (2001). SNARE mediated membrane fusion. *Nature Reviews Molecular Cell Biology* **2**:98-106.

Chidgey M.A.J. (1993). Protein targeting to dense-core secretory granules. *Bioessays* **15**:317-321.

Cifone M.G., Migliorati G., Parroni R., Marchetti C., Millimaggi D., Santoni A., and Riccardi C. (1999). Dexamethasone-induced thymocyte apoptosis: Apoptotic signal

involves the sequential activation of phosphoinositide-specific phospholipase C, acidic sphingomyelinase, and caspases. *Blood* **93**:2282-2296.

Clary D.O., Griff I.C., and Rothman J.E. (1990). SNAPs, a family of NSF attachment proteins involved in intracellular membrane fusion in animals and yeast. *Cell* **61**:709-721.

Collins B.M., Mccoy A.J., Kent H.M., Evans P.R., and Owen D.J. (2002). Molecular architecture and functional model of the endocytic AP2 complex. *Cell* **109**:523-535.

Desjardins M., Huber L.A., Parton R.G., and Griffiths G. (1994). Biogenesis of phagolysosomes proceeds through a sequential series of interactions with the endocytic apparatus. *Journal of Cell Biology* **124**:677-688.

Di Fiore P.P. and Gill G.N. (1999). Endocytosis and mitogenic signaling. *Current Opinion in Cell Biology* **11**:483-488.

Dulubova I., Sugita S., Hill S., Hosaka M., Fernandez I., Sudhof T.C., and Rizo J. (1999). A conformational switch in syntaxin during exocytosis: role of munc18. *EMBO Journal* **18**:4372-4382.

Dunn K.W., Mcgraw T.E., and Maxfield F.R. (1989). Iterative fractionation of recycling receptors from lysosomally destined ligands in an early sorting endosome. *Journal of Cell Biology* **109**:3303-3314.

Elferink L.A., Trimble W.S., and Scheller R.H. (1989). 2 Vesicle-Associated Membrane-Protein Genes Are Differentially Expressed in the Rat Central Nervous-System. *Journal of Biological Chemistry* **264**:11061-11064.

Fayyazi A., Eichmeyer B., Soruri A., Schweyer S., Herms J., Schwarz P., and Radzun H.J. (2000). Apoptosis of macrophages and T cells in tuberculosis associated caseous necrosis. *Journal of Pathology* **191**:417-425.

Felder S., Miller K., Moehren G., Ullrich A., Schlessinger J., and Hopkins C.R. (1990). Kinase-activity controls the sorting of the epidermal growth-factor receptor within the multivesicular body. *Cell* **61**:623-634.

Galli T., Chilcote T., Mundigl O., Binz T., Niemann H., and Decamilli P. (1994). Tetanus toxin-mediated cleavage of cellubrevin impairs exocytosis of transferrin receptor-containing vesicles in CHO cells. *Journal of Cell Biology* **125**:1015-1024.

Geuze H.J., Slot J.W., Strous G.J.A.M., Lodish H.F., and Schwartz A.L. (1983). Intracellular site of asialoglycoprotein receptor ligand uncoupling - double-label immunoelectron microscopy during receptor-mediated endocytosis. *Cell* **32**:277-287.

Ghosh R.N., Gelman D.L., and Maxfield F.R. (1994). Quantification of low-density-lipoprotein and transferrin endocytic sorting in Hep2 cells using confocal microscopy. *Journal of Cell Science* **107**:2177-2189.

Goldsby R.A., Kindt T.J., and Osborne B.A. (2000). Cells and organs of the immune system. **4th**:47-50.

Greenberg S., Burridge K., and Silverstein S.C. (1990). Colocalization of F-Actin and Talin during Fc receptor mediated phagocytosis in mouse macrophages. *Journal of Experimental Medicine* **172**:1853-1856.

Griffiths G. (2002). What's special about secretory lysosomes? *Seminars in Cell & Developmental Biology* **13**:279-284.

Griffiths G.M. (1996). Secretory lysosomes - A special mechanism of regulated secretion in haemopoietic cells. *Trends in Cell Biology* **6**:329-332.

Gross S.K., Shea T.B., and McCluer R.H. (1985). Altered secretion and accumulation of kidney glycosphingolipids by mouse pigmentation mutants with lysosomal dysfunctions. *Journal of Biological Chemistry* **260**:5033-5039.

Gruenberg J., Griffiths G., and Howell K.E. (1989). Characterization of the early endosome and putative endocytic carrier vesicles *in-vivo* and with an assay of vesicle fusion *in-vitro*. *Journal of Cell Biology* **108**:1301-1316.

Gruenberg J. and Maxfield F.R. (1995). Membrane transport in the endocytic pathway. *Current Opinion in Cell Biology* **7**:552-563.

Guo Z.H., Turner C., and Castle D. (1998). Relocation of the t-SNARE SNAP-23 from lamellipodia-like cell surface projections regulates compound exocytosis in mast cells. *Cell* **94**:537-548.

Gustavsson J., Parpal S., Karlsson M., Ramsing C., Thorn H., Borg M., Lindroth M., Peterson K.H., Magnusson K., and Stralfors P. (1999). Localization of the insulin receptor in caveolae of adipocyte plasma membrane. *FASEB Journal* **13**:1961-1971.

Hanson P.I., Roth R., Morisaki H., Jahn R., and Heuser J.E. (1997). Structure and conformational changes in NSF and its membrane receptor complexes visualized by quick-freeze/deep-etch electron microscopy. *Cell* **90**:523-535.

Hata Y., Slaughter C.A., and Sudhof T.C. (1993). Synaptic vesicle fusion complex contains Unc-18 homolog bound to syntaxin. *Nature* **366**:347-351.

Heijnen H.F.G., Debili N., Vainchencker W., Breton-Gorius J., Geuze H.J., and Sixma J.J. (1998). Multivesicular bodies are an intermediate stage in the formation of platelet α -granules. *Blood* **91**:2313-2325.

Henning S.W., Galandrini R., Hall A., and Cantrell D.A. (1997). The GTPase Rho has a critical regulatory role in thymus development. *EMBO Journal* **16**:2397-2407.

Hirling H., Steiner P., Chaperon C., Marsault R., Regazzi R., and Catsicas S. (2000). Syntaxin 13 is a developmentally regulated SNARE involved in neurite outgrowth and endosomal trafficking. *European Journal of Neuroscience* **12**:1913-1923.

Hollander G.A., Wang B.P., Nichogiannopoulou A., Platenburg P.P., Vanewijk W., Burakoff S.J., Gutierrezramos J.C., and Terhorst C. (1995). Developmental control point in induction of thymic cortex regulated by a subpopulation of prothymocytes. *Nature* **373**:350-353.

Holt M., Varoqueaux F., Wiederhold K., , rlaub H., assbauer D., and ahn R. (2006). Identification of SNAP-47, A novel Q_{bc}-SNARE with ubiquitous expression. *Journal of Biological Chemistry*.

Hong W. (2005). Cytotoxic T lymphocyte exocytosis: bring on the SNAREs. *Trends in Cell Biology* **15**:644-650.

Hopkins C.R. (1983). Intracellular routing of transferrin and transferrin receptors in epidermoid carcinoma A431-cells. *Cell* **35**:321-330.

Hsu S.C., Hazuka C.D., Foletti D.L., and Scheller R.H. (1999). Targeting vesicles to specific sites on the plasma membrane: the role of the sec6/8 complex. *Trends in Cell Biology* **9**:150-153.

Huizing M., Sarangarajan R., Strovel E., Zhao Y., Gahl W.A., and Boissy R.E. (2001). AP-3 mediates tyrosinase but not TRP-1 trafficking in human melanocytes. *Molecular Biology of the Cell* **12**:2075-2085.

Jahn R., Lang T., and Sudhof T.C. (2003). Membrane fusion. *Cell* **112**:519-533.

Jahn R. and Sudhof T.C. (1994). Synaptic vesicles and exocytosis. *Annual Review of Neuroscience* **17**:219-246.

Jahn R. and Sudhof T.C. (1999). Membrane fusion and exocytosis. *Annual Review of Biochemistry* **68**:863-911.

Janeway C.A., Travers P., Wallport M., and Sclomchik M.J. (2001a). T cell mediated immunity. **5th**:295-340.

Janeway C.A., Travers P., Wallport M., and Sclomchik M.J. (2001b). The development and survival of lymphocytes. **5th**:221-293.

Katzmann D.J., Odorizzi G., and Emr S.D. (2002). Receptor downregulation and multivesicular-body sorting. *Nature Reviews Molecular Cell Biology* **3**:893-905.

- Kishimoto T., Narazaki M., Matsumoto T., and Naka T. (1998). Negative regulation of cytokine signals by STAT-induced STAT-inhibitor-1 (SSI-1). *Experimental Hematology* **26**:759-759.
- Kornfeld S. and Mellman I. (1989). The biogenesis of lysosomes. *Annual Review of Cell Biology* **5**:483-525.
- Koster A., Saftig P., Matzner U., Vonfigura K., Peters C., and Pohlmann R. (1993). Targeted Disruption of the M(R) 46-000 Mannose 6-Phosphate Receptor Gene in Mice Results in Misrouting of Lysosomal Proteins. *EMBO Journal* **12**:5219-5223.
- Kreykenbohm V., Wenzel D., Antonin W., Atlachkine V., and von Mollard G.F. (2002). The SNAREs vtila and vtilb have distinct localization and SNARE complex partners. *European Journal of Cell Biology* **81**:273-280.
- Kyewski B.A., Schirmacher V., and Allison J.P. (1989). Antibodies against the T-Cell receptor CD3 complex interfere with distinct intra-thymic cell-cell interactions *in vivo* - correlation with arrest of T-Cell differentiation. *European Journal of Immunology* **19**:857-863.
- Lacorazza H.D., Porritt H.E., and Nikolich-Zugich J. (2001). Dysregulated expression of pre-T α reveals the opposite effects of Pre-TCR at successive stages of T cell development. *Journal of Immunology* **167**:5689-5696.
- Lin R.C. and Scheller R.H. (2000). Mechanisms of synaptic vesicle exocytosis. *Annual Review of Cell and Developmental Biology* **16**:19-49.
- Lind E.F., Prockop S.E., Porritt H.E., and Petrie H.T. (2001). Mapping precursor movement through the postnatal thymus reveals specific microenvironments supporting defined stages of early lymphoid development. *Journal of Experimental Medicine* **194**:127-134.
- Link E., Edelmann L., Chou J.H., Binz T., Yamasaki S., Eisel U., Baumert M., Sudhof T.C., Niemann H., and Jahn R. (1992). Tetanus toxin action - inhibition of neurotransmitter release linked to synaptobrevin proteolysis. *Biochemical and Biophysical Research Communications* **189**:1017-1023.
- Lobie P.E., Sadir R., Graichen R., Mertani H.C., and Morel G. (1999). Caveolar internalization of growth hormone. *Experimental Cell Research* **246**:47-55.
- Lodish H., Berk A., Zipursky S.L., Matsudaira P., Baltimore D., and Darnell J.E. (2001). Protein sorting: organelle biogenesis and protein secretion. **4th**:691-743.
- Low S.H., Li X., Miura M., Kudo N., Quinones B., and Weimbs T. (2003). Syntaxin 2 and endobrevin are required for the terminal step of cytokinesis in mammalian cells. *Developmental Cell* **4**:753-759.

- Lupashin V.V., Pokrovskaya I.D., Mcnew J.A., and Waters M.G. (1997). Characterization of a novel yeast SNARE protein implicated in Golgi retrograde traffic. *Molecular Biology of the Cell* **8**:2659-2676.
- Mallard F., Tang B.L., Galli T., Tenza D., Saint-Pol A., Yue X., Antony C., Hong W.J., Goud B., and Johannes L. (2002). Early/recycling endosomes-to-TGN transport involves two SNARE complexes and a Rab6 isoform. *Journal of Cell Biology* **156**:653-664.
- Marjomaki V., Pietiainen V., Matilainen H., Upla P., Ivaska J., Nissinen L., Reunanen H., Huttunen P., Hyypia T., and Heino J. (2002). Internalization of Echovirus 1 in caveolae. *Journal of Virology* **76**:1856-1865.
- Marsh E.W., Leopold P.L., Jones N.L., and Maxfield F.R. (1995). Oligomerized transferrin receptors are selectively retained by a luminal sorting signal in a long-lived endocytic recycling compartment. *Journal of Cell Biology* **129**:1509-1522.
- Marsh M., Griffiths G., Dean G.E., Mellman I., and Helenius A. (1986). 3-Dimensional structure of endosomes in BHK-21-cells. *Proceedings of the National Academy of Sciences of the United States of America* **83**:2899-2903.
- Martinez-Arca S., Alberts P., Zahraoui A., Louvard D., and Galli T. (2000). Role of tetanus neurotoxin insensitive vesicle-associated membrane protein (TI-VAMP) in vesicular transport mediating neurite outgrowth. *Journal of Cell Biology* **149**:889-899.
- Mayor S., Presley J.F., and Maxfield F.R. (1993). Sorting of membrane-components from endosomes and subsequent recycling to the cell-surface occurs by a bulk flow process. *Journal of Cell Biology* **121**:1257-1269.
- McMahon H.T., Ushkaryov Y.A., Edelman L., Link E., Binz T., Niemann H., Jahn R., and Sudhof T.C. (1993b). Cellubrevin is a ubiquitous tetanus-toxin substrate homologous to a putative synaptic vesicle fusion protein. *Nature* **364**:346-349.
- McMahon H.T., Ushkaryov Y.A., Edelman L., Link E., Binz T., Niemann H., Jahn R., and Sudhof T.C. (1993a). Cellubrevin Is a ubiquitous tetanus-toxin substrate homologous to a putative synaptic vesicle fusion protein. *Nature* **364**:346-349.
- Mellman I. (1996). Endocytosis and molecular sorting. *Annual Review of Cell and Developmental Biology* **12**:575-625.
- Mellman I. and Steinman R.M. (2001). Dendritic cells: Specialized and regulated antigen processing machines. *Cell* **106**:255-258.
- Miller J.F.A. and Osoba D. (1967). Current concepts of immunological function of thymus. *Physiological Reviews* **47**:437-&.

- Minter L.M. and Osborne B.A. (2003). Cell death in the thymus - it's all a matter of contacts. *Seminars in Immunology* **15**:135-144.
- Monck J.R. and Fernandez J.M. (1996). The fusion pore and mechanisms of biological membrane fusion. *Current Opinion in Cell Biology* **8**:524-533.
- Moroy T. and Karsunky H. (2000). Regulation of pre-T-cell development. *Cellular and Molecular Life Sciences* **57**:957-975.
- Mukherjee S., Ghosh R.N., and Maxfield F.R. (1997). Endocytosis. *Physiological Reviews* **77**:759-803.
- Mullock B.M., Smith C.W., Ihrke G., Bright N.A., Lindsay M., Parkinson E.J., Brooks D.A., Parton R.G., James D.E., Luzio J.P., and Piper R.C. (2000). Syntaxin 7 is localized to late endosome compartments, associates with Vamp 8, and is required for late endosome-lysosome fusion. *Molecular Biology of the Cell* **11**:3137-3153.
- Munoz J.J., Alfaro D., Garcia-Ceca J., Alonso L.M., Jimenez E., and Zapata A. (2006). Thymic alterations in EphA4-deficient mice. *Journal of Immunology* **177**:804-813.
- Murray R.Z., Wylie F.G., Khromykh T., Hume D.A., and Stow J.L. (2005). Syntaxin 6 and Vti1b form a novel SNARE complex, which is up-regulated in activated macrophages to facilitate exocytosis of tumor necrosis factor-alpha. *Journal of Biological Chemistry* **280**:10478-10483.
- Nakatsu F. and Ohno H. (2003). Adaptor protein complexes as the key regulators of protein sorting in the post-Golgi network. *Cell Structure and Function* **28**:419-429.
- Naramura M., Jang I.K., Kole H., Huang F., Haines D., and Gu H. (2002). c-Cbl and Cbl-b regulate T cell responsiveness by promoting ligand-induced TCR down-modulation. *Nature Immunology* **3**:1192-1199.
- Nosaka T., Morita S., Kitamura H., Nakajima H., Shibata F., Morikawa Y., Kataoka Y., Ebihara Y., Kawashima T., Itoh T., Ozaki K., Senba E., Tsuji K., Makishima F., Yoshida N., and Kitamura T. (2003). Mammalian twisted gastrulation is essential for skeletolymphogenesis. *Molecular and Cellular Biology* **23**:2969-2980.
- Nossal G.J.V. (1994). Negative Selection of Lymphocytes. *Cell* **76**:229-239.
- Nunnari J. and Walter P. (1996). Regulation of organelle biogenesis. *Cell* **84**:389-394.
- Ohno H. (2006). Physiological roles of clathrin adaptor AP complexes: lessons from mutant animals. *Journal of Biochemistry* **139**:943-948.

Ohno H., Stewart J., Fournier M.C., Bosshart H., Rhee I., Miyatake S., Saito T., Gallusser A., Kirchhausen T., and Bonifacino J.S. (1995). Interaction of Tyrosine-based sorting signals with clathrin-associated proteins. *Science* **269**:1872-1875.

Orlandi P.A. and Fishman P.H. (1998). Filipin-dependent inhibition of cholera toxin: Evidence for toxin internalization and activation through caveolae-like domains. *Journal of Cell Biology* **141**:905-915.

Owen D.J., Collins B.M., and Evans P.R. (2004). Adaptors for clathrin coats: Structure and function. *Annual Review of Cell and Developmental Biology* **20**:153-191.

Owen D.J. and Luzio J.P. (2000). Structural insights into clathrin-mediated endocytosis. *Current Opinion in Cell Biology* **12**:467-474.

Owen M.J. and Venkitaraman A.R. (1996). Signalling in lymphocyte development. *Current Opinion in Immunology* **8**:191-198.

Oyler G.A., Higgins G.A., Hart R.A., Battenberg E., Billingsley M., Bloom F.E., and Wilson M.C. (1989). The identification of a novel synaptosomal-associated protein, Snap-25, differentially expressed by neuronal subpopulations. *Journal of Cell Biology* **109**:3039-3052.

Pagan J.K., Wylie F.G., Joseph S., Widberg C., Bryant N.J., James D.E., and Stow J.L. (2003). The t-SNARE syntaxin 4 is regulated during macrophage activation to function in membrane traffic and cytokine secretion. *Current Biology* **13**:156-160.

Palmer A. and Klein R. (2003). Multiple roles of ephrins in morphogenesis, neuronal networking, and brain function. *Genes & Development* **17**:1429-1450.

Panigada M., Porcellini S., Barbier E., Hoeflinger S., Cazenave P.A., Gu H., Band H., von Boehmer H., and Grassi F. (2002). Constitutive endocytosis and degradation of the pre-T cell receptor. *Journal of Experimental Medicine* **195**:1585-1597.

Paumet F., Le Mao J., Martin S., Galli T., David B., Blank U., and Roa M. (2000a). Soluble NSF attachment protein receptors (SNAREs) in RBL-2H3 mast cells: Functional role of syntaxin 4 in exocytosis and identification of a vesicle-associated membrane protein 8-containing secretory compartment. *Journal of Immunology* **164**:5850-5857.

Paumet F., Le Mao J., Martin S., Galli T., David B., Blank U., and Roa M. (2000b). Soluble NSF attachment protein receptors (SNAREs) in RBL-2H3 mast cells: Functional role of syntaxin 4 in exocytosis and identification of a vesicle-associated membrane protein 8-containing secretory compartment. *Journal of Immunology* **164**:5850-5857.

Pazirandeh A., Xue Y.T., Rafter I., Sjovall J., Jondal M., and Okret S. (1999). Paracrine glucocorticoid activity produced by mouse thymic epithelial cells. *FASEB Journal* **13**:893-901.

Pearse B.M.F. (1988). Receptors compete for adaptors found in plasma-membrane coated pits. *EMBO Journal* **7**:3331-3336.

Pfeffer S.R. (1999). Transport-vesicle targeting: tethers before SNAREs. *Nature Cell Biology* **1**:E17-E22.

Philpott K.L., Viney J.L., Kay G., Rastan S., Gardiner E.M., Chae S., Hayday A.C., and Owen M.J. (1992). Lymphoid development in mice congenitally lacking T-Cell receptor- α - β expressing cells. *Science* **256**:1448-1452.

Polgar J., Chung S.H., and Reed G.L. (2002). Vesicle-associated membrane protein 3 (VAMP-3) and VAMP-8 are present in human platelets and are required for granule secretion. *Blood* **100**:1081-1083.

Prekeris R., Klumperman J., and Scheller R.H. (2000). Syntaxin 11 is an atypical SNARE abundant in the immune system. *European Journal of Cell Biology* **79**:771-780.

Pryor P.R., Mullock B.M., Bright N.A., Lindsay M.R., Gray S.R., Richardson S.C.W., Stewart A., James D.E., Piper R.C., and Luzio J.P. (2004). Combinatorial SNARE complexes with VAMP7 or VAMP8 define different late endocytic fusion events. *EMBO Reports* **5**:590-595.

Puri N., Kruhlak M.J., Whiteheart S.W., and Roche P.A. (2003). Mast cell degranulation requires N-ethylmaleimide-sensitive factor-mediated SNARE disassembly. *Journal of Immunology* **171**:5345-5352.

Rabinowitz S., Horstmann H., Gordon S., and Griffiths G. (1992). Immunocytochemical characterization of the endocytic and phagolysosomal compartments in peritoneal macrophages. *Journal of Cell Biology* **116**:95-112.

Ravichandran V., Chawla A., and Roche P.A. (1996). Identification of a novel syntaxin- and synaptobrevin/VAMP-binding protein, SNAP-23, expressed in non-neuronal tissues. *Journal of Biological Chemistry* **271**:13300-13303.

Regazzi R., Wollheim C.B., Lang J., Theler J.M., Rossetto O., Montecucco C., Sadoul K., Weller U., Palmer M., and Thorens B. (1995). Vamp-2 and cellubrevin are expressed in pancreatic β -cells and are essential for Ca^{2+} - but not for Gtp-Gamma-S-induced insulin-secretion. *EMBO Journal* **14**:2723-2730.

Ren Q., Barber H.K., Crawford G.L., Karim Z.A., Zhao C., Choi W., Wang C.C., Hong W., and Whiteheart S.W. (2006). Endobrevin/VAMP-8 Is the primary v-SNARE for the platelet release reaction. *Molecular and Cellular Biology* **Nov 1**.

Ridley A.J. (2001). Rho family proteins: coordinating cell responses. *Trends in Cell Biology* **11**:471-477.

Ritter M.A. and Boyd R.L. (1993). Development in the thymus - It takes 2 to tango. *Immunology Today* **14**:462-469.

Rizo J. and Sudhof T.C. (2002). SNAREs and Munc18 in synaptic vesicle fusion. *Nature Reviews Neuroscience* **3**:641-653.

Rothman J.E., Balch W.E., Braell W.A., Glick B., Hino Y., and Wattenberg B. (1984). Reconstitution of protein-transport in the Golgi. *Journal of Cell Biology* **99**:A230-A230.

Rothman J.E. and Wieland F.T. (1996). Protein sorting by transport vesicles. *Science* **272**:227-234.

Sano S., Takahama Y., Sugawara T., Kosaka H., Itami S., Yoshikawa K., Miyazaki J., van Ewijk W., and Takeda J. (2001). Stat3 in thymic epithelial cells is essential for postnatal maintenance of thymic architecture and thymocyte survival. *Immunity* **15**:261-273.

Schiavo G., Benfenati F., Poulain B., Rossetto O., Delaureto P.P., Dasgupta B.R., and Montecucco C. (1992). Tetanus and Botulinum-B Neurotoxins block neurotransmitter release by proteolytic cleavage of synaptobrevin. *Nature* **359**:832-835.

Schubert W., Frank P.G., Razani B., Park D.S., Chow C.W., and Lisanti M.P. (2001). Caveolae-deficient endothelial cells show defects in the uptake and transport of albumin in vivo. *Journal of Biological Chemistry* **276**:48619-48622.

Shen Y., Schlessinger K., Zhu X., Meffre E., Quimby F., Levy D.E., and Darnell J.E.Jr. (2004). Essential role of STAT3 in postnatal survival and growth revealed by mice lacking STAT3 serine 727 phosphorylation. *Molecular and Cellular Biology* **24**:407-419.

Shores E.W., Ewijk W.V., and Singer A. (2005). Disorganization and restoration of thymic medullary epithelial cells in T cell receptor-negative scid mice: Evidence that receptor-bearing lymphocytes influence maturation of the thymic microenvironment. *European Journal of Immunology* **21**:1657-1661.

Shores E.W., Sharrow S.O., Uppenkamp I., and Singer A. (1990). T-Cell receptor-negative thymocytes from scid mice can be Induced to enter the Cd4/Cd8 differentiation pathway. *European Journal of Immunology* **20**:69-77.

Shores E.W., Vanewijk W., and Singer A. (1991). Disorganization and restoration of thymic medullary epithelial-cells in T-Cell receptor-negative scid mice - evidence that receptor-bearing lymphocytes influence maturation of the thymic microenvironment. *European Journal of Immunology* **21**:1657-1661.

Sikorra S., Henke T., Swaminathan S., Galli T., and Binz T. (2006). Identification of the amino acid residues rendering TI-VAMP insensitive toward botulinum neurotoxin B. *Journal of Molecular Biology* **357**:574-582.

Simmen T., Honing S., Icking A., Tikkanen R., and Hunziker W. (2002). AP-4 binds basolateral signals and participates in basolateral sorting in epithelial MDCK cells. *Nature Cell Biology* **4**:154-159.

Simonsen A., Lippe R., Christoforidis S., Gaullier J.M., Brech A., Callaghan J., Toh B.H., Murphy C., Zerial M., and Stenmark H. (1998). EEA1 links PI(3)K function to Rab5 regulation of endosome fusion. *Nature* **394**:494-498.

Singh R.D., Puri V., Valiyaveetil J.T., Marks D.L., Bittman R., and Pagano R.E. (2003). Selective caveolin-1-dependent endocytosis of glycosphingolipids. *Molecular Biology of the Cell* **14**:3254-3265.

Sollner T., Bennett M.K., Whiteheart S.W., Scheller R.H., and Rothman J.E. (1993a). A protein assembly-disassembly pathway *in-vitro* that may correspond to sequential steps of synaptic vesicle docking, activation, and fusion. *Cell* **75**:409-418.

Sollner T., Whitehart S.W., Brunner M., Erdjumentbromage H., Geromanos S., Tempst P., and Rothman J.E. (1993b). SNAP receptors implicated in vesicle targeting and fusion. *Nature* **362**:318-324.

Sorkin A., Mckinsey T., Shih W., Kirchhausen T., and Carpenter G. (1995). Stoichiometric interaction of the epidermal growth-factor receptor with the clathrin-associated protein complex Ap-2. *Journal of Biological Chemistry* **270**:619-625.

Sprent J., Lo D., Gao E.K., and Ron Y. (1988). T-Cell selection in the thymus. *Immunological Reviews* **101**:173-190.

Steegmaier M., Klumperman J., Foletti D.L., Yoo J.S., and Scheller R.H. (1999a). Vesicle-associated membrane protein 4 is implicated in trans-Golgi network vesicle trafficking. *Molecular Biology of the Cell* **10**:1957-1972.

Steegmaier M., Klumperman J., Foletti D.L., Yoo J.S., and Scheller R.H. (1999b). Vesicle-associated membrane protein 4 is implicated in trans-golgi network vesicle trafficking. *Molecular Biology of the Cell* **10**:1957-1972.

Steegmaier M., Yang B., Yoo J.S., Huang B., Shen M., Yu S., Luo Y., and Scheller R.H. (1998). Three novel proteins of the syntaxin/SNAP-25 family. *Journal of Biological Chemistry* **273**:34171-34179.

Steinman R.M. and Swanson J. (1995). The endocytic activity of dendritic cells. *Journal of Experimental Medicine* **182**:283-288.

Stenmark H., Vitale G., Ullrich O., and Zerial M. (1995). Rabaptin-5 is a direct effector of the small GTPase Rab5 in endocytic membrane fusion. *Cell* **83**:423-432.

Sudhof T.C. (2004). The synaptic vesicle cycle. *Annual Review of Neuroscience* **27**:509-547.

Sudhof T.C., Baumert M., Perin M.S., and Jahn R. (1989). A synaptic vesicle membrane protein is conserved from mammals to drosophila. *Neuron* **2**:1475-1481.

Sutton R.B., Fasshauer D., Jahn R., and Brunger A.T. (1998). Crystal structure of a SNARE complex involved in synaptic exocytosis at 2.4 angstrom resolution. *Nature* **395**:347-353.

Takahama Y. (2006). Journey through the thymus: stromal guides for T-cell development and selection. *Nature Reviews Immunology* **6**:127-135.

Teng F.Y.H., Wang Y., and Tang B.L. (2001). The syntaxins. *Genome Biology* **2**:243-251.

ter Beest M.B.A., Chapin S.J., Avrahami D., and Mostov K.E. (2005). The role of syntaxins in the specificity of vesicle targeting in polarized epithelial cells. *Molecular Biology of the Cell* **16**:5784-5792.

ter Bush D.R., Maurice T., Roth D., and Novick P. (1996). The Exocyst is a multiprotein complex required for exocytosis in *Saccharomyces cerevisiae*. *EMBO Journal* **15**:6483-6494.

Thien C.B.F., Blystad F.D., Zhan Y., Lew A.M., Voigt V., Andoniou C.E., and Langdon W.Y. (2005a). Loss of the c-cbl RING finger function induces increased TCR signalling and thymic deletion. *Tissue Antigens* **66**:561-561.

Thien C.B.F., Blystad F.D., Zhan Y.F., Lew A.M., Voigt V., Andoniou C.E., and Langdon W.Y. (2005b). Loss of c-Cbl RING finger function results in high-intensity TCR signaling and thymic deletion. *EMBO Journal* **24**:3807-3819.

Trimble W.S., Cowan D.M., and Scheller R.H. (1988). VAMP-1 - A synaptic vesicle associated integral membrane protein. *Proceedings of the National Academy of Sciences of the United States of America* **85**:4538-4542.

van Ewijk W. (1991). T-Cell differentiation is influenced by thymic microenvironments. *Annual Review of Immunology* **9**:591-615.

Vandeurs B., Holm P.K., Kayser L., Sandvig K., and Hansen S.H. (1993). Multivesicular bodies in Hep-2 cells are maturing endosomes. *European Journal of Cell Biology* **61**:208-224.

Verhage M., Maia A.S., Plomp J.J., Brussaard A.B., Heeroma J.H., Vermeer H., Toonen R.F., Hammer R.E., van den Berg T.K., Missler M., Geuze H.J., and Sudhof T.C. (2000). Synaptic assembly of the brain in the absence of neurotransmitter secretion. *Science* **287**:864-869.

von Boehmer H. (1992). Thymic selection - A matter of life and death. *Immunology Today* **13**:454-458.

von Boehmer H. (1994). Positive selection of lymphocytes. *Cell* **76**:219-228.

von Figura K. and Hasilik A. (1986). Lysosomal enzymes and their receptors. *Annual Review of Biochemistry* **55**:167-193.

von Mollard G.F., Nothwehr S.F., and Stevens T.H. (1997). The yeast v-SNARE Vti1p mediates two vesicle transport pathways through interactions with the t-SNAREs Sed5p and Pep12p. *Journal of Cell Biology* **137**:1511-1524.

von Mollard G.F. and Stevens T.H. (1998). A human homolog can functionally replace the yeast vesicle-associated SNARE Vti1p in two vesicle transport pathways. *Journal of Biological Chemistry* **273**:2624-2630.

von Boehmer H. (1992). Thymic selection - A matter of life and death. *Immunology Today* **13**:454-458.

Wang C.C., Ng C.P., Lu L., Atlashkin V., Zhang W., Seet L.F., and Hong W.J. (2004). A role of VAMP8/endobrevin in regulated exocytosis of pancreatic acinar cells. *Developmental Cell* **7**:359-371.

Ward D.M., Pevsner J., Scullion M.A., Vaughn M., and Kaplan J. (2000). Syntaxin 7 and VAMP-7 are soluble N-ethylmaleimide-sensitive factor attachment protein receptors required for late endosome-lysosome and homotypic lysosome fusion in alveolar macrophages. *Molecular Biology of the Cell* **11**:2327-2333.

Waters M.G., Clary D.O., and Rothman J.E. (1992). A Novel 115-Kd peripheral membrane protein is required for intercisternal transport in the Golgi stack. *Journal of Cell Biology* **118**:1015-1026.

Weimbs T., Low S.H., Chapin S.J., Mostov K.E., Bucher P., and Hofmann K. (1997). A conserved domain is present in different families of vesicular fusion proteins: A new superfamily. *Proceedings of the National Academy of Sciences of the United States of America* **94**:3046-3051.

Wong S.H., Zhang T., Xu Y., Subramaniam V.N., Griffiths G., and Hong W.J. (1998). Endobrevin, a novel synaptobrevin/VAMP-like protein preferentially associated with the early endosome. *Molecular Biology of the Cell* **9**:1549-1563.

Xu Y., Wong S.H., Tang B.L., Subramaniam V.N., Zhang T., and Hong W.J. (1998). A 29-kilodalton Golgi soluble N-ethylmaleimide-sensitive factor attachment protein receptor (Vti1-rp2) implicated in protein trafficking in the secretory pathway. *Journal of Biological Chemistry* **273**:21783-21789.

Yamashiro D.J., Tycko B., Fluss S.R., and Maxfield F.R. (1984). Segregation of transferrin to a mildly acidic (Ph 6.5) para-Golgi compartment in the recycling pathway. *Cell* **37**:789-800.

Yang C.M., Mora S., Ryder J.W., Coker K.J., Hansen P., Allen L.A., and Pessin J.E. (2001). VAMP3 null mice display normal constitutive, insulin- and exercise-regulated vesicle trafficking. *Molecular and Cellular Biology* **21**:1573-1580.

Yoshihara M., Adolfsen B., and Littleton J.T. (2003). Is synaptotagmin the calcium sensor? *Current Opinion in Neurobiology* **13**:315-323.

Zambrowicz B.P., Friedrich G.A., Buxton E.C., Lilleberg S.L., Person C., and Sands A.T. (1998). Disruption and sequence identification of 2,000 genes in mouse embryonic stem cells. *Nature* **392**:608-611.

Zeng Q., Subramaniam V.N., Wong S.H., Tang B.L., Parton R.G., Rea S., James D.E., and Hong W.J. (1998a). A novel synaptobrevin/VAMP homologous protein (VAMP5) is increased during in vitro myogenesis and present in the plasma membrane. *Molecular Biology of the Cell* **9**:2423-2437.

Zeng Q., Subramaniam V.N., Wong S.H., Tang B.L., Parton R.G., Rea S., James D.E., and Hong W.J. (1998b). A novel synaptobrevin/VAMP homologous protein (VAMP5) is increased during in vitro myogenesis and present in the plasma membrane. *Molecular Biology of the Cell* **9**:2423-2437.

Zeng Q., Tran T.T.H., Tan H.X., and Hong W.J. (2003). The cytoplasmic domain of Vamp4 and Vamp5 is responsible for their correct subcellular targeting - The N-terminal extension of Vamp4 contains a dominant autonomous targeting signal for the trans-Golgi network. *Journal of Biological Chemistry* **278**:23046-23054.

Zimmerberg J., Vogel S.S., and Chernomordik L.V. (1993). Mechanisms of Membrane-Fusion. *Annual Review of Biophysics and Biomolecular Structure* **22**:433-466.

Publications

Kanwar N., Dressel R., Fayyazi A., Fischer von Mollard G., Lack of endosomal SNARE VAMP8 in mice leads to defect in the thymus. *Manuscript in preparation*

Curriculum Vitae

Personal data

Name Namita Kanwar
Born 23 July 1981, Faridabad (India)
Marital status Single

Education - School

Xth Grade 1997 St. Joseph's Convent School, Faridabad, India
XIIth Grade 1999 APJ Public School, Faridabad, India

Education -University

1999-2002 Bachelor of Science, University of Delhi, Delhi, India

Enrollment at : Acharya Narendra Dev College
Field of study : Biomedimedical Sciences
Degree awarded : B.Sc. Biomedical Sciences

B.Sc. project: Analysis of physico-chemical properties of drugs

Division for Pharmaceutical Research, Ranbaxy Research Laboratories,
India

2002-2003 Master of Science, Georg-August Universität Göttingen, Germany

Enrollment at : Max Planck Research School, International
 Program for Molecular Biology
Field of study : Molecular Biology
Degree awarded : M.Sc. Molecular Biology

M.Sc. Project: Analysis of mice deficient in late endosomal SNARE proteins
Vti1b and VAMP8/ Endobrevin

Department for Biochemistry II, Georg- August Universität Göttingen

(Major advisor: Professor Dr. Gabriele Fischer von Mollard)
